Master of Science Thesis

# Offshore Wind Farm Optimisation

## A Comparison of Performance between Regular and Irregular Wind Turbine Layouts

M. V. Sickler

31 July 2020

DTU

EWEM

TU Delft

Ventolines

# Offshore Wind Farm Optimisation

## A Comparison of Performance between Regular and Irregular Wind Turbine Layouts

by

M.V. Sickler

to obtain the degree of Master of Science
at the Danish University of Technology and Delft University of Technology,
to be defended publicly on August 13, 2020.




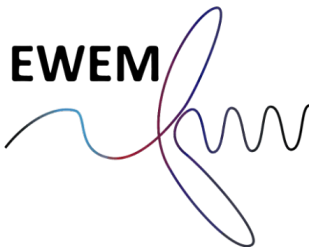


| | | | |
|---|---|---|---|
| Student number TU Delft: | 4354052 | | |
| Student number DTU: | s183288 | | |
| Project duration: | November 1, 2019 – August 13, 2020 | | |
| Thesis committee: | Dr. K. Dykes | DTU | Supervisor |
| | Ir. J. A. Melkert | TU Delft | Quality control |
| | Dr. ir. B. C. Ummels | Ventolines | Supervisor |
| | Dr. ing. R. Schmehl | DTU | External supervisor |
| | Dr. ir. M. B. Zaaijer | TU Delft | Supervisor |

An electronic version of this thesis is available at http://repository.tudelft.nl/.

# Abstract

Wind farm layouts in industry show a range of patterns with an overall trend from regular to irregular patterns over time. Wind farm layout optimisation studies in literature generally result in irregular wind turbine patterns. Review of existing literature shows that the performance of irregular and regular wind farm layouts has not been compared in a consistent way. Although there are indications that irregular layouts outperform regular layouts, it is yet to be determined if this is the case for the overall performance and if so, to what degree. In this research the effect of regular and irregular wind farm layouts on selected performance indicators is quantified. This quantification is performed through means of a comparative case study.

The performance of both regular and irregular wind farm layouts is assessed on the basis of three performance indicator groups: (1) power performance; (2) wake-induced tower fatigue; and (3) inter-array cabling system. The performance indicators in these groups are affected by a change in wind farm layout, feasible, site independent, and technical as concluded from a multi-criteria decision analysis.

The irregular wind farm layout has a higher annual energy production and a higher persistence to wind direction. The net present value of this increase in cash flow over the lifetime of the wind farm is estimated at 10 million Euros. A higher persistence to wind direction means that the power output is less sensitive to fluctuations in wind direction. This characteristic increases the predictability of the wind farm power, which can indirectly lead to a decrease in imbalance cost on the electricity market.

The wake induced tower fatigue is found to be negatively impacted by an irregular wind farm layout. Implementation of the Frandsen model shows that the maximum effective turbulence of the irregular wind farm is 23.8% higher than that of the regular wind farm layout. For fatigue-driven tower design, this leads to an increase in tower wall thickness, which in turn results in an increase in tower material consumption. The increase in tower cost in the wind farm is estimated at 4 million Euros. Application of a minimum inter-turbine spacing to ameliorate the negative effect on effective turbulence is can lead to a decrease of 20 % (as compared to the case study).

The inter-array cable design results show a marginal increase in cable cost of 1.15 % for the irregular wind farm. The analysis reveals that this performance indicator is strongly dependent on site-specific input data. Due to this marginal change and dependency on site specific input data, this performance indicator is omitted from further conclusions.

Comparing the negative effect of the tower cost and the increase in revenue due to the higher AEP, the net present value is computed. With a discount rate of 5 %, the net present value of the AEP reduced by the increase in tower cost results in an increase of 6 million Euros.

For improved performance in future wind farm layouts, the implementation of irregular wind turbine patterns is advisable. That is, with the proviso that the minimum inter-turbine spacing is taken into consideration with respect to wake-added turbulence levels.

# Acknowledgements

First and foremost, I would like to express my deepest appreciation to Bart Ummels, who provided me with encouragement and patience throughout the duration of this research project. I am very grateful for the trust and unparalleled support I have received and his profound belief in my work and abilities. With his unlimited enthusiasm for wind energy and technology he has managed to make my thesis a positive and fun experience.

At TU Delft and DTU, I would like to extend my sincere thanks to Katherine Dykes and Michiel Zaaijer for the many meetings in which we discussed the progress of my research. The development of this project is in large part thanks to the knowledge, constructive criticism, and general advice they shared with me. Guiding me in the right direction and employing alternative and helicopter-view perspectives have been very valuable for my progress throughout this project. Furthermore, I would like to thank Roland Schmehl and Joris Melkert for completing my thesis committee.

Performing my thesis in collaboration with Ventolines, I have come to strongly appreciate the Ventolines team for their collegiality. It has been very rewarding and encouraging to be surrounded by such a diverse and talented team, and therefore I am grateful for the opportunity and freedom Ventolines has given me. Several people at Ventolines played an important role in the process of this thesis. First, I would like to express my gratitude to Boy Koppenol and Ardaan Walvis who provided a great amount of assistance. I highly appreciate the advice and brainstorming sessions with Boy which greatly contributed to my understanding of the wind turbine industry. Many thanks to Ardaan who was especially helpful to me during the starting phase of my thesis, where he guided and supported me whilst working with WindPRO. Also, I would like to thank Ana-Maria Ringlever-Dospinescu (van Oord), Michel Tellman, Albert Ploeg, Benjamin Stobbe, Erik Smid (Siemens Gamesa), and Daniël Vree for their time and expert knowledge and advice. They have all, in different ways, given me insightful information and valuable data, as well as invaluable knowledge obtained from their field of expertise. In addition, thank-you to Guus Mulders for saving me an extensive amount of time by allowing me to use his laptop with WindPRO installed for the duration of my project.

The completion of this thesis would not have been possible without the help of my friends: Janneke Blok, Sieglinde Goossenaerts, Diederik van Binsbergen, Madelon Nijman, Ruben Wink, Robin Vervaat, and Kees ’t Hooft. I thank them for their support and time to thoroughly check my work, providing me with helpful advice.

On a personal note, I am deeply indebted to Chimène Jongejans and Joost Hagens, who supported me during the strange and challenging times originating from the Covid-19 pandemic. Last, but certainly not least, I wish to thank my family for their love and encouragement, without whom I would never have enjoyed so many opportunities.

*M.V. Sickler*
*Delft, July 2020*

# Contents


**1 Introduction** **1**
- 1.1 Offshore Wind Farms . . . 1
  - 1.1.1 Performance . . . 1
  - 1.1.2 Timeline of Wind Turbine Patterns in History . . . 2
- 1.2 Literature on Wind Farm Layouts . . . 3
- 1.3 Problem Statement . . . 4
- 1.4 Research Objective and Research Questions . . . 5
  - 1.4.1 Research Objective . . . 5
  - 1.4.2 Research Questions . . . 5
- 1.5 Methodology and Thesis Outline . . . 5

**2 Performance Indicator Selection and Case Selection** **7**
- 2.1 Introduction . . . 7
- 2.2 Performance Indicator Selection . . . 7
  - 2.2.1 Overarching Key Performance Indicator . . . 7
  - 2.2.2 Performance Indicator Inventory . . . 8
  - 2.2.3 Multi-Criteria Decision Analysis . . . 9
  - 2.2.4 Multi-Criteria Decision Analysis Results . . . 10
- 2.3 Case Selection . . . 11
  - 2.3.1 Case Layout Specifications . . . 11
  - 2.3.2 Wind Climate . . . 12
  - 2.3.3 Wind Turbine Specification . . . 13
- 2.4 Conclusion . . . 14

**3 Performance Indicator 1: Power Performance** **15**
- 3.1 Introduction . . . 15
- 3.2 Annual Energy Production . . . 15
  - 3.2.1 Annual Energy Production in WindPRO . . . 16
  - 3.2.2 Annual Energy Production Analysis Borssele . . . 16
  - 3.2.3 Individual Turbine AEP Performance . . . 17
- 3.3 Persistence to Wind Direction . . . 19
  - 3.3.1 Omni-directional Power Calculations in WindPRO . . . 19
  - 3.3.2 Persistence to Wind Direction Assessment Borssele . . . 20
  - 3.3.3 Value on the Electricity Market . . . 22
- 3.4 Conclusion . . . 23

**4 Performance Indicator 2: Wake Induced Tower Fatigue** **24**
- 4.1 Introduction . . . 24
- 4.2 Fatigue Models . . . 25
- 4.3 Wake Added Tower Fatigue . . . 26
  - 4.3.1 Effective Turbulence . . . 26
  - 4.3.2 Tower-wall Thickness Relation to Effective Turbulence . . . 27
- 4.4 Wake Added Tower Fatigue Borssele . . . 27
  - 4.4.1 Wake Added Damage . . . 28
  - 4.4.2 Tower Dimensions and Cost . . . 29
- 4.5 Conclusion . . . 30

**5 Performance Indicator 3: Electrical Inter-Array Cabling System** **31**
5.1 Introduction . . . 31
5.2 Inter-Array Cable Design . . . 32
5.3 Preliminary Cable Design Process for Borssele . . . 34
5.3.1 Input Parameters . . . 34
5.3.2 Calculation and Decision Phase . . . 34
5.3.3 Cable Length . . . 35
5.3.4 Impact on Cost, Revenue, and Profit . . . 36
5.4 Conclusion . . . 37

**6 General Applicability of Results** **38**
6.1 Rotor Diameter Sensitivity . . . 38
6.1.1 Down-scaling the IEA Wind Turbine . . . 38
6.1.2 Sensitivity: Energy Yield . . . 39
6.1.3 Sensitivity: Persistence to Wind Direction . . . 40
6.1.4 Sensitivity: Wake Induced Tower Fatigue . . . 41
6.1.5 Rotor Diameter Sensitivity Conclusion . . . 43
6.2 Wind Climate Sensitivity . . . 43
6.2.1 Sensitivity: Energy Yield . . . 44
6.2.2 Sensitivity: Persistence to Wind Direction . . . 44
6.2.3 Sensitivity: Wake Induced Tower Fatigue . . . 45
6.2.4 Windrose Climate Sensitivity Conclusion . . . 46
6.3 Re-optimisation of Wind Farm Layouts . . . 47
6.3.1 Rotor Diameter Optimisation . . . 48
6.3.2 Wind Climate Optimisation . . . 48
6.4 Additional Optimised Layout Cases . . . 49
6.4.1 Optimised Layouts Selection . . . 49
6.4.2 Annual Energy Production . . . 51
6.4.3 Persistence to Wind Direction . . . 51
6.4.4 Wake Induced Tower Fatigue . . . 52
6.4.5 Additional Layout Conclusion . . . 53
6.5 Conclusion . . . 55

**7 Mitigation of Effective Turbulence for Irregular Wind Farms** **56**
7.1 Introduction . . . 56
7.2 Minimum Spacing Limit . . . 57
7.3 Wake Energy Loss . . . 57
7.4 Implementation of the Minimum Spacing Limit . . . 58
7.4.1 Annual Energy Yield . . . 59
7.4.2 Effective Turbulence . . . 59
7.5 Conclusion . . . 60

**8 Conclusion and Recommendation** **61**
8.1 Conclusions . . . 61
8.2 Recommendations . . . 62

**A Multi-Criteria Decision Analysis** **63**
A.1 Performance Indicator Inventory & Rating . . . 63
A.2 Selected Performance Indicator Groups . . . 64

**B Optimised Layouts** **65**
B.1 MDAO Design Approach . . . 65
B.2 WindPRO Optimisation Module . . . 65
B.2.1 Regular Optimisation . . . 65
B.2.2 Irregular Layout Optimisation WindPRO . . . 66
B.3 WindPRO Optimised Layout Results . . . 67

**C Wind Direction Distribution** **68**

**D Sensitivity Overview** **70**

**E Sensitivity Study Inter-Array Cable Layout** **71**
E.1 Detailed Design Loop . . . . . 71
E.2 Cable Selection . . . . . 72
E.3 Substation Location . . . . . 74

**Bibliography** **76**

# 1 Introduction

## 1.1. Offshore Wind Farms

Increasing the renewable energy share on the electrical grid is partially facilitated through means of wind energy, by utilising wind turbines to convert kinetic energy from the wind to electrical power [1]. A comparison between wind energy and other renewable energy sources performed by Jacobson [2], shows that wind energy performs best with respect to air pollution, energy security and effects of global warming related emissions. When multiple wind turbines are placed in a confined space this is called a wind farm. Offshore wind farms are particularly interesting as this poses less geographical and social constraints compared to onshore wind farms. Additionally, due to the increase in population near the coast, there is also a higher demand for electricity near the coastal regions [3].

### 1.1.1. Performance

The performance of an offshore wind farm indicates how efficient the system is at achieving its main objective [4]. Improving the performance of wind farms lays the foundation for the wind farm layout optimisation problem: finding the best position of turbines in a defined region taking into account certain design objectives [5]. Due to the increased installed capacity and increasing size of offshore wind farms, research regarding the optimal placement of turbines within a wind farm is discussed thoroughly in literature. Until recently, the main driver for wind farm research and development has been the levelised cost of energy (LCOE). This is computed as the total cost of a wind farm divided by the total electrical energy generated by the wind farm over the lifetime. The LCOE entails multiple components such as the annual energy production (AEP), number of turbines, installation cost, operational cost, and many more. Some wind farm layout optimisation studies employ a single objective of maximising the AEP due to its relatively considerable effect on the LCOE [6]. The LCOE for offshore wind energy has significantly decreased, by more than 60% in the last 7 years as shown in Figure 1.1.

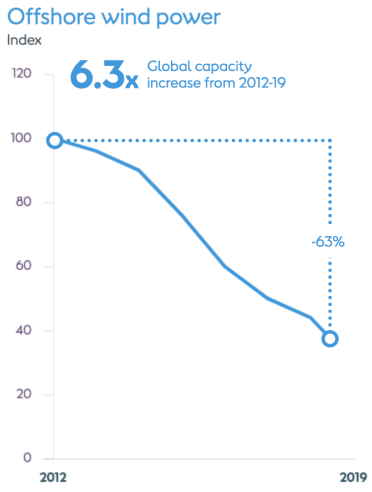


Figure 1.1: Global reduction in cost of energy (LCOE) for offshore wind. [7]

Although wind farm layout optimisation is extensively covered in literature, there is a lack of well-defined best practices for the performance assessment of a wind farm. This problem was previously identified by González-Longatt et al. [8], who developed an inventory of the performance indicators for the operation and maintenance phase of wind farms. However, a lack of performance indicator identification beyond the scope of this operations and maintenance phase remains in literature. This can also be observed in the variation in optimisation objectives between different wind farm layout optimisation studies [9].

One performance indicator which is included in all wind farm layout optimisation algorithms is the AEP. This was previously identified as (one of) the most important performance indicators for an offshore wind farm. Extracting kinetic energy from the wind results in a velocity deficit behind the rotor disk causing a decrease in power production for downstream turbines. According to Barthelmie et al. [10], on average the power output loss of a large wind farm can reach up to 10-20 % of the total power output due to wake losses. Therefore, the layout of the wind farm to a large degree determines its AEP performance [11]. Numerous wind farm layouts exist in operational wind farms, as well as theoretical layouts resulting from optimisation studies.

### 1.1.2. Timeline of Wind Turbine Patterns in History

Looking at wind farm layouts over time, a range of patterns can be recognised. The patterns can be distinguished based on their regularity. Regular patterns are defined as '*Arranged in or constituting a constant or definite pattern, especially with the same space between individual instances.*' [12]. An example of a strictly regular pattern could be a square with equal inter-turbine spacing (left-most wind farm in Figure 1.2). Irregular patterns are defined as '*Not even or balanced in shape or arrangement*' [13]. The second wind farm from the right in Figure 1.2 shows an irregular wind turbine pattern with an irregular outline. There are however different degrees of regularity ranging between these strictly regular and irregular patterns. The right-most wind turbine in Figure 1.2 for example shows an irregular wind turbine pattern with a regular outline.

Examining wind farm layouts which are operational in industry, a range of patterns can be recognised in relation to time. Earlier wind farms show regular patterns such as the wind farms Horns Rev 1 (2002) [14] and Prinses Amalia (2008) [15]. More recent and larger wind farms show more variation in patterns such as the wind farms Horns Rev 2 (2009) [16] and Rødsand (2010) [17], and partial irregularity such as Anholt (2013) [16] and many more. Multiple desktop optimisation studies even suggest fully irregular wind farms such as Research Layout 1 and 2 which are obtained from existing research [18, 19].

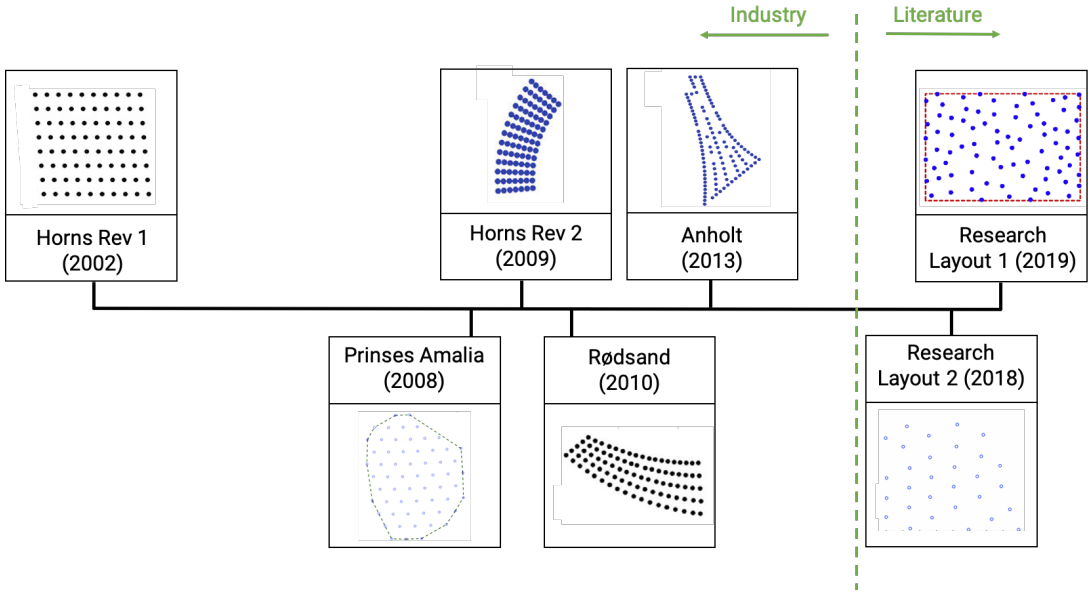


Figure 1.2: Timeline of wind farm patterns in history. Left of the green dashed line wind farm layouts operational in industry are depicted [14–17], and right of the green dashed line optimised layouts from literature studies are depicted [18, 19].

From left to right, Figure 1.2 shows a gradual change from regular to irregular wind farms. Horns Rev 1 has a high degree of regularity, where the optimisation algorithms resulting from [18, 19], show more

irregular patterns. To complete the image sketched in Figure 1.2, Triton Knoll wind farm should be added at the right-most position in 2022 [20]. As the wind farm is still under development it does not belong in the history timeline, but it is worth mentioning. This wind farm has a highly irregular wind turbine pattern and thus substantiates the gradual change from regular to irregular layouts.

Regulation changes amplify the interest to optimise the performance of offshore wind farms. The permit change implemented in the Netherlands on the $1^{st}$ of July 2015 [21] is an example. A site decision is designated by the Minister of Economic Affairs which contains, among other things, the maximum number of turbines, minimum rotor surface, minimum and maximum capacity of each turbine and the minimum distance required between the turbines. Previously, permits were granted for a given number of turbines with a set position within the wind farm. This change facilitates the optimisation of the layout after the permit has been granted.

## 1.2. Literature on Wind Farm Layouts

Observing this gradual change from regular to irregular wind farm layouts, a literature study is performed. In this section, the existing literature on regular and irregular layouts is presented. A study performed by Perez-Moreno et al. [22] investigated the preliminary design development of the layout, electrical collection system, and support structures of an offshore wind farm. This is done based on two different approaches. In the first, sequential approach, the interaction between the three performance characteristics are neglected. In the second approach, which is called the 'Multidisciplinary Design Analysis and Optimisation' (MDAO) approach, their interaction is taken into account. The objective of both approaches is to optimise for the total system levelised cost of energy (LCOE). This study is performed using a regular and irregular layout, however, the aim is not to compare the performance of the different geometric patterns.

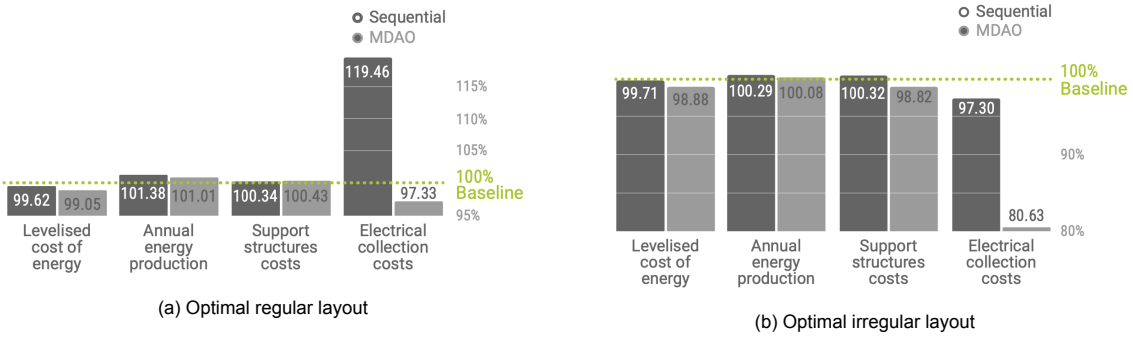


(a) Optimal regular layout

(b) Optimal irregular layout

Figure 1.3: Levelised cost of energy, annual energy production, electrical costs, and support structure costs of the optimal layouts found with the sequential and MDAO approaches [22].

Looking at the results for the regular (Figure 1.3a) optimisation, the difference between the sequential and MDAO approach is investigated. In Figure 1.3b, the same is done for the irregular wind farm. The performance can, however, not be compared between the regular and irregular results, as the baseline design for the regular and irregular wind farm are not identical.

In a study performed by Chen et al. [23], an innovative method for optimisation is proposed and tested with real wind conditions which is applicable for both regular and irregular layouts. The research is based on a multi-objective genetic algorithm with the objective to maximize the wind farm efficiency and minimize the cost per unit power. Four case studies are conducted, one regular and three irregular. They are compared with each other, all with the same total geographical area. From this comparison, it is suggested that irregular geometric patterns may perform better than regular layouts, but no final conclusion is drawn.

Charhouni et al. [24] compares different wind farm layout options (regular and irregular) with the aim to extract as much wind power whilst simultaneously minimising cost. The resulting power, capacity factor and efficiency of the study for the layout designs shows that the irregular layout has a higher power production, capacity factor and efficiency than the regular layout. It should be noted that this study considers a constant wind speed and direction. To make the comparison between the two layouts fair, the study should be conducted with variable wind speed and direction.

Although all three studies mentioned above [22–24] touch upon the performance of regular and irregular layouts, the aim of these studies is to assess the performance of the optimisation itself. Considering the change in geometric patterns for wind farms over the years as mentioned in subsection 1.1.2, the effect of this on the performance of the wind farm should be investigated.

## 1.3. Problem Statement

The difference in performance between regular and irregular wind farms is largely unknown. To make an informed decision on the turbine placement of a new wind farm, the benefits and drawbacks of choosing for a regular or irregular wind farm layouts should be identified. Three aspects should be addressed in light of this problem statement.

First, the performance indicators by which the performance of a wind farm can be quantified are not well-defined in literature. An overview of all the possible performance indicators, and which performance indicators affect the overall performance to what extent is lacking. The degree to which these performance indicators are influenced by the geometry of the wind farm is also not investigated.

Second, the effect of optimised wind farm layouts on all performance indicators are either unknown or only partially investigated in literature. The existing studies which include regular and irregular wind farm layouts focus on the performance of the optimisation tools. The aim of these optimisation studies is not to compare the overall performance between the regular and irregular wind farms.

Third, it should be noted that irregularity is inherent to the used optimisation algorithms. In literature, most optimisation studies result in irregular wind farms [25–28]. This is due to the enormous design space of irregular patterns with many local optima. A particle swarm optimisation (PSO) or genetic algorithm (GA) is therefore unlikely to find a regular pattern. Based on the nature of the optimisation algorithms many optimisation studies are bias toward irregular wind farm layouts.

In existing literature there are no studies dedicated to compare regular and irregular wind farms based on a complete set of performance assessment criteria. A consistent comparative analysis of multiple regular and irregular wind farms has not been conducted. Specifically, objective performance assessment criteria appear to be lacking. Although there are indications that irregular layouts outperform regular layouts with respect to yield, it is yet to be confirmed if irregular layouts indeed provide a better performance overall (e.g. a higher profit).

## 1.4. Research Objective and Research Questions

In this section the boundaries of the research executed in this master thesis project are mapped out. First, the research objective is formulated, from which the research question and sub-questions are derived, which form the basis of this research.

### 1.4.1. Research Objective

To alleviate the problem identified in section 1.3, the following research objective is formulated:

*To quantify the effect of regular and irregular offshore wind farm layouts on selected performance indicators by means of a comparative case study using state-of-the-art simulation tools and models.*

### 1.4.2. Research Questions

From the research objective the main research questions can be derived which give an indication by what means the objective is set out to be achieved. The research questions also provide a guideline to what steps need to be carried out to achieve the objective of this project in a feasible manner. The main research question for this master thesis is formulated as follows:

*To what extent does a regular or irregular geometrical pattern of wind turbines affect the performance of an offshore wind farm?*

In order to answer this research question, an additional set of questions is formulated referred to as sub-questions:

- What performance indicators can be identified to quantify the performance of an offshore wind farm layout?
- What considerations apply when comparing selected performance indicators between regular and irregular layouts?
- What is the difference in performance of selected performance indicators between the case regular and irregular layouts?
- To what extent are the results found to be generally applicable to regular and irregular layouts?
- Is there a possibility to ameliorate the worst performing indicator for the (overall) better wind farm layout?

## 1.5. Methodology and Thesis Outline

The structure of this thesis is outlined in Figure 1.4. In chapter 1, an introduction is presented, followed by a discussion on the state-of-the-art research on the layout of offshore wind farms. This is followed by the research objective and research questions. chapter 2 forms the basis of this research. The performance indicators for offshore wind farms are investigated and the relevant indicators for this research are selected. Then, the input parameters and choice of wind farm layout for the case study are selected. This is followed by chapter 3, chapter 4, and chapter 5 where an analysis of the three selected performance indicators is performed. This is followed by an analysis of the general applicability of the obtained results in chapter 6. In chapter 7, as an addition to the main research, the potential to mitigate negative performance result is explored. Finally, the conclusions from this research and recommendations for further research are presented in chapter 8.

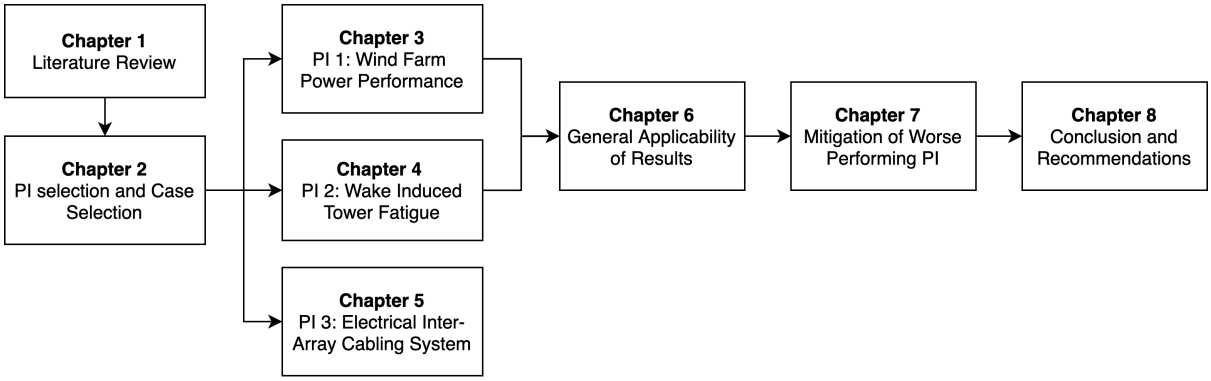


Figure 1.4: Schematic representation of report structure and methodology with corresponding chapter numbers. PI = performance indicator.

The research includes multiple expert interviews to verify findings and develop methods to analyse the performance indicators. The wind farm simulations are performed using readily available tools. Software packages such as Windfarmer [29], WindPRO [30], and OpenWind [9] are designed for wind farm calculations. This master thesis is conducted in collaboration with Ventolines which grants access to WindPRO. Low-fidelity models are developed when these tools are not available or lack in accuracy.

# 2

# Performance Indicator Selection and Case Selection

## 2.1. Introduction

In this section, the basis for the research comparing regular and irregular wind farm layouts is established. An inventory is made of all wind farm performance indicators by which the performance of a wind farm can be quantified. From this inventory, the performance indicators that are used for this research are selected. These steps are performed in section 2.2. Next, in section 2.3 the case regular and irregular wind farm layouts which are used for the comparative case study are selected. This is presented together with background information and their corresponding wind climate, and wind turbine type.

## 2.2. Performance Indicator Selection

To compare the performance between the regular and irregular wind farms, a selection must be made of the performance indicators which will be analysed. As previously found in subsection 1.1.1, there is a lack of well-defined best practices for the performance assessment of a wind farm. An inventory of possible performance indicators is established. Before this inventory and selection can be made, an overarching key performance indicator must be selected.

### 2.2.1. Overarching Key Performance Indicator

The performance of a wind farm can be assessed with a single and overarching key performance indicator (OKPI) according to SETIS - TPWind [31]. This suggested OKPI is the levelised cost of energy (LCOE), which is expressed in Euro per Megawatt-hour [€/MWh].

In a recent study performed by Tao and Finenko [4], it is suggested that the LCOE is no longer suitable as OKPI. For decision making in the power generating industry, using LCOE estimates as a base for achieving grid parity[1] forms an incomplete benchmark [4]. A recent study performed by Nissen and Harfst [32] shows that an investment can be profitable (generating positive net present value (NPV)) while the LCOE is higher than the current grid price for energy. This is caused by neglecting energy price changes. Bertalero et al. [33] therefore suggest to take into account the timely variation of the value of energy. The objective for producing energy in industry is now no longer to produce the cheapest possible power, but to generate the highest value over the lifetime of a renewable power plant, according to Dykes et al. [34].

Therefore, instead of choosing the LCOE as the OKPI, profit is deemed a more suitable candidate. According to Remer and Nieto [35], profit is often evaluated using one of the following techniques: net present value (NPV), internal rate of return (IRR), return on investment (ROI), cost/benefit analysis (CBA) and payback period (PP) methods. In this research the cost/benefit analysis is chosen, dividing the profit in cost and revenue.

[1] Grid parity indicates potential profit. This is achieved when the electricity is generated at the same or lower price than the prevailing energy tariff [4].

### 2.2.2. Performance Indicator Inventory

An overview of all performance indicators affecting the OKPI is established using the study on performance indicators for the operations and maintenance phase of the wind farm lifetime by Gonzalez et al. [36]. The results of this study are re-organised and expanded using the research performed by Shafiee et al. [37], presenting a cost breakdown structure for offshore wind farms over the lifetime. The aim when developing a wind farm is increasing this profit, which is a trade-off between the revenue (related to power production) and cost.

These studies and cost-breakdown structure are used to form the PI tree as shown in Figure 2.1. This AND-tree is assembled consisting of four different levels: overarching key performance indicator (OKPI), key performance indicators (KPI), performance indicators (PI), and sub-performance indicators (SPI). All sub-components together encompass the higher-level entry.

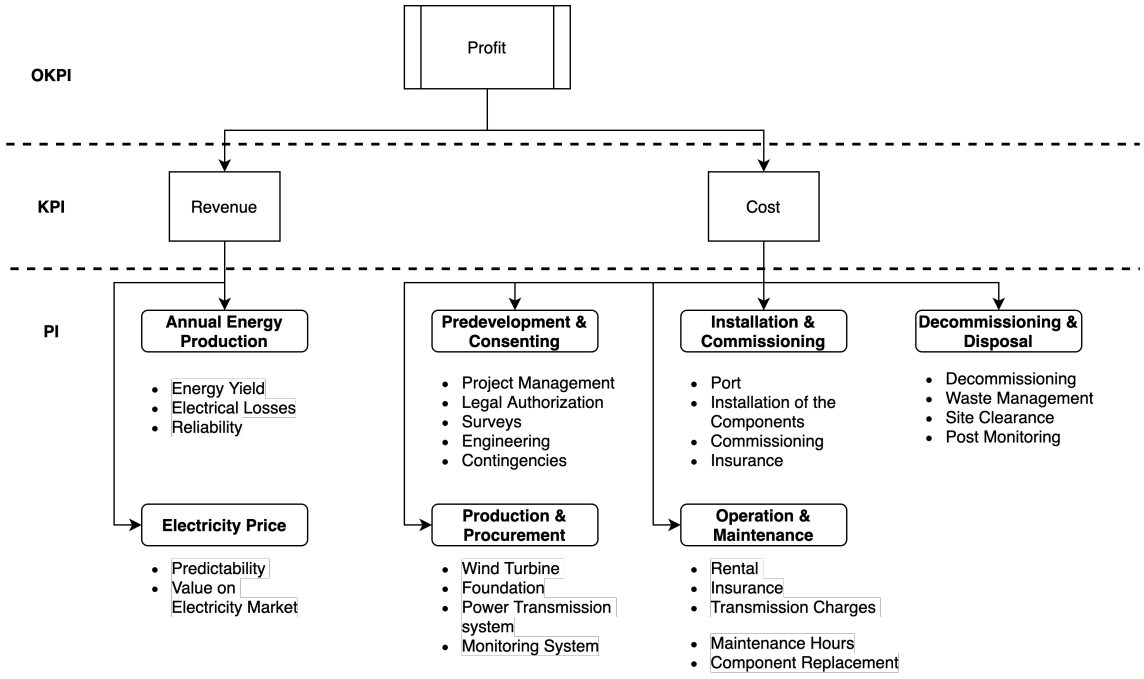


Figure 2.1: Breakdown of Performance Indicators

Some SPI's are very similar or overlapping with SPI's under different PI's, which, in a complex system like an offshore wind farm is inevitable. Insurance is included both in the production & acquisition and installation & commissioning PI's for example. In this case, the SPI is analysed based on its effect on the most relevant PI. Now, to substantiate the decision making, the interpretation of SPI's which are not straightforward in the PI diagram are presented below:

- The SPI **wind turbine** listed under PI production & procurement consists of many different components. For simplicity only the two cost driving components, the tower and rotor blades are considered. These account for 29.4% and 24.9% of the turbine cost respectively [38]. The cost breakdown is presented in a pie chart in Figure 2.2.

  The blades of a wind turbine are designed according to a certain wind class in the IEC standard [39], which is in turn determined by the location of the wind farm as a whole. The location of the turbine in the wind farm do not influence the blade design. The placement of the turbines in the wind farm does affect the turbine tower design. The worst-case turbine in the wind farm determines the tower design according to ir. B. Koppenol [2]. Therefore, only the tower design is considered for the wind turbine SPI.

[2]Technical Project Manager at Ventolines B.V. including turbine package management and support structure design.

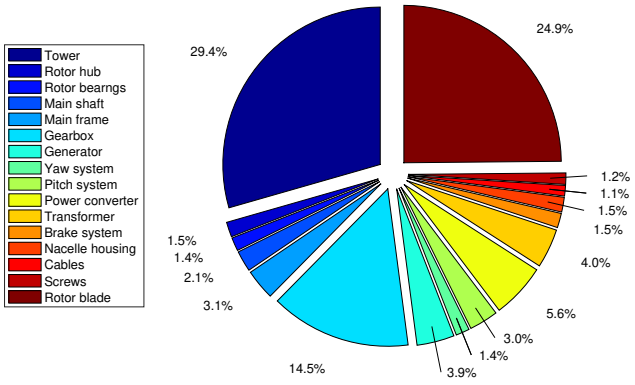


Figure 2.2: Pie chart representing the cost breakdown of wind turbine components according to [38]. The turbine tower and blades show the largest contribution to the total wind turbine cost.

- The **value on the energy market (e-market)** SPI listed under the PI electricity price, refers to the value that wind power has on the electricity market. This varies constantly depending on for example the power production and forecast errors of available wind. In the Netherlands the responsibility of balancing the energy output of the wind farm lies with the program responsible parties [40]. Related power imbalance cost that accompany this are payed by the program responsible parties.
- The **power transmission system** SPI considers the inter-array cabling system of the wind farm only. As the export cable, substation and other components are considered to show marginal differences for the same rated output of the wind farms, with only a change in wind turbine positioning. The same holds for the SPI **electrical losses** which is closely related to the power transmission system.
- For the **foundation** SPI under production & procurement PI, there are different definitions identified in literature. In this research, the structure on which the turbine tower is mounted is considered as the foundation. For offshore wind turbines this can be jacket-pile, monopile, gravity-type, tripod and suction caissons [41]. However, the choice of foundation type and the design is heavily dependent on the site, like water depth, wave conditions and soil conditions.

Elaborating on the ambiguous sub-performance indicators in Figure 2.1 clarifies how each sub-performance indicator is interpreted for the selection phase.

### 2.2.3. Multi-Criteria Decision Analysis

In the next step a decision is made on which sub-performance indicators are the most relevant to investigate in the scope and context of this thesis. A choice is made between quantifiable and non-quantifiable components as well as multiple criteria to assess the results. A suitable approach to this type of problem is the multiple criteria decision analysis (MCDA) [42]. The weighted sum method (WSM) is used for this application. Before scoring the sub-performance indicators and selection of the criteria, the context of the project is specified. The criteria for the MCDA are derived from the research question, it is important that the assessed sub-performance indicators are in order of importance:

- **Affected by layout**, as the research question aims to identify the differences in performance indicators between regular and irregular layout, it is one of the most important criteria and therefore given a weight of 2.
- **Feasible**, the selected SPI must be feasible to quantify within the scope and time frame of the research. This means that sufficient input data and validated models must be available, or reliable models can be developed within the framework of this research. This is crucial to answer the research question and thus given a weight of 2.

- **Site independent**, the aim of this research is to assess the difference between the performance indicators for a regular and irregular wind farm layout, which is only comparable for the same location, wave conditions, wind climate, wind directions etc. However, in order to obtain generally applicable results, the influence of the specific site condition such as soil condition/distance to shore etc. should be excluded from the analysis as much as possible. This criterion is weighed 1.
- **Technical**, many topics around the wind farm layout design are concerned with logistical, environmental, financial aspects etc. This criterion is weighed 0.5.
- **Relevance MSc. degree**, aerodynamics need to be included in the SPI selection as this is the environment of the research, thus given a weight of 0.5.

The sub-performance indicators are assigned a weight, this is done using a scale from one to three. The best alternatives are then calculated using Equation 2.1 [42].

$$A_{WSM} = \sum_{i}^{N} \sum_{j}^{M} a_{ij} w_j \tag{2.1}$$

Here, $A_{WSM}$ is the WSM score of the alternative i, $a_{ij}$ is the weight given to $i^{th}$ alternative corresponding to criteria j, and $w_j$ is the weight given to the $j^{th}$ criterion. N and M are the number of alternatives and criteria respectively. This is then normalised with the maximum obtainable score and multiplied to get a score out of 10.

### 2.2.4. Multi-Criteria Decision Analysis Results

The results for the sub-performance indicators with the highest scores are shown in Table 2.1, which are all selected for further research in this thesis. Scores of the other sub-performance indicators and scores on individual criteria can be found in Appendix A.

Table 2.1: Performance indicator multi-criteria decision analysis result summary.

| PI Group | SPI | Score |
|---|---|---|
| **Power Performance** | Energy Yield | 10.0 |
| | Predictability | 10.0 |
| | Value on e-market | 8.3 |
| **Wake Induced Tower Fatigue** | Wind turbine | 8.9 |
| | Component replacement | 8.9 |
| **Electrical System** | Electrical losses | 8.6 |
| | Power transmission system | 9.7 |

Since the sub-performance indicators are interrelated, groups are formed of the SPI's that can be considered in one analysis.

- **Power Performance** is identified as one performance indicator group. In this PI group, the following SPI's are included: yield/wake losses, predictability, and value on e-market. The AEP is driving for the revenue of the wind farm which is in turn a driving factor for the overarching key performance indicator: profit.

  Persistence of power output for varying wind directions is expected to influence the value of energy on the e-market. Small changes in wind direction can have a large impact on the total power output. In order to optimise the integration of the wind farm with the electrical grid, it is important that the power variability and output can be predicted accurately. Balancing between the generated and demanded power forms a fundamental issue in the control and operation of electrical power systems [43].

- **Wake Induced Tower Fatigue**, the SPI's wind turbine and component replacement cost can be grouped through fatigue loads in a wind farm and tower material consumption. Mikitarenko and

Perelmuter [44] showed that the tower fatigue loading is significantly affected by the wake effects in the wind farm. Assessing the effect of the wind farm layout on the wake added fatigue damage of the tower can potentially increase the initial investment cost of the wind farm, which directly affects the overarching key performance indicator: profit. Logically, the component replacement cost of the tower changes with tower cost changes.

- **Electrical System**, the final group of interest concerns the electrical losses and power transmission system. The cable length is a driving factor of the cost and electrical losses of the inter-array cables. The effect on the cable length and losses of different wind farm layouts is expected to affect both the revenue through the electrical losses, and the cost through the initial investment of inter-array cable and installation cost.

The performance indicator groups are assigned names for future reference in this report. Now that the performance indicator groups are identified, the last step before analysing the performance is to select a regular and irregular wind farm as input to the comparative case study. This is done in section 2.3.

## 2.3. Case Selection

For each of the three identified performance indicator groups, the results for both regular and irregular offshore wind farm patterns need to be investigated. The performance indicator group results are quantified through means of a case study containing both a regular and irregular wind farm. In this section, the wind farm layout, turbine type and wind climate are presented along with other relevant case input data.

### 2.3.1. Case Layout Specifications

In the literature review, an optimisation study was identified performed by Sanchez Perez Moreno [45]. The regular and irregular wind farm are used as input case wind farm layouts. In his study, Sanchez Perez Moreno [45] develops two optimisation approaches: the sequential approach and the multidisciplinary design analysis and optimisation (MDAO) approach.

The sequential design approach is as follows; first, the layout is optimised for the annual energy production (AEP), taking into consideration 12 wind direction sectors with a steady wake-effect to determine local wind speeds. Then, the support structure for every wind turbine is considered. Finally, the infield collection system is optimised after which the levelised cost of energy (LCOE) is calculated. In the sequential design, there is no iteration or feedback between the consequent design steps.

The optimisation procedure for the MDAO approach couples different components and disciplines represented by computational tools in a workflow to simulate the entire system. Additional information on the MDAO workflow can be found in Appendix B. Since the MDAO approach is not commonly used in industry, the sequential design is selected as the baseline case design.

The selected reference site on which the research is performed is Borssele III and IV. This wind farm consists of 74 turbines [46], located near the border between the Netherlands and Belgium, in the Southern part of the Dutch North Sea. This reference wind plant was selected by Sanchez Perez Moreno [45] due to the readily available data, such as: wind climate, soil conditions, water depth etc, and is also utilized in this research. The resulting layouts are shown in Figure 2.3 below.

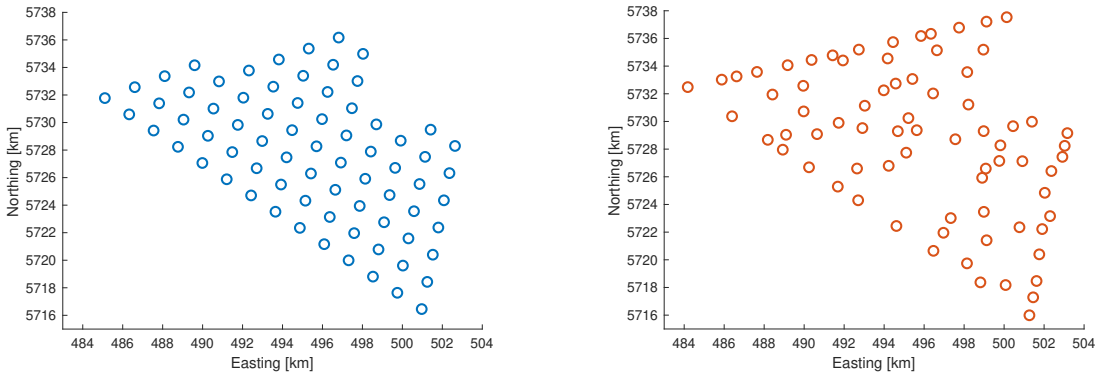


(a) Regular (b) Irregular

Figure 2.3: Regular and irregular layout from Sanchez Perez Moreno [45] consisting of 74 turbines with a rated power of 10 MW at Borssele.

To obtain a rough feeling for the measure of irregularity, the sum of the distance to a selection of the surrounding turbines is computed for each turbine in the wind farms. If the number of turbines with a unique value of this sum is high, this indicates an irregular wind turbine pattern. The embedded turbines of the regular wind farm are expected to have identical values for the sum of the distance to surrounding turbines.

Looking more closely at the spacing in Figure 2.3, some initial observations are quantified. First, for each turbine in the wind farm, the sum of the distances to each surrounding turbine in a 10 rotor diameter (10 RD) radius is computed. Second, it is observed that the minimum distance between two turbines is smaller for the irregular wind farm. The results are presented in Table 2.2.

Table 2.2: Number of turbines with the same unique sum of distances to surrounding turbines with a tolerance of 0.001 RD ($N_{turb}$), and the minimum inter-turbine spacing ($x_{min}$).

| | $\mathbf{N_{turb}}$ ($\sum d_i$) [-] | $\mathbf{x_{min}}$ [RD] |
|---|---|---|
| **Regular** | 66 | 8.88 |
| **Irregular** | 5 | 2.73 |

In the regular wind farm, there are 5 unique values for this sum, where in the irregular wind farm there are 66 unique values. More sophisticated methods to determine the measure of regularity exist, but this method serves as an initial indication which is deemed sufficient for the purpose of this research.

For the irregular wind farm, it can be observed that the turbine density at some edges of the wind farm is higher than the regular wind farm. As described in the work of Guirguis et al. [47], wind farm area edges attract wind turbines which have lower efficiency when placed inside the wind farm. This increase in turbine density at the edges of the wind farm cause a lower (average) spacing between the turbines.

### 2.3.2. Wind Climate

The meteorological data is obtained from Wind and Zone [48]. The data set consists of hourly mean wind speeds at 10 m height in m/s and corresponding wind directions in degrees. The data stems from HARMONIE, which is a numerical weather prediction (NWP) model used by the Royal Netherlands Meteorological Institute (KNMI). The measurements cover the period from 1979 until 2013, at a measurement point 3.02°E 51.70°N. When a measurement period of at least six months is available, and the long- and short-term wind direction distribution is similar, the measurements can be assumed to represent long-term turbulence conditions [39]. The measurement period of the Borssele turbulence data is gathered over a time period of approximately 3.3 years [48], which conforms to this IEC requirement.

The hub-height data is required to analyse the performance of the wind farm as this resembles the incoming flow to the rotor disk. To extrapolate the data to hub-height, the power-law profile is found to be the most suitable method according to the study performed in Wind and Zone [48]. The suggested power exponent for this extrapolation is $\alpha$ = 0.08.

The wind rose can then be obtained at hub-height for further analysis of the wind climate. For this the wind direction distribution is divided into 12 sectors of each 30°. For each wind direction bin, the probability of that wind direction occurring, Weibull distribution, and mean wind speed are calculated. The visualisation of this wind rose is shown in Figure 2.4, where the wind speeds in the wind direction bin are divided into five wind speed bins.

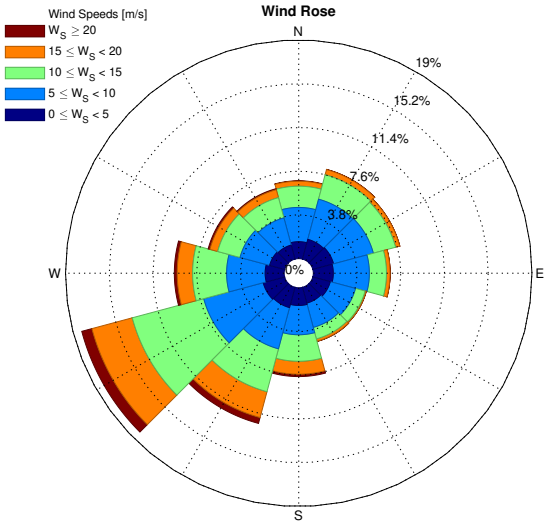


Figure 2.4: Wind rose obtained from Borssele IV data set provided by Wind and Zone [48], extrapolated to hub-height with power-law exponent 0.08.

It can clearly be observed that the prevailing wind is from the southwest direction (sector 9). The wind speed bin containing wind speeds above 20 m/s is larger than the other sectors, indicating this wind speed occurs more frequently in this wind direction sector. The corresponding values are presented in Appendix C. The omni-directional mean wind speed is 9.5 m/s with a shape and scale parameter of 10.7 and 2.1 respectively. The obtained results are verified with the 100 m height Weibull parameters presented in Wind and Zone [48].

### 2.3.3. Wind Turbine Specification

The optimisation performed by Sanchez Perez Moreno [45] is based on the IEA Wind Task 37 reference wind turbine with 10 MW rated power [49]. This turbine will from now on be referred to as the IEW Wind turbine. The turbine specifications are presented in Table 2.3 below.

Table 2.3: Key parameters of the 10 MW IEA Wind Task 37 reference wind turbine [45]

| Parameter | 10 MW Turbine | Unit |
|---|---|---|
| Wind regime | IEC class IA | [-] |
| Rated power | 10 | [MW] |
| Rated wind speed | 11.4 | [m/s] |
| Rotor diameter | 190.8 | [m] |
| Hub-height | 119 | [m] |
| Cut-in wind speed | 4 | [m/s] |
| Cut-out wind speed | 25 | [m/s] |

Identical parameters as the report of Sanchez Perez Moreno [45] are chosen to adhere to the optimisation input parameters. The thrust coefficient and power curve of the IEA Wind turbine are shown in Figure 2.5.

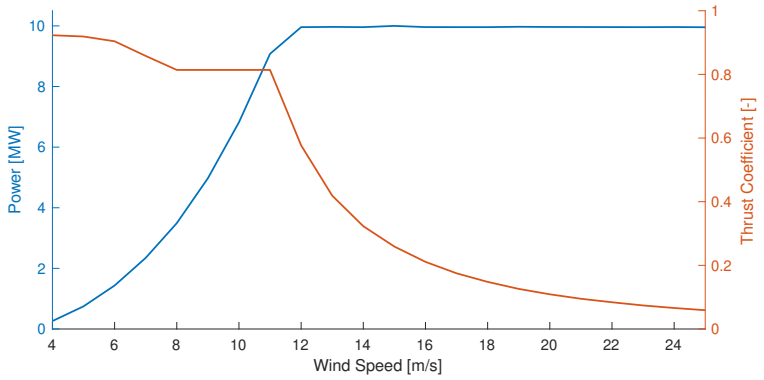


Figure 2.5: The thrust coefficient and power curve of the IEA Wind turbine used in the optimisation algorithm developed by Sanchez Perez Moreno [45].

In this report these input parameters are used unless otherwise stated.

## 2.4. Conclusion

An overview of performance indicators (PI) is developed with the overarching key performance indicator profit. Profit is divided into cost and revenue, which in turn can be divided in several performance and sub-performance indicators. Implementing a multi-criteria decision analysis method, three performance indicator groups are selected: power performance, wake induced tower fatigue, and the electrical system. The selection of sub-performance indicators in the PI groups is based on a set of 5 criteria: affected by layout, feasible, site-independent, technical, and relevant to the MSc. degree. The comparative study between regular and irregular layouts will be performed by analysis of the PI groups on two pre-defined layouts with 74 turbines of 10MW each, based on the conditions at Borssele III and IV.

# 3

# Performance Indicator 1: Power Performance

## 3.1. Introduction

In this chapter, the performance indicator (PI) group called 'power performance' is analysed. This PI group includes the following sub-performance indicators: energy yield, predictability, and value on the electricity market. Here, the performance indicator results are quantified for the regular and irregular wind farm layout presented in the case selection. As schematically presented in Figure 3.1, the relation between the layout and profit is investigated with the annual energy production (AEP) and persistence to wind direction. The velocity deficit in the wake causes a reduction in the power output of the wind farm depending on the orientation of the wake. This has effect on the annual energy production and the variability of the power output as a function of wind direction.

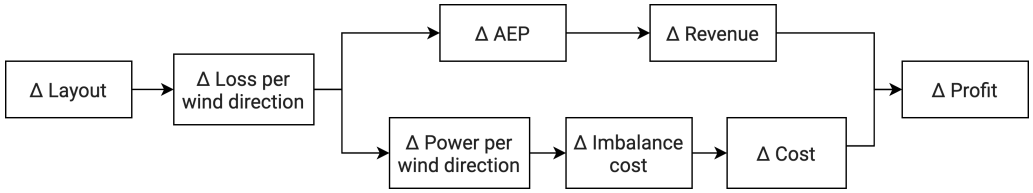


Figure 3.1: Schematic representation of layout, power production, and cost & profit relation

These two aspects will be analysed separately in the following sections.

## 3.2. Annual Energy Production

Previously, in section 1.2, it was found that most wind farm layout optimisation algorithms focus on the maximisation of energy output [25, 26, 50–53]. The aim of this section is to quantify the influence of the regular or irregular wind farm layout on the AEP. The AEP is an estimate of the energy production of a wind farm during a one-year period[1], assuming 100 % availability of the turbines [54]. The annual energy production is calculated with Equation 3.1.

$$AEP = T \int_{0}^{2\pi} \int_{U_{cut-in}}^{U_{cut-out}} P(U) f(U,\theta) d\theta dU \tag{3.1}$$

The annual energy production is often measured in megawatt hours. This can be obtained when the power curve and the frequency of wind speed distributions is known for a specific location. In Equation 3.1, T is the number of hours in a year, P is the power curve of the specific wind turbine, f is the wind speed frequency distribution, U represents the operational wind speeds, and $\theta$ represents the wind speed directions.

[1]The transmission losses stemming from the electrical inter-array cabling system are excluded from this analysis.

A difference in AEP for the regular and irregular wind farm is expected, as the placement of the turbines in the wind farm combined with the wind rose will determine the orientation of the wakes in the wind farm. The wind farm will generate more energy when the wake losses are minimised.

### 3.2.1. Annual Energy Production in WindPRO

A readily available software tool to estimate the AEP is WindPRO. The PARK model in WindPRO with wind statistics based calculations with MEASURE model is designed to estimate the annual energy production [30]. WindPRO PARK calculations are commonly applied as the basis for the business case and financing of offshore wind parks. Investment banks trust WindPRO as a wind farm modelling tool to create wind energy assessment for determining the wind farm finance [55].

First, the wind distribution at each wind turbine generator (WTG) position is determined based on wind measurement data imported by the user. The wind measurements in this research are imported in the form of Weibull-parameters for each wind direction sector.

Then, the wind distribution from this previous step is adjusted to account for the array losses using the PARK model. The PARK model is the most popular approach to predict the wake deficit behind a wind turbine and wake losses in a wind farm [56]. Inputs for the PARK module like the wind climate and the wind farm layout are known as well as the performance curves of the WTG model [57]. Also, as part of the PARK model, the wake-decay constant for the N.O. Jensen wake model is selected. The default value for the wake-decay constant (WDC) of 0.04 is selected. This wake decay constant determines the rate of expansion behind the turbine. A lower expansion means a higher wake deficit behind the rotor meaning the wake losses are larger. A wake decay coefficient of 0.04 is recommended both by Barthelmie et al. [58] and in the EMD WindPRO manual [30] for offshore wind farms.

Finally, for the energy yield calculation, the adjusted wind distribution resulting from the PARK module is integrated with the performance curves of the WTG. Importing the IEA Wind turbine, wind rose, and setting up the PARK model with a WDC of 0.04, the AEP of each individual turbine in the wind farm is computed. With this individual AEP of the turbines, two analyses are performed:

- The total AEP of the wind farm is calculated by summation of the individual turbine results. The wake loss percentage and an estimate of the corresponding revenue from the AEP are computed.
- The individual AEP results from WindPRO can also be used to compare the performance of the wind turbines in both wind farms. First, the best and worst performing turbines are compared within the wind farm. This can be established by arranging the AEP results per turbine from high-performance to low-performance, which visualises the difference in annual energy production obtained for the entire wind farm. Second, the position of the turbines is identified by generating a colour scheme for the turbine AEP results. This visualises at what positions within the wind farm the high-performance and low-performance turbines are located.

The analysis of the total wind farm AEP and the AEP of the individual turbines in the wind farm are elaborated upon in the following sections.

### 3.2.2. Annual Energy Production Analysis Borssele

The farm layout, wind conditions and turbine specifications established in section 2.3 are imported to WindPRO. The total annual energy production of the regular and irregular layouts is then computed for all 74 turbines within the Borssele case wind farm using the PARK model described in subsection 3.2.1. Both wind farm layouts are subjected to the exact same input parameters which resemble the Borssele wind farm site. The PARK result is shown in Table 3.1 below in the first two columns.

Table 3.1: Regular and irregular annual energy production with real Weibull distribution and IEA Wind turbine results from WindPRO.

| | **AEP [GWh/y]** | **Wake Loss [%]** | **Revenue [$10^3$ €]** |
|---|---|---|---|
| **Regular** | 3138.7 | 8.1 | 144 802 |
| **Irregular** | 3159.5 | 7.5 | 145 501 |
| **Difference** | + 0.66 % | - 7.41 % | 700 |

The total AEP of the irregular wind farm is higher (0.66%) than the regular AEP. This difference is 15.6 GWh/year. Looking at the European Power Exchange (EPEX) history in the Netherlands between 2007 and 2020, the price per MWh was on average €44.90 obtained in collaboration with ir. Michel Tellman [2]. The total increase in revenue per year is then approximately €700 000. Today's value of this increase in revenue over the lifetime of the wind turbine is estimated using Equation 3.2.

$$NPV = \sum_{t=1}^{n} \frac{R_t}{(1+i)^t} \tag{3.2}$$

In which $R_t$ is the net cash inflow during a 1-year period, i is the discount rate, n is the lifetime of the wind farm in years, and t loops over the n years. With a discount rate of 5 % and lifetime of 25 years, the net present value of the added AEP revenue is approximately 10 million Euros. This additional step is presented to emphasise the effect of the AEP on the profit of the wind farm. A seemingly small increase in AEP results in a significant increase of overall wind farm profit.

The regular wind farm produces 94% of its potential power, and the irregular wind farm produces 94.5% of this power. This is in line with the objective of Sanchez Perez Moreno [45] to increase the power production by decreasing the power losses due to wake effects. The relative results are verified with the research of Sanchez Perez Moreno [45]. The percentage difference between the irregular wind farms (Base and MDAO) from his research are known and utilised to compute the expected total AEP of the MDAO irregular wind farm. The difference between the AEP computed with the percentages from Sanchez Perez Moreno [45], and the AEP obtained with WindPRO is 0.0096%. This research project focuses on the difference between the regular and irregular wind farm layout which means that this relative verification is sufficient.

### 3.2.3. Individual Turbine AEP Performance

To investigate the source of this difference in energy yield between the two case wind farms, the individual turbine behaviour is investigated. The individual turbine energy yield depends on its position in the wind farm. The AEP of the individual turbines are arranged from high-performance to low-performance for both the regular and irregular wind farm as shown in Figure 3.2.

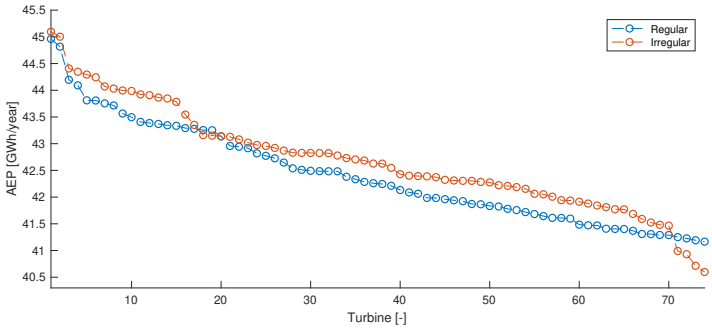


Figure 3.2: Individual turbine annual energy production for the regular and irregular wind farm layout arranged from high-performance to low-performance.

The turbines with the lowest performance in the irregular wind farm show a lower AEP than the turbines with the lowest performance in the regular wind farm. The increase in AEP of the overall wind farm can therefore not be attributed to the outliers. The best- and worst-performing turbine of the regular and irregular layout are identified with their corresponding yield as shown in Table 3.2.

[2]Head of power purchase agreements at Ventolines B.V., has experience on both sides of the energy trade formerly taking the position as Head of Structuring and Origination at Eneco Energy Trade.

Table 3.2: Comparison of the difference between the worst (-) and best (-) performing turbines in the regular and irregular wind farm.

| | **Turbine AEP [GWh/year]** | |
|---|---|---|
| | (-) | (+) |
| **Regular** | 41.2 | 44.9 |
| **Irregular** | 40.6 | 45.1 |
| **Difference** | - 1.4 % | + 0.3 % |

The worst-performing turbine in the irregular wind farm produces 1.4 % less energy compared to the worst-performing turbine in the regular wind farm. For the best-performing turbine, the opposite is observed. The best-performing turbine in the irregular wind farm performs 0.3 % better than the best-performing turbine in the regular wind farm. The difference in AEP for the outliers in Figure 3.2 show why these are not the cause for the higher performance of the irregular wind farm. If only the four best- and worst-performing turbines are taken from both wind farms, the regular wind farm would outperform the irregular layout with 2.39 GWh per year. From this it can be concluded that the optimisation program sacrifices the energy yield of certain turbines in the wind farm for an overall higher total energy yield. The relatively small but constant higher performance of the irregular wind farm turbines results in the final higher AEP of 15.6 GWh per year as previously found.

The position of the turbines in the wind farm based on their performance is identified in Figure 3.3. The four best- and worst- performing turbines are emphasised with dark-green and black lines.

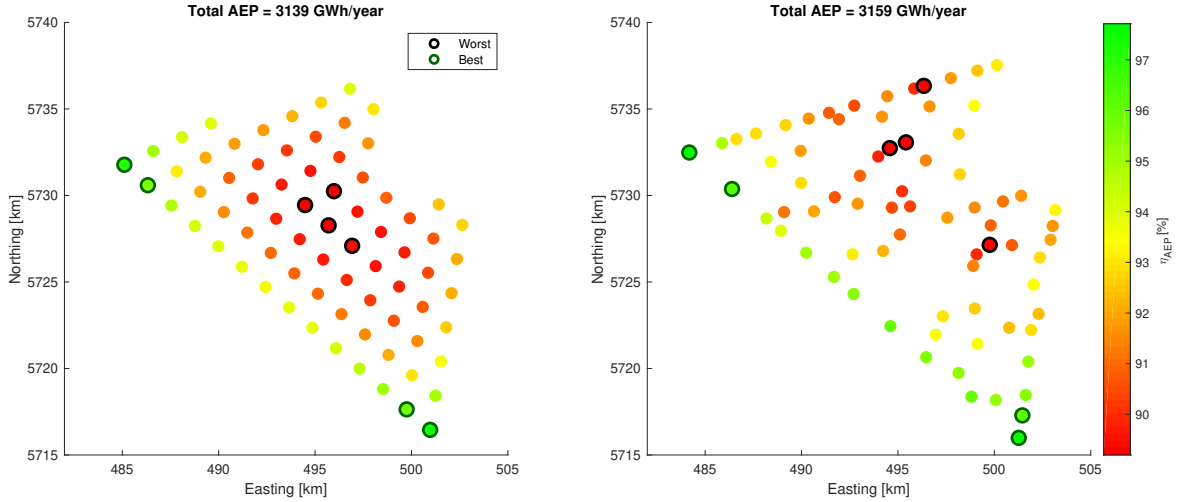


Figure 3.3: Individual turbines of the regular and irregular wind farm layout coloured from red to green based on their performance. The four best- and worst- performing turbines are encircled.

A clear difference in the distribution of performance between the regular and irregular wind farm can be observed. On the left, in the regular layout, a clear distinction can be made in performance based on the location of the turbines within the wind farm.

The regular wind farm shows a 'smooth' distribution of performance in the wind farm. A gradual change from green to orange to red is observed moving along the prevailing wind direction (south-west-west). Looking at the best-performing turbines, it can be observed that for most wind directions these turbines will experience an undisturbed incoming wind speed. For the worst-performing turbines, the opposite can be said. No matter the wind direction, these turbines will always be subjected to wakes of their neighboring turbines.

In the irregular wind farm, a smooth distribution in performance (as observed for the regular wind farm) is not observed. The high-performance of the turbines on the south-west border looks similar to the regular turbines as this edge faces the prevailing wind direction. The turbines embedded in the wind farm show larger variation to their neighboring turbines than the regular wind farm. Two factors

cause the lower performance of the worst-performing turbines. First, the turbines are located on the lee side of their neighboring turbine for the prevailing wind direction. This means that these turbines will experience a velocity deficit caused by their upstream neighboring turbine. With the prevailing wind direction causing this situation, the effect is greater than for other wind directions. Second, the spacing to their neighbor affects the performance. The inter-turbine spacing between the worst-performing turbines and their neighbor is small. The low performance of these turbines is caused by a combination of these two factors.

The results of the sub-performance indicator 'energy yield' are in favour of the irregular wind farm. The overall wind farm AEP of the irregular wind farm is 0.66% higher than the regular wind farm. This is caused by the relatively small but constant higher performance of the irregular wind farm turbines. Noteworthy is that the worst-performing turbines in the irregular wind farm actually have a lower individual turbine AEP than the worst-performing in the regular wind farm.

## 3.3. Persistence to Wind Direction

In this section, two sub-performance indicators: predictability and value on the electricity market, are investigated. The persistence to wind direction of the regular and irregular wind farm is assessed. The aim of exploring this performance indicator is to establish the relation between the layout, change in wind direction, associated (power) losses, imbalance cost, and hence profit as shown in the lower branch of Figure 3.1.

The power in a wind farm can vary with time depending on the variability of wind speed [43], but also with changing wind directions [59]. Forecasting wind power production is a challenging task due to this variable nature of wind speed and direction. Research is performed to develop tools which can accurately predict the day-ahead power production of wind farms [60]. The electricity market, in a nutshell, is driven by supply and demand. The day-ahead market is settled at the most cost-effective way based on supply and demand bidding. Producers that have wind energy or another variable energy source in their generation mix need to be able to forecast their day ahead production to substantiate their bids [60]. When a wind farm yields more energy than predicted, this leads to a supply of more energy than the bid [61]. If this is not corrected by the producer, this will lead to imbalance costs. Imbalance costs decrease the net income for the producer. The balancing cost for a study performed on prediction errors and balancing costs in Finland is estimated at 0.7 € per MWh which is calculated per MWh of the total energy production.

Choosing a wind farm layout which potentially has higher persistence to changes in wind direction increases the predictability of the wind farm production according to Othman et al. [62]. Power production as a function of wind direction can be seen as a metric to assess the wind farm's ability to maintain its performance of power production with changing wind direction [63], and would reduce the risk of relatively sudden, significant changes in output due to modest changes in wind direction. If the predictability of the wind farm power production increases, the imbalance cost is therefore expected to decrease. In the following section, the power output as a function of wind direction is analysed for the regular and irregular wind farm layout.

### 3.3.1. Omni-directional Power Calculations in WindPRO

The PARK module in WindPRO can be utilised to assess the power output of the wind farm at different wind directions. For this analysis, the time-series based on measurements PARK module[3] is chosen instead of the wind statistics based PARK with MEASURE model used for the AEP calculations. The power is sampled for all wind directions, with steps of 1°. On both wind farm layouts, the same wind rose is placed with a uniform wind direction distribution and mean wind speed found from the Borssele wind climate data.

At the mean wind speed at Borssele of 9.5 m/s, the wake losses play a significant role in the power output of the wind farm. When a significantly higher wind speed is chosen (+ 15 m/s) the wake losses would decrease significantly and might even disappear completely. At higher wind speeds, the deficit

[3] In this module of WindPRO, a more detailed wake decay factor can be implemented. For this, a 35% linear weight and 65% RSS (Root Sum Square) weight is chosen. In the original N.O. Jensen wake model, multiple wakes are summarised using the RSS method. An alternative method is to use the linear method to summarise the deficits. For large wind farms, the RSS method is found to underestimate the velocity deficit, where the linear method overestimates it far too much. Therefore, it is recommended in the EMD WindPRO manual [30] to use a combination of the two methods with a 35% linear weight and 65% RSS (Root Sum Square) weight.

velocity in the wake still results in rated power, meaning the turbine downstream still produces the maximum power regardless of whether it is located in the wake or not.

### 3.3.2. Persistence to Wind Direction Assessment Borssele

The procedure described above is implemented in WindPRO with a mean wind speed of 9.5 m/s. The obtained power results are then post-processed to form a multi-directional power curve with constant wind speed to visualise the difference in power output as presented in Figure 3.4.

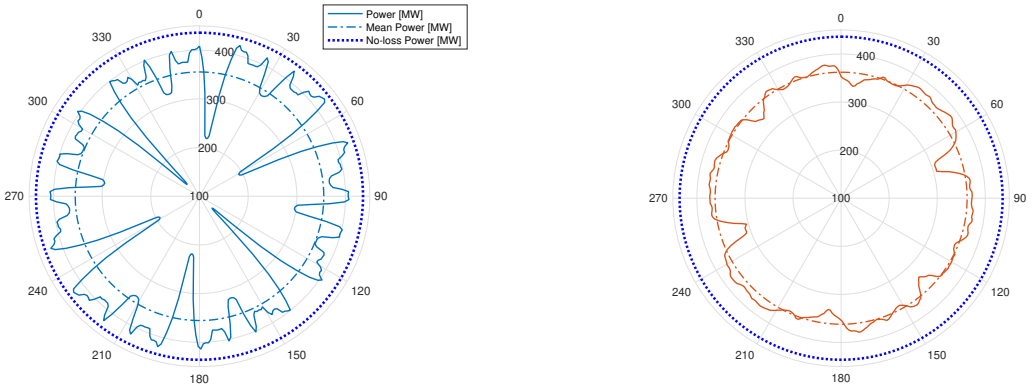


(a) Regular (b) Irregular

Figure 3.4: Power output of the regular and irregular wind farm subjected to a mean wind speed of 9.5 m/s in steps of 1°.

In Figure 3.4, the power production per wind direction is represented by the continuous blue and red lines for the regular and irregular wind farm respectively. The disrupted coloured lines indicate the mean power production over all wind directions and the navy blue disrupted lines represent the no-loss power production.

The regular wind farm layout has significantly higher changes in power output as a function of wind direction than the irregular wind farm layout. Not only the magnitude of the power drop varies, but also the amount of wind directions at which this occurs is higher for the regular wind farm. Both this magnitude and the wind direction at which they occur can be related to the regular wind farm layout. The wind direction at which the wind farm power deficits are expected are indicated with arrows in Figure 3.5.

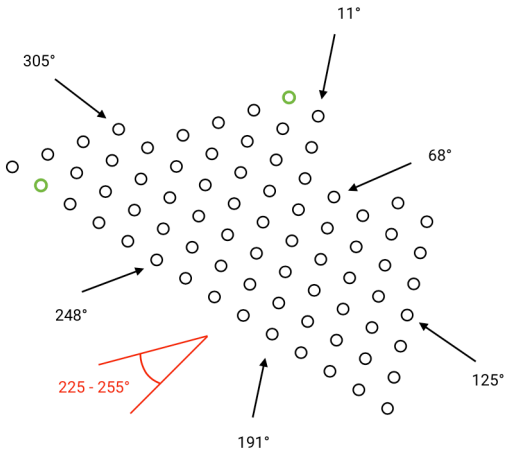


Figure 3.5: Visualisation of inflow angles with low power production for regular wind farm. The prevailing wind direction sector is indicated in red.

The visualisation in Figure 3.5 in combination with Figure 3.4 show a relation between the wind direction and wind turbine positioning. The low power performance in the regular layout is directly related to the alignment of the wind direction with the wind turbine rows. For the regular layout, these rows are clearly visible at the indicated angles. A distinction can be made between the magnitudes of the power deficit

in the regular layout. This can be related to the number of wind turbines positioned in each row. For a higher number of turbines the power deficit increases in magnitude as more turbines experience a full wake and thus generate less power. Turbines arranged in large arrays are also known to restrict the wake recovery. This is referred to as the deep-array effect [17]. The large arrays change the flow of air in the atmosphere above the wind farm. This decreases the exchange of momentum from this air stream which decrease the wake recovery. The negative effect of this alignment of wind turbines in rows is thus increased by the deep-array effect.

For the irregular wind farm, the magnitude of the power drops is significantly smaller compared to the irregular wind farm. The relation between the wind turbine rows and power deficit is not as apparent as it is for the regular wind farm. With a denser turbine population near the edges of the wind farm (Figure 3.6), alignment with these edges does lead to a relatively small power deficit compared to the regular wind farm.

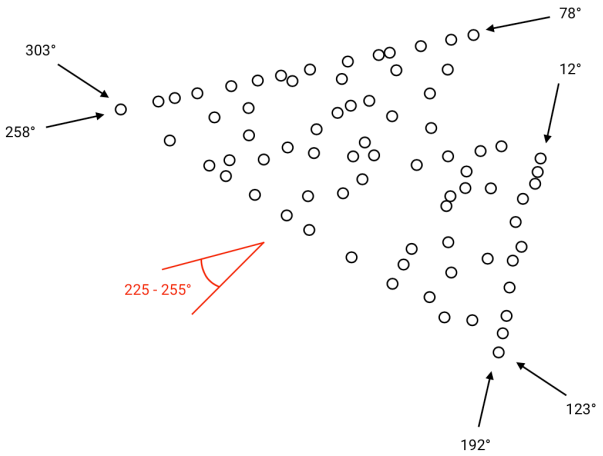


Figure 3.6: Visualisation of inflow angles with low power production for irregular wind farm. The prevailing wind direction sector is indicated in red.

The highest wind farm power deficit is expected when the wind direction aligns with the turbine rows on the north-side of the wind farm. The turbines in this row are closely spaced and mostly oriented along the same row. Zooming in on the wind directions with the highest change in power output for both the regular and irregular wind farm results in Figure 3.7.

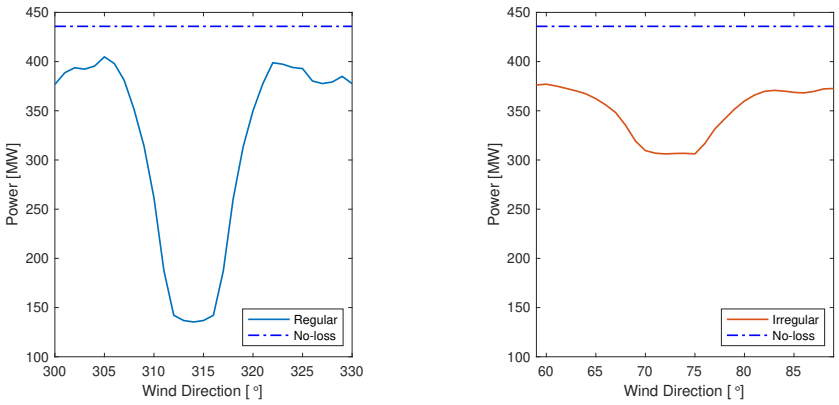


(a) Regular (b) Irregular

Figure 3.7: Power output as a function of wind direction for the regular and irregular wind farms subjected to a wind speed of 9.5 m/s, zoomed in on the wind directions with the highest power drops.

The difference in magnitude is clearly visible between the regular and irregular power. The change in wind direction over which the power deficit occurs is approximately the same for both wind farm

layouts. The power in the regular wind farm between 300° and 330° drops from approximately 405 MW to 135 MW, equal to a decrease of approximately 66.6 %. This wind farm power deficit occurs over a wind direction change of approximately 7°. The power in the irregular wind farm between 60° and 90° drops from 377 MW to 306 MW, equal to a decrease of approximately 18.8 %. This change occurs over a wind direction change of approximately 8°. The difference in maximum wind farm power deficit, imbalance cost for a prediction error of 7°, and the standard deviation of the power as a function of wind direction, are presented in Table 3.3.

Table 3.3: Maximum wind farm power deficit, corresponding imbalance cost, and standard deviation of the power as a function of wind direction.

| | Max. $P_{drop}$ [MW] | $\sigma$ P [MW] |
|---|---|---|
| **Regular** | 269.5 | 67.6 |
| **Irregular** | 70.9 | 16.6 |
| **Difference** | - 73.7 % | - 75.5 % |

From Table 3.3 it can be observed that this irregular layout performs better than the regular layout. The maximum difference in power deficit over a wind sector bin is approximately 73.7% lower than that found in the regular wind farm. The standard deviation as a function of wind direction is approximately 75.5% lower than the regular wind farm. The low standard deviation of the irregular wind farm indicates that the multi-directional power curve in Figure 3.7b is closely spaced around the mean. For the regular wind farm this is not the case as the multi-directional power curve fluctuates more significantly as a function of wind direction. Furthermore, the prevailing wind direction of Borssele site is found to be from 225° to 255° which includes the large power drop around 240° in the regular wind farm. This high probability increases the negative effect of the regular wind farm even further.

It should be noted that this analysis is not performed as a function of time. The effect of this time variation is explained using the regular wind farm. In Figure 3.5, two turbines are indicated in green. If the wind direction is set to 248°, the turbine on the left will feel the change in wind speed earlier than the turbine at the end of the row (right). With a wind speed of 9.5 m/s and the distance between these turbines estimated at 12 km, this delay would be approximately 21 minutes. This effect is expected to smooth out the power output curves in Figure 3.4.

### 3.3.3. Value on the Electricity Market

An expert interview with ir. M. Tellman [4] was conducted to explore the possibility of relating the persistence to wind direction with the revenue. Quantifying this relation is deemed too ambitious for the scope of this thesis, due to the high complexity and uncertainty of the electricity market. Although quantification is not feasible in this research scope, a positive effect of the higher persistence to wind direction of the irregular wind farm is expected[4] for the revenue of the wind farm. The more stable power behaviour of the irregular wind farm as a function of wind direction is expected to result in lower uncertainties with predicting power output.

In an attempt to indicate the degree to which the imbalance cost affects the revenue, the wind climate data and an indicative price for the imbalance cost based on history is used. A visualisation of the wind direction over a period of 24 hours is presented in Figure 3.8.

The first five hours of this 24-hour time period in the Borssele wind climate data set show a change in wind direction of approximately 68 °. The average slope of this decrease is 11.3 °per hour. An even more significant change is observed from 7 ° to 8 °, with a wind direction change of 38° per hour. Such changes in wind direction could result in higher prediction errors. According to Obersteiner et al. [61], the prediction errors for flat terrain 12-hour forecasting ranges between 9 to 12 %.

The relation between this predictability of the power output and the imbalance cost is not quantified in this research. However, using historical data from a research conducted on wind farms in Finland, an indication of the magnitude of the imbalance cost can be obtained. Assuming an imbalance cost of approximately 0.7 € per MWh as indicated by Holttinen [60], this would lead to approximately 2.2 million Euros per year. The total revenue of the AEP (excluding the imbalance costs) based on the average

[4]Head of power purchase agreements at Ventolines B.V., M. Tellman has experience on both sides of the energy trade formerly taking the position as Head of Structuring and Origination at Eneco Energy Trade.

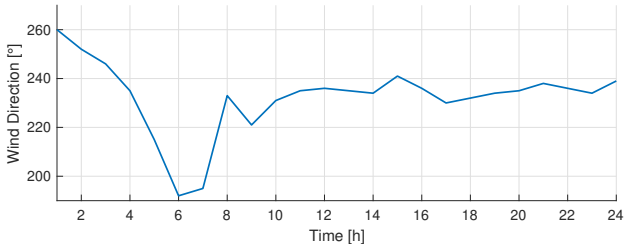


Figure 3.8: Wind direction for a time period of 24 hours obtained from Borssele wind climate data [48].

price per MWh in the Netherlands between 2007 and 2020, is approximately 141 million Euros per year. The imbalance cost would then amount to approximately 1.6% of the AEP revenue of one year. In this 1.6 % the difference between the regular and irregular wind farm layout could cause a change.

The sub-performance indicators predictability and value on the electricity market are thus both found to perform better for the irregular wind farm in this analysis. Note that the analysis is only performed at a mean wind speed of 9.5 m/s. Furthermore, the relation between the imbalance cost and power output of the wind farm is not as simple as portrayed in the estimation of this section. It greatly varies between different studies and between wind farms in industry.

## 3.4. Conclusion

From the annual energy production analysis executed in WindPRO, the absolute difference between the regular and irregular wind farm energy yield is analysed. This shows a higher AEP of approximately 0.66% for the irregular wind farm layout, corresponding to approximately €700 000 according to the average EPEX price in the Netherlands between 2007 and 2020. The individual turbine performance shows that the difference in AEP is not caused by the outliers (best-performing and worst-performing turbines) but by the average performing turbines in the wind farm. Relating the performance and positions shows that the distribution of the lower performing turbines is more evenly spread for the regular wind farm than for the irregular wind farm.

Estimating the difference in persistence to wind direction for both wind farm layouts results in a significant difference. The maximum power drop decreases with 73.7 % for the irregular wind farm compared to the regular wind farm layout. The turbine rows in the wind farm with regular layout are driving for the angle at which the power drops occur as well as their magnitude. A higher number of turbines in a turbine row correspond to a larger power drop. This effect might worsen even more due to deep-array effects. It is expected that a wind farm layout with a higher persistence to wind direction will lead to a decrease in prediction errors. This is likely to result in lower imbalance costs. A rough estimation based on historical imbalance cost data shows that the imbalance cost would amount to approximately 1.6 % of the AEP revenue. The difference between the imbalance cost of the regular and irregular wind farm would then become visible within this 1.6 %.

It should be noted that the analysis for persistence to wind direction is executed using a mean constant wind speed of 9.5 m/s. This simplification likely overestimates the power drops as a function of wind direction, as the time-dependent change of wake losses in the wind farm is not considered. Also, the wind speed is below rated power, which means that the wake losses here play a significant role. For higher wind speeds (+ 15 m/s) the effect of wake losses diminish or even disappear completely. The difference between the regular and irregular wind farm layout at these wind speeds would thus decrease significantly or even goes to zero.

Based on the analysis and assumptions in this section, the irregular wind farm layout performs better for all three sub-performance indicators analysed: the energy yield, predictability, and value on the electricity market.

# 4

# Performance Indicator 2: Wake Induced Tower Fatigue

## 4.1. Introduction

In this chapter, the performance indicator (PI) group called 'wake induced tower fatigue' is analysed. This PI group includes the following sub-performance indicators: wind turbine, and component replacement. As discussed in subsection 2.2.2, only the tower design is considered for these sub-performance indicators[1].

The positioning of wind turbines inside a wind farm and the wind climate indicate the amount of wake effects the downstream turbines will experience. Especially in offshore conditions these wake effects are driving for the wind turbine fatigue loading [64]. With low terrain roughness and low ambient turbulence intensities, the effects of these wakes is higher than onshore wind farms. Multiple studies performed confirm that one of the fundamental parameters which determine the wall thickness of the tower design is fatigue [64–67].

Assuming the fatigue is indeed the determining factor for the tower wall thickness, in this chapter, the relation between the wind farm layout and fatigue loads is investigated with respect to the overarching key performance indicator: profit. The schematic representation of this relation is presented in Figure 4.1 below.

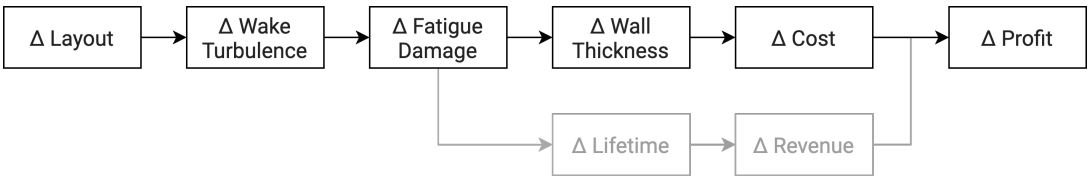


Figure 4.1: Schematic overview of the layout, fatigue loads, and added material cost

Figure 4.1 starts with the wind farm layout, the positioning of turbines within a wind farm determines the amount of wake effects on downstream turbines. The higher turbulence intensity in the wake causes increased fatigue loads on the wind turbine structures. Increased fatigue loads in turn cause higher fatigue damage. From this point there are two possibilities:

- Designing for a set lifetime aiming for minimal material consumption
- Designing for the expected fatigue loads with the aim to maximise the lifetime of the turbine

Both the wind turbine design & manufacturing company and wind farm developer may be interested in considering both objectives. Offshore wind turbines are often designed for a lifespan of 25 years. A turbine's lifespan is determined by multiple factors among which reliability and failure. Moving and exposed components are worn out at a higher rate than shielded components, making the driving

[1]Note that only the tower added fatigue due to wake induced turbulence is investigated because in industry the rotor-nacelle assembly is designed according to a wind class in the IEC standard [39], where the tower is designed site-specifically as confirmed by experts ir. B. Koppenol and dr. ir. B. Ummels.

components for a wind turbine lifetime the blades and gearbox [68]. Due to both the complexity, and uncertainty of the effect of the tower fatigue on the lifetime of a wind turbine, the latter objective is disregarded in this research. Therefore, in this analysis, the lifetime is set and the fatigue loading is investigated for possible changes in the material consumption.
The analysis in this chapter is based on the assumption that the tower design is fatigue-driven. The tower design of a wind turbine is however highly complicated and includes among others the following design drivers:

- The tower design must ensure that the tower natural frequency does not overlap with the 1P (rotor rotational) and 3P (blade passing) frequencies. Excitation at these frequencies might lead to resonance which causes large amplitude loads resulting in increased fatigue damage [69].
- In industry the certification of a wind turbine is based on load calculations according to wind turbine requirements stated in the IEC standard [39]. Using this the fatigue load cases on the turbine are calculated, to confirm that the turbine performance is adequate. Looking at the design load basis (DLB) in IEC 61400-1 [39], there are five design load cases (DLC) that include fatigue loads. These are presented in Table 4.1 below.

Table 4.1: Design Load Cases concerning fatigue loads [39]

| DLC | Design Situation | Wind Condition | Other Conditions |
|---|---|---|---|
| **1.2** | Power production | NTM $V_{in} < V_{hub} < V_{out}$ | |
| **2.4** | Power production + occurrence of fault | NTM $V_{in} < V_{hub} < V_{out}$ | Control, protection, or electrical system faults including loss of electrical network |
| **3.1** | Start-up | NWP $V_{in} < V_{hub} < V_{out}$t | |
| **4.1** | Normal shut-down | NWP $V_{in} < V_{hub} < V_{out}$ | |
| **6.4** | Parked (standing still or idling) | NTM $V_{hub} < 0.7V_{ref}$ | |

NTM here is the normal turbulence model and NWP is the normal wind profile model as specified in [39]. Although literature confirms that the wake added fatigue loads are driving for the thickness of the WTG tower wall, the design should be verified to withstand both extreme and fatigue load cases.

- A minimum wall thickness is required for a fixed diameter to prevent local buckling of the tower.
- The maximum diameter of the turbine can be determined by logistical (transport) constraints, such as tunnels, bridges and other conditions. This may lead to a non-optimised design [70], which would not allow for a reduction in material consumption based solely on the fatigue damage.

Although these aspects of the tower design should not be neglected, literature suggests that the wake added fatigue loads are likely to be the driving factor for the tower wall thickness [64, 66, 67]. Therefore, it is of interest to study layout impacts on the fatigue loading of the WTG tower.

## 4.2. Fatigue Models

Many fatigue modeling approaches and tools exist for the estimation of fatigue loads. Aeroelastic and aero-servo-elastic tools can be utilised to simulate stochastic turbulence, either in the time- or frequency domain. With this, the dynamic behaviour can be simulated and consequently the damage equivalent loads can be determined using rainflow counting [71]. Examples of such tools are BLADED, FAST, PHATAS, and HAWC2 [72]. From these, HAWC2 [73] and FAST [14] are commonly used in literature.

According to Frandsen [66] it is argued and justified that models considering only the effective turbulence intensity are representable for estimating the increased fatigue loads in wind farms. The effective turbulence intensity is defined by Frandsen [66] as the turbulence intensity which causes the same fatigue-load damage as the actual direction dependent turbulence intensity [74]. Two such low-fidelity models are: IEC 61400-1 (IEC 2005) [39] and Frandsen [66]. The Frandsen approach implicitly assumes that the structural load ranges vary linearly with the turbulence intensity [74]. The

difference between the IEC 61400-1 and Frandsen effective turbulence equation is shown in Equation 4.1 and Equation 4.2.

$$I_{add}^2 = \frac{1}{(1.5 + 0.8 s_i \sqrt{C_T(u)})^2} \qquad (Frandsen, [66]) \tag{4.1}$$

$$= \frac{0.9}{(1.5 + 0.3 s_i \sqrt{1/u})^2} \qquad (IEC, [39]) \tag{4.2}$$

In which $s_i$ is the distance to neighbouring turbines normalized by the rotor diameter, $C_T$ is the turbine thrust coefficient and $u$ is the wind speed at which the added wake is investigated. The IEC standard suggests to use the latter equation as a simplified worst case value [67], assuming a generic thrust coefficient rather than a turbine and wind speed specific thrust coefficient.

In order to select a suitable model to estimate the fatigue loading, a preliminary trade-off is performed based on the accessibility to the tools, feasibility, accuracy, computational effort and development date. Using the comparative study performed by Ageze et al. [75], the trade-off is presented in Table 4.2.

Table 4.2: Comparison of fatigue models

| | Accessibility | Feasible | Accuracy | Computational effort | Developed Date |
|---|---|---|---|---|---|
| **Effective turbulence** | | | | | |
| IEC 61400-1 | +++ | +++ | + | +++ | 2005 |
| Frandsen | +++ | +++ | ++ | +++ | 2007 |
| **Aeroelastic Models** | | | | | |
| HAWC2 | ++ | + | +++ | + | 2006 |
| FAST | ++ | ++ | +++ | ++ | 2005 |
| PHATAS | + | ++ | +++ | ++ | 1993 |

From the trade-off, it is found that for the preliminary analysis of the wake induced tower fatigue, the low fidelity Frandsen model will be the most suitable option for this research. Allowing for more accuracy than the IEC approach, while simultaneously having low computational effort compared to the dynamic analysis tools. Ahlstr [72] confirms the use of Frandsen by concluding that the effective turbulence model suggested by Frandsen [66] can be considered good and only slightly conservative in his research.

## 4.3. Wake Added Tower Fatigue

In this section the effective turbulence calculation procedure is described using the Frandsen model in subsection 4.3.1. Then, in subsection 4.3.2, the effective turbulence is related to the added fatigue damage which is related to the difference in tower wall thickness.

### 4.3.1. Effective Turbulence

The effective turbulence intensity should not be seen as a physical representation of the wake but serves as a method to obtain the same fatigue loading as the actual flow conditions. The calculations are performed for hub-height and the mean wind speed from the prevailing wind direction from the selected data set. The effective turbulence can then be calculated using Equation 4.3 [66].

$$I_{eff}(\bar{U}_a) = \left[ \int_0^{2\pi} p(\theta|\bar{U}_a) I^m(\theta|\bar{U}_a) d\theta \right]^{\frac{1}{m}} \tag{4.3}$$

Where $p$ is the probability of a certain wind direction occurring at hub-height, $\theta$ is the wind direction, $\bar{U}_a$ is the mean wind speed at hub-height. $I$ I is the turbulence intensity in the wake, which is made up of the ambient turbulence intensity and the wake added turbulence intensity. $m$ is the Wöhler exponent of the material determined by the SN-curve. Equation 4.3 can be simplified to Equation 4.4 [66].

$$I_{eff} = \frac{\sigma_{eff}}{\bar{U}_a} = \frac{1}{\bar{U}_a}\left[(1 - N \cdot p_w)\sigma_a^m + p_w \sum_{i=1}^{N} \sigma_T^m(s_i)\right]^{\frac{1}{m}} \tag{4.4}$$

N is the number of surrounding turbines. Equation 4.4 is only valid for turbines within a 10 RD radius distance from the turbine under investigation. Furthermore, it is assumed that there is no reduction in the mean wind speed inside the wind farm. $p_w$ is the probability of wake condition from wake number $i$ which is defined for this method at 0.06. This standard value used for the probability of wake condition from a certain turbine is based on the assumption that each wind direction occurs with an equal probability, and a deterministic assessment of the wake geometry. $m$ is the Wöhler exponent of the material determined by the SN-curve, $s_i$ is the distance normalized by the rotor diameter, to the neighbouring turbine $i$. $\sigma_T$ is the standard deviation of the ambient and wake turbulence combined, this can be determined using Equation 4.5 [66].

$$\sigma_T = \sqrt{\frac{(U_{a,sec})^2}{1.5 + 0.8 s_i \sqrt{C_T (U_{a,sec})^2} + \sigma_a^2}} \tag{4.5}$$

The effective turbulence can then be calculated for each turbine in the wind farm. Note that in Equation 4.5, the ambient wind speed no longer has a mean value, but the value changes depending on which wind direction sector the surrounding wind turbine is located in.

### 4.3.2. Tower-wall Thickness Relation to Effective Turbulence

The Frandsen model implicitly assumes that the structural load ranges vary linearly with the turbulence intensity.

$$\sigma_{DEL} \propto \frac{M_{YT,DEL}}{t} \tag{4.6}$$

In which $M_{YT,DEL}$ is the tower bottom fore-aft bending moment, t is the thickness, and $\sigma_{DEL}$ is the damage equivalent stress. To maintain the same damage equivalent stress, the wall thickness of the tower thus needs to increase proportional to the damage equivalent load [2]. A damage equivalent load is convenient to use as this indicates the additional material consumption when the same exterior geometry is maintained. The new wall-thickness is determines using Equation 4.7.

$$t_{new} = t_{old}\left(\frac{I_{eff}}{I_a}\right) \tag{4.7}$$

In which $t_{new}$ is the wall thickness after the increase, $t_{old}$ is the initial wall thickness, and $I_a$ is the ambient turbulence intensity. This method overestimates the added tower wall thickness because it assumes that the increase in damage equivalent load is applicable to all sections of the tower. Assuming that the design driver for all tower sections are fatigue driven [76]. It is therefore recommended by Shan [76] to increase the thickness with only 50% of the value computed from Equation 4.7.

## 4.4. Wake Added Tower Fatigue Borssele

The previously described methodology to determine the added fatigue damage is applied to the Borssele case. To implement Equation 4.4, the mean wind speed at hub-height, number of surrounding turbines, ambient standard deviation, Wöhler exponent, and combined standard deviation of wake and ambient turbulence combined needs to be determined. From the hourly measurement data available for the Borssele site and literature these values are computed and estimated.

Then, the ambient turbulence intensity needs to be determined from the Borssele hourly mean wind speed measurements. Once the standard deviation is determined, the turbulence intensity can easily be obtained using the mean wind speed obtained from the Borssele wind data. To obtain the standard deviation, Equation 4.8 is used as recommended in [77].

[2]Damage equivalent load is a load with constant amplitude and fixed frequency which would cause the same damage as the actual variation of loads over a lifetime

$$\sigma_a = 0.03\bar{U}_a + 0.455 \tag{4.8}$$

In which $\sigma_a$ is the standard deviation and $\bar{U}_a$ is the ambient wind speed. This results in an omni-directional mean turbulence intensity of approximately 8.14% which is in line with the values obtained in Wind and Zone [48]. A code is developed in MATLAB to calculate the effective turbulence as presented in Equation 4.4. For each turbine the surrounding turbines are identified with their distance to the turbine of interest, in which wind direction sector they are positioned, and the mean wind speed and turbulence intensity corresponding to that wind direction sector.

### 4.4.1. Wake Added Damage

A Wöhler exponent of 4 is chosen as wind turbine towers are commonly made of welded steel [78]. The thrust coefficient of the IEA Wind turbine is determined for each wind direction sector. Using these input parameters and the rotor diameter of 190.8 m, the fraction between the effective and ambient turbulence is then computed as presented in Figure 4.2.

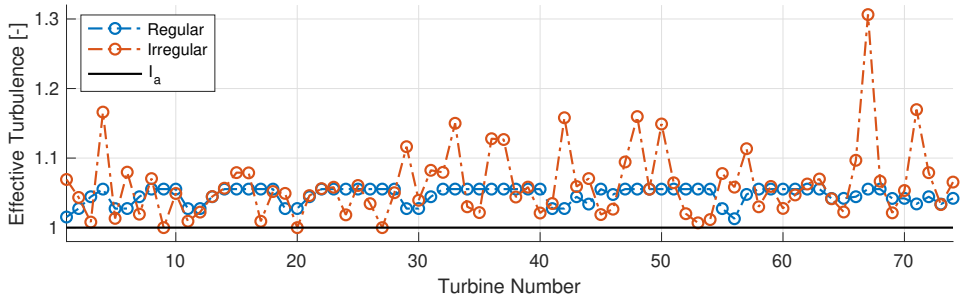


Figure 4.2: Fraction of effective turbulence divided by the ambient turbulence ($I_a$) for each turbine in the regular (blue) and irregular (red) wind farm layout due to wake added turbulence using Frandsen [66].

In Figure 4.2, the black horizontal line represents the case with zero added wake turbulence. The irregular wind farm (red) shows three turbines with no added fatigue due to wake effects. This is due to the fact that the surrounding turbines have a greater distance than 10 RD. The positions of the turbines with no added wake fatigue are identified in green in Figure 4.3. The worst-fatigue positions are identified in red and the second-worst turbines in yellow. From the positioning, it can be derived that both the wind direction and spacing between the turbines are driving factors for the effective turbulence.

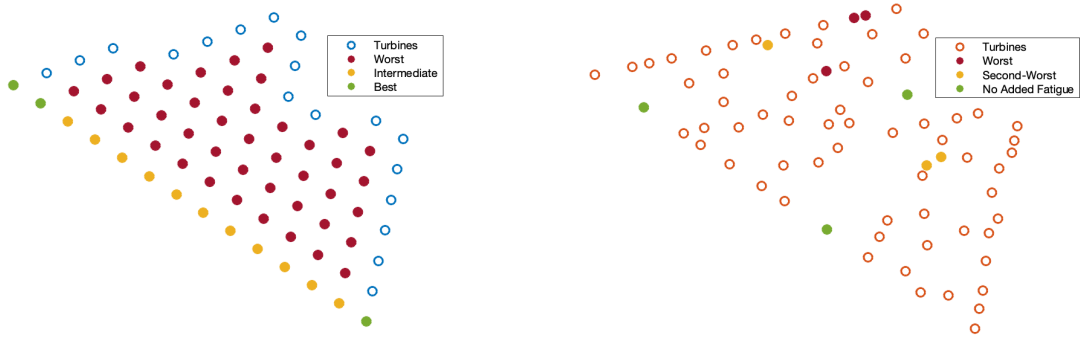


(a) Regular

(b) Irregular

Figure 4.3: Positioning of the different effective turbulence levels in the wind farm for the regular and irregular turbine placement.

Two of the worst-performing turbines are closely spaced together, with an inter-turbine distance of 2.73 RD. By re-positioning one of the two turbines, the effective turbulence of both turbines decreases. To quantify the difference between the regular and irregular wind farm, the turbines are assigned to bins

of 0.001 effective turbulence. From this, the number of turbines with the highest effective turbulence (driving the tower design) is computed. This is visualised with bins of 0.005 (for better visualisation) in Figure 4.4.

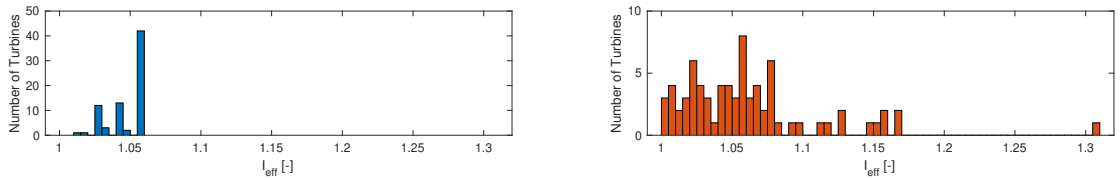


(a) Regular (b) Irregular

Figure 4.4: Number of turbines per effective turbulence bin with bin-size of 0.005.

First, it can be observed that the range of effective turbulence for the regular wind farm is significantly smaller than the irregular wind farm. Meaning, the effective turbulence intensity levels are more constant for the regular layout. Second, it is observed that the regular wind farm has 42 turbines with the highest effective turbulence where this is only 1 turbine for the irregular wind farm. This is also seen in Figure 4.3. It indicates a significantly higher potential to reduce the effective turbulence of the irregular wind farm. The ambient turbulence and mean wind speed are site-specific and not changeable. Therefore, the effective turbulence can only be changed by adjusting the wind turbine positions, increasing the minimum inter-turbine spacing. Surmising that the effective turbulence can indeed be reduced by increasing the minimum inter-turbine spacing, re-positioning the worst-case fatigue turbine could potentially reduce the effective turbulence with 11.68%.

In Table 4.3 the maximum effective turbulence, the corresponding turbine spacing in rotor diameters, number of turbines with that effective turbulence, and the standard deviation are presented.

Table 4.3: Maximum effective turbulence computed with Frandsen normalised with ambient turbulence intensity. Minimum spacing ($x_{min}$) of the corresponding turbines of the regular and irregular layout in rotor diameter. Additionally, the number of turbines with this highest effective turbulence and the standard deviation.

| | **Max. $I_{eff}$ [-]** | **$x_{min}$ [RD]** | **$N_{turb}$ [-]** | **$\sigma$ $I_{eff}$ [-]** |
|---|---|---|---|---|
| **Regular** | 1.055 | 8.75 | 42 | 0.0119 |
| **Irregular** | 1.306 | 2.73 | 1 | 0.0508 |
| **Difference** | 23.8% | - 69.2 % | | 325.4 % |

With an increase of 23.8%, the irregular wind farm performs significantly worse on effective turbulence than the regular wind farm. This corresponds, among other factors, to the spacing of the turbines which is much smaller in the irregular layout. Another interesting observation is the number of turbines with the highest effective turbulence. This number substantiates the previous expectation of higher potential to decrease the effective turbulence of the irregular wind farm.

### 4.4.2. Tower Dimensions and Cost

The maximum effective turbulence found in section 4.4 is used to assess the effect on the material cost of the wind turbine tower. The wall thickness of the IEA Wind turbine is increased with the additional thickness and the new volume is computed. It is assumed that the increase in damage is applicable to all sections of the tower, and that fatigue due to bending is thus the design driver for all sections. Using a cost estimation of 740€ per ton of S355 steel [79], the cost of the tower material is estimated and presented in Table 4.4 together with the change in damage equivalent bending moment and added thickness to the base of the tower.

Table 4.4: Added fatigue damage due to effective turbulence, resulting increase in tower volume, and total increase in tower material cost in the wind farm. The values in this table are based on the maximum effective turbulence intensity found for the regular and irregular wind farm.

| | $\alpha_{DEL}$ [-] | Volume [$m^3$] | Tower Cost [$10^6$ €] |
|---|---|---|---|
| **Base** | - | 73.9 | 2.68 |
| **Regular** | 1.055 | 78.0 | 2.69 |
| **Irregular** | 1.306 | 96.4 | 2.74 |
| **Difference** | + 23.8 % | + 23.6 % | + 2.0 % |

Looking at the change in tower cost for the irregular wind farm, the increase in cost initially seems rather high. The cost is put in perspective using Figure 2.2. The cost-breakdown here shows that the tower cost amounts to approximately 29.4% of the total turbine cost. A turbine average cost is approximately 0.9 million euros per MW according to [80]. This means approximately 2.6 million euros is an estimate of the total tower cost of each IEA Wind turbine. An increase of 23.6% in weight due to the increased material consumption of the irregular wind turbine would then be equal to approximately 2.45% of the total tower cost. The additional material consumption cost is thus deemed reasonable for an initial estimate.

Comparing the regular and irregular wind farm it can be seen that the added damage equivalent load and volume increase with approximately the same percentage. This is due to the linear relation between volume and added damage equivalent load. The tower cost per turbine in the irregular layout increases with approximately 2% compared to the tower cost of the regular layout. For one tower this results in a difference of approximately € 53500, but implementing this for all turbines in the wind farm causes the irregular wind farm to have an increase in total tower cost of 3.9 million Euros, which is significant for the profit of the wind farm. The net present value of the irregular wind farm is investigated. A 700000 Euros increase in cash flow per year is expected due to the higher annual energy production. Today's value of this increase in cash flow is approximately 10 million Euros. This is achieved at the expense of an increase in total tower cost of 4 million Euros. The irregular wind farm has a higher net present value of approximately 6 million Euros based on the energy yield and increased tower material consumption than the regular wind farm.

## 4.5. Conclusion

The effective turbulence intensity is quantified using the Frandsen model. It is observed that the effective turbulence intensity is driven by the distance between the turbines over the number of turbines in the 10 RD distance radius. The irregular wind farm has a 23.8 % higher effective turbulence than the regular wind farm. The tower wall thickness increases linearly with the increase in damage equivalent load which results from this increase in effective turbulence.

The change in tower wall thickness due to the increased effective turbulence is expected to increase the turbine tower cost in the irregular wind farm with approximately 2% compared to the regular wind farm. With a steel price of 740€ per ton of S355 steel [79], this would lead to an increase of 3.9 million euros for the entire wind farm. The sub-performance indicators wind turbine (tower) and component replacement cost thus perform better in the regular wind farm. That is, assuming that the same tower design is applied to all towers based on the worst-case fatigue position in the wind farm. It could however also be considered to use multiple tower designs in one wind farm, this would significantly decrease the total tower cost in the wind farm.

It should be noted that the wake added fatigue damage is calculated using a low fidelity model to generate an initial estimation rather than developing a detailed fatigue analysis. The Frandsen model is known to overestimate the effective turbulence intensity [81]. Also, investigating the combined fatigue loads of both the wave and wake induced effects should be considered when determining the actual thickness of the tower wall. The relative increase of the tower cost is thus expected to decrease based on the overestimation of the Frandsen model. If more than one tower design is considered for the wind farm, this effect could be ameliorated.

Based on the assumptions and analysis performed in this chapter it is found that the regular wind farm performs better for the sub-performance indicators wind turbine and component replacement. The effective turbulence increases with 23.8% for the irregular wind farm compared to the regular wind farm resulting in an estimated 3.9 million euros of tower material cost.

# 5

# Performance Indicator 3: Electrical Inter-Array Cabling System

## 5.1. Introduction

In this chapter, the performance indicator (PI) group called 'electrical system' is analysed. This PI group includes the following sub-performance indicators: electrical losses and power transmission system.

For offshore wind farms, the overall electrical infrastructure cost is increasing over time [82]. This is governed by the power and number of turbines, location of the wind farms and the increased demand concerning requirements from the transmission system operators. According to Sun et al. [83], the electrical infrastructure cost can lead up to 15% of the total capital expenses of a wind farm. In this project, the collection grid is defined as the electrical grid connecting the wind turbines in the wind farm to the substation(s). The electrical infrastructure of offshore wind farms consists of:

- **WTG transformer** converting low voltage to high voltage (66 kV) and **WTG switch-gear**, to minimise consequences for equipment failure [84].
- **Inter-array cabling** connecting the WTGs to the offshore substation.
- **Offshore substation** including power transformers to step-up the voltage from 66 kV to (typically) 132-220 kV.
- **Export cabling** transporting the high-voltage power to an on-shore connection to the grid.

In this research, only the difference in inter-array cabling costs and losses are considered. The aim of this chapter is to quantify the relation between the turbine layout, electrical inter-array cabling system, and the cost and revenue of the wind farm. This relation is schematically visualized in Figure 5.1.

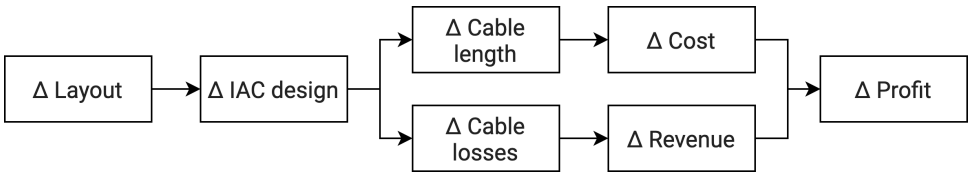


Figure 5.1: Schematic representation of the relation between the wind turbine positioning, electrical inter-array cable (IAC) design and profit of an offshore wind farm.

The objective of designing the inter-array cable routing is twofold [85]:

- Minimise initial cost of the cable and installation
- Minimise reduced revenue due to electrical power losses

The objective of the inter-array cabling design is thus a transfer of the available electricity generated by the turbines to the offshore substation at the lowest possible cost. In this research project, the internal

collection grid is not integrated with the wind farm layout design approach, as the wind farm layout in industry is often determined without taking into account the cable layout according to experts working in offshore wind farm development; ir. B. Koppenol [1], ing. A. Ploeg [2], Dr. ir. B. Ummels, and ir. A. Ringlever-Dospinescu [3]. In theory, a trade-off could be made between the decreased wake losses and increased cabling cost and losses with increasing spacing between the wind turbines [86]. Integrally including the inter-array cabling cost in the optimisation algorithm of the wind farm layout is challenging. This is due to the inherent design complexities and many design constraints for offshore wind turbine layouts, in combination with those for inter-array cabling (in particular soil conditions).

## 5.2. Inter-Array Cable Design

When designing the electrical array cabling system for an offshore wind farm, one has to take into consideration many inter-dependent design variables [86]. In this section a general overview is presented for the design process. The aim of the inter-array cable design is twofold. First, to address the considerations and sequence of choices that need to be made to design an internal connection grid for offshore wind farms. Second, the acquired insights are used to address differences between regular and irregular layouts. The approach is representative for the common approach with which IAC are designed: first, a first-order design, based on standard cable diameters and rules-of-thumb. Second, a validation of that design based on (much) more detailed inputs such as soil conditions, installation considerations and electrical losses (among others) and subsequent updates of the design. This research provides an overview of such considerations, but will be limited to the first step of the design process only, plus a number of sensitivity analyses.

The main design drivers for the electrical collection grid are overall cost (and risk) minimisation, subject to constraints, and reliability. Commonly, redundancy in IAC is considered sub-optimal and wind turbines are connected in strings, not loops [84]. Despite a number of offshore cable outages in the past decade, this approach is still considered as the most efficient (in combination with strong quality due diligence during manufacturing and installation, and a form of business interruption insurance).

The initial investment cost is an important factor when designing the collection grid, however lower power losses may result in lower overall cost due to higher profit. A number of constraints have to be considered.

- Cable crossing increases the risk of damage and installation cost, therefore this should be avoided.
- Obstacles might be present within the wind farm causing restrictions [85]. This is not taken into consideration in this preliminary analysis due to its site-specific nature.
- The energy flow on each connection is limited to the capacity of the installed cable [87].
- A variety of cables is available where capacities, electrical resistance, and cost vary per cable type. In this research, a limited number of representative cable types is used.

Reliability of the individual component as well as the electrical system as a whole is also an important design driver. Offshore, the replacement or repair of malfunctioning parts can lead to extremely complex and expensive operations [86]. A trade-off between the additional investment cost and repair/replacement cost is therefore necessary to assess the benefit for the wind farm. Franken [88] describes a reliability optimisation method for sub-sea cable systems which can be implemented in the decision-making phase of offshore wind farms. The high-level design process visualisation through means of a flowchart is presented in Figure 5.2.
An additional explanation for this will be provided in section 5.3, where this flowchart will be utilised for a preliminary offshore wind farm layout case. The second design loop is entered for the detailed design phase of the electrical inter-array cabling system. The detailed design loop is elaborated upon in Appendix E. Due to both the complexity and the need to use site-specific input parameters from the wind farm, the second design loop is not implemented in this preliminary estimation of the IAC performance.

[1] Technical Project Manager at Ventolines B.V. including turbine package management and support structure design.
[2] Offshore wind design and installation expert at Ventolines B.V.
[3] Senior Electrical Engineer at van Oord, responsible for developing and designing various electrical aspects for offshore wind projects. Involved with the design phase as well as the implementation phase.

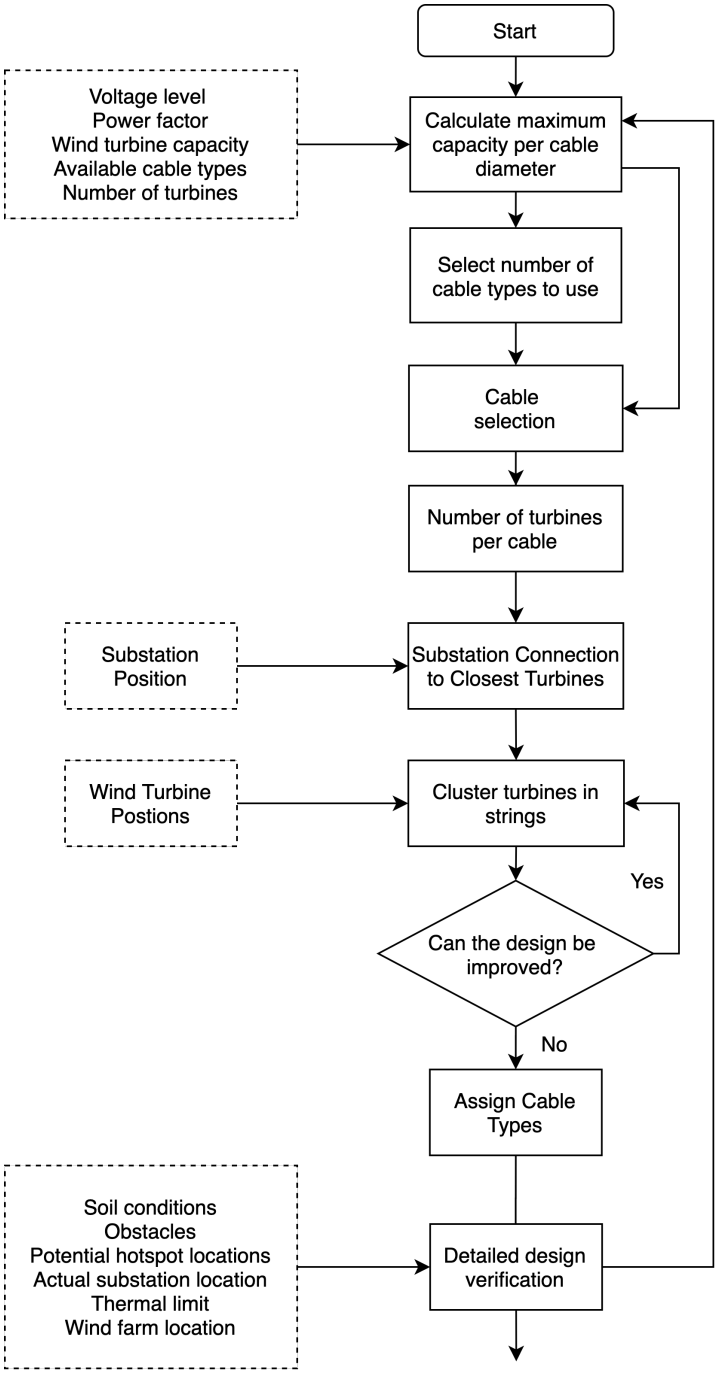


Figure 5.2: High-level design process flowchart for the design of the electrical inter-array cable design of an offshore wind farm. Interrupted square boxes are input parameters for the design process, diamond shaped boxes represent verification points, and square boxes represent calculation/decision points.

## 5.3. Preliminary Cable Design Process for Borssele

Applying the design process described in section 5.2, a preliminary electrical array cabling system is designed for the internal connection grid of the case wind farm.

### 5.3.1. Input Parameters

First, the voltage level of the system is selected. According to [89] the cost of energy can be reduced by 1.5% by making use of higher intra-array voltages. The 66 kV cables are readily available and selected for this IAC design. Using 66 kV cabled instead of 33 kV cables means more turbines can be connected to a single string, system losses can be reduced, and thus the overall cable length can be reduced.

The power factor used for these calculations is 0.9. The power factor often ranges between 0.9 and 0.95, but to stay on the conservative side 0.9 is selected [90]. The power factor indicates the ratio between the real and apparent power. It can be seen as a measure of the efficiency of the electrical power utilisation as discussed with ir. A. Ringlever-Dospinescu[3]. The nominal Borssele wind farm output is estimated at 740 MW provided by 74 turbines of each 10 MW.

The most commonly used type of cables in the offshore wind industry are cross-linked polyethylene (XLPE) insulated submarine cables, which are environmentally friendly, reliable, and have low electrical losses according to Endegnanew et al. [86]. Both aluminium and copper conductors are available in industry. Aluminium conductors have lower current carrying capacities which result in larger diameters [89]. For this design, three-core cables are selected, here three cables are bundled together which each carry one phase. A benefit of this cable type opposed to the single-core cables is that the phases do not have magnetic coupling which results in a balanced system [86]. Furthermore, the three-core cable is cheaper as it can be installed in one go, opposed to the separate method which is used to lay the single-core cables.

### 5.3.2. Calculation and Decision Phase

With the cable type selected, the voltage level known and the estimated power factor, the maximum electrical power carrying capabilities of the cables can be calculated using Equation 5.1.

$$P_{max} = \sqrt{3} V I \cos(\theta) \tag{5.1}$$

Another decision that needs to be made is the number of internal connection cables that will be used in the electrical array cabling system. The increase of installation cost needs to be considered when this is determined. In practice, a low number of cable types is used in the design phase. Consulting with ir. A. Ringlever-Dospinescu [3], using three cable types for the case design deemed a suitable choice. The cable types selected due to availability and suitability are the 400 $mm^2$, 630 $mm^2$, and 800 $mm^2$, aluminium 3-phase AC cables used by Ventolines in WindPark Friesland.

The number of turbines that can be supported by each cable follows from the maximum electrical power carrying capacity of each cable, which is divided by the nominal electrical power of the turbines (10 MW). In this case study, a spare of 50 A is included in the ampacity to allow for unforeseen extra electrical power conditions, as was suggested by ir. A. Ringlever-Dospinescu [3]. The maximum electrical power carrying capabilities of the cables are calculated to be approximately 43.4, 60.0, and 77.2 MW. This means, 4, 6, and 7 turbines can be connected to the 400 $mm^2$, 630 $mm^2$, and 800 $mm^2$ cables respectively. The cable specifications as well as the maximum electrical power that can be supported by the cables is presented in Table 5.1.

Table 5.1: Selected cable types with their corresponding specifications for the case study of Borssele.

| | **Type [$mm^2$]** | **Ampacity [A]** | **Conductor resistance [Ω/ km]** | **Phase operating voltage [kV]** | **Number of turbines [-]** | **Cost [€/m]** |
|---|---|---|---|---|---|---|
| **Cable 1** | 400 | 424 | 0.101 | 66 | 4 | 145 - 160 |
| **Cable 2** | 630 | 584 | 0.063 | 66 | 6 | 165 - 180 |
| **Cable 3** | 800 | 750 | 0.037 | 66 | 7 | 240 - 255 |

When a suitable set of cables is selected, the substation is connected to the number of turbines surrounding it equal to the minimum number of strings needed to connect all turbines. The number of strings needed to connect all turbines to the substation can thus easily be obtained when the maximum electrical power

capacity of each cable is known. To connect all 74 turbines of the case design and a maximum of 7 turbines per string, the minimum amount of strings required is 11. In this research a single sub-station is placed at a suitable location in the wind farm. In further design stages a choice can be made to use multiple substations. For simplicity of the design as well as minimisation of the installation procedures, only the regular string connections are utilised.

Next, the turbines are clustered in strings, avoiding cable crossings and unnecessary use of cable length. Clusters of 6-7 turbines are made which are in line with these first turbines connected to the substation. The objective in this phase of the initial design is to use as little of the higher rated cables as possible to reduce the initial investment cost. The cables situated near the substation are required to have the highest current carrying capacity to allow for the transmission of the electrical power of all turbines on the string. The cables near the end of each string can be smaller in size as less turbines are connected. After this design step a verification is performed to establish whether a simple improvement can be made with the cable use. Rearranging strings can result in a decrease of cable length, and long distances are covered preferably with the lower rated cables. When the strings are optimised, the cable types are assigned to each connection between the turbines and substation.

### 5.3.3. Cable Length

Following this procedure, a preliminary design for the regular and irregular case layout from Borssele results in Figure 5.3 [4].

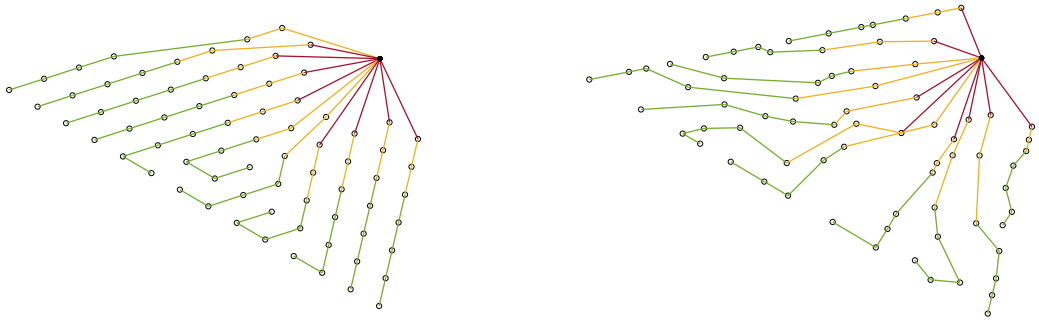

(a) Regular 11 string layout

(b) Irregular 11 string layout

Figure 5.3: Preliminary electrical inter-array cable design for Borssele regular and irregular case study using 400, 630, and 800 $mm^2$, 66 kV, 3-phase AC cables.

A comparison between the length of the cables, affecting the initial investment and the revenue of the wind farm over time, respectively, is presented for both layouts in Table 5.2. A cluster of turbines can be observed at the top left corner of the irregular layout which causes the total length of the internal connection cables to be higher than for the regular case. In order to reach the turbines in this corner, with a maximum of 7 turbines, several turbines have to be skipped to reach all turbines. It can be seen that the substation position is not ideal for the irregular layout, and thus a sensitivity study to assess the effect of the substation placement should be performed.

[4]Note that the cables are connected in straight lines, in reality the cables are installed with curves to avoid cable crossing.

Table 5.2: Resulting length per cable type using 400, 630, and 800 $mm^2$ cables regular and irregular layout, and the difference comparing the irregular layout to the regular layout.

| | **Length [km]** | |
|---|---|---|
| | Regular | Irregular |
| **Cable 1** | 74.76 | 78.26 |
| **Cable 2** | 45.24 | 54.17 |
| **Cable 3** | 28.17 | 18.98 |
| **Total** | **148.17** | **151.42** |
| **Difference** | + 2.19 % | |

Looking at the total cable length of both layouts, it can be observed that the regular layout uses less internal connection cables than the irregular layout. However, the average size of the cables in the irregular grid is smaller compared with the regular grid due to the shorter length of the total use of cable 3. As this cable is more expensive, the total investment cost of the electrical array cabling system of the irregular grid is expected to result in better performance.

### 5.3.4. Impact on Cost, Revenue, and Profit

In this section, the assessment of the difference in cost and revenue for both the regular and irregular electrical inter-array cabling system is investigated. First, the cost component is assessed, linking the cable length to the initial investment related to the offshore inter-array cable cost. Second, the effect on the revenue is assessed looking at the losses the cables cause per unit length.

The initial investment cost of both the regular and irregular IAC is estimated based on the established length in subsection 5.3.3. As previously found, the total length of the irregular layout is larger than the regular layout. However, due to the difference in cable type lengths, this does not automatically mean a cheaper inter-array cabling system. Therefore, a cost estimation is performed in this subsection. The cost per unit length is presented in Table 5.1, where the values are obtained from an expert interview conducted with ir. Ana-Maria Ringlever-Dospinescu [3]. It is emphasised that the cable costs vary greatly with specific site conditions. The total cost in million is only slightly higher for the irregular layout when comparing to the regular layout. An indicative cost per m for the offshore inter-array cables is presented in Table 5.3 below.

Table 5.3: Resulting estimates of the direct offshore inter-array cable cost and approximate full load losses of the inter-array cable design for the regular and irregular Borssele.

| | **Cost [$10^6$ €]** | | **Full load loss [MW]** | |
|---|---|---|---|---|
| | Regular | Irregular | Regular | Irregular |
| **Cable 1** | 11.36 | 11.90 | 5.75 | 6.01 |
| **Cable 2** | 7.42 | 8.88 | 4.15 | 4.97 |
| **Cable 3** | 7.04 | 4.75 | 2.81 | 1.90 |
| **Total** | **25.83** | **25.53** | **12.70** | **12.87** |
| **Difference** | - 1.16% | | + 1.35% | |

The losses per unit meter can be established using the conductor resistance. The losses in megawatt can then be established using the lengths calculated in subsection 5.3.3. This results in the losses shown in the two rightmost columns of Table 5.3. A relatively small difference between the losses is seen, as was also the case for the initial investment cost of the IAC design for both layouts. The same reasoning can be implemented for the losses as for this initial investment cost of the offshore inter-array cables. The largest losses are obtained in the second cable which is used more in the regular design than the irregular design. However, due to the much shorter length used for cable 1, the total losses are 1.35% higher for the irregular layout than for the regular layout. From this it can be concluded that the difference between the regular and irregular layout with respect to the electrical power losses and initial investment cost of the IAC design is negligible.

An additional study is performed with alternative cable type and substation location in Appendix E.

This is done to assess the sensitivity of the cable length, cost, and full load losses to changes in these input parameters. The results of the irregular IAC design for these studies are presented in Table 5.4.

Table 5.4: Sensitivity study results of the irregular wind farm for alternative cable selection: 240 mm², 400 mm², and 630 mm², and alternative substation location (position = $4.955 \cdot 10^5$ m northing and $5.725 \cdot 10^6$ m Southing).

| | Total Length [km] | Difference | Total Cost [$10^6$ €] | Difference | Full Load Loss [MW] | Difference |
|---|---|---|---|---|---|---|
| **Base** | 151.42 | | 25.53 | | 12.87 | |
| **Cable Type** | 172.68 | + 14.0 % | 24.96 | - 2.2 % | 12.94 | + 0.5 % |
| **Substation** | 117.76 | - 22.2 % | 20.22 | - 20.8 % | 10.12 | - 21.4 % |

The percentage difference presented in Table 5.4 is relative to the base irregular IAC layout. Noteworthy, is that the results found in this study are not in line with the results of the base study. Especially the total length of the cables changes significantly between the three cases. For an alternative cable type selection the total length increases with 14%, where for a change in substation location it decreases with 22.2%. The cable type selection changes the results less significantly than the substation location. Due to the significant decrease in total cable length for the alternative substation position, the cost and full load losses decrease significantly. Due to the high sensitivity of the results to especially the substation location, no final conclusions can be drawn from the relatively small differences of the base results.

## 5.4. Conclusion

The main distinction in offshore electrical systems is due to the difference in the inter-array cable design. However, the electrical inter-array cables of offshore wind farms are highly dependent on site-specific aspects such as soil resistivity and other constraints. Therefore, a preliminary design process is developed and implemented on the case of Borssele. From the case study performed in section 5.3 and the sensitivity study performed in Appendix E the following conclusions can be drawn.

First, the difference in the length, approximate full load losses, and cost between the regular and irregular wind farm layout were found to be limited. The irregular grid has a total increased length of 2.19% compared to the regular positioning of the turbines. This causes an increase in both cost and the approximated full load losses.

Two sensitivity studies are performed for the irregular layout to assess the effect of changes in cable type and substation location on the results. The change in cable type shows a significant change in cable length, but the total cost and full load losses are marginal. Changing the substation location results in significant changes in the results. The total cable length decreases with 22.2% and the total cost with 20.8%. Promising as these results may sound, the substation position is largely determined by the energy transmission company, which in turn depends on national regulations, which results in a fixed substation position.

The difference in inter-array cable performance between the regular and irregular wind farm layout from this preliminary analysis is found to be marginal. Due to the high sensitivity to especially the substation location, no final conclusions are drawn for this performance indicator group. With a fixed substation location, and the same cable types selected, the difference between the regular and irregular inter-array cable length, cost, and full load losses are considered to be negligible.

# 6

# General Applicability of Results

The preceding results are obtained using only the specific Borssele case study. In order to look at more general applicability for regular and irregular layouts on the performance indicators (PI) the sensitivity analysis is performed with changes of input parameters. The models used are deterministic, meaning that the same results are obtained when the same input parameters are used.

First, a sensitivity study will quantify how much the output parameters change with varying input parameters [91]. A local sensitivity analysis approach is chosen to analyse the effect of small changes in the input parameters on the output parameters [92]. While this may not inform global effects of different layouts, it provides a first step towards evaluating the general trends of their effects. This sensitivity study is performed with the OAT (one factor at a time) method. To assess the performance of the wind farm, one input parameter is changed at a time, for which the performance indicator results are analysed. To select the input parameters that will be altered, a qualitative assessment is performed of how the sub-performance indicators are affected. More detail on this qualitative assessment is presented in Appendix D.

Second, it is recognised that the sensitivity studies without re-optimising the wind farm layout are not a fair comparison for performance. Therefore, additional optimised layouts are developed using an optimisation tool integrated in WindPRO [30]. The additional layout pairs form a basis to compare the effect of alternative layouts on the results. With the WindPRO and MDAO optimised layouts [45], additional case studies are performed as a means to verify to general applicability of the results.

The PI groups that will be analysed in both the sensitivity study and the alternative case studies are the power performance and the wake induced tower fatigue. The PI group electrical system is left out as the effect of the layout on this PI group is found marginal and too dependent on site-specific input data as concluded in section 5.4. The analyses in this chapter are performed up to the point where the determinative parameter for the profit is obtained.

## 6.1. Rotor Diameter Sensitivity

In this section, the sensitivity of the performance results to a change in rotor diameter is analysed. In industry, turbines with identical nominal power but varying rotor diameters exist. A change in rotor diameter will affect both the power and the wake losses in the wind farm, while the nominal power of the wind park as a whole is the same. Therefore, this allows for an isolated comparison of different rotors. In this chapter, the thrust and power curves of different commercially available offshore wind turbines are used to model the IEA Wind turbine with a smaller rotor size. Initially, a brief analysis of the changes in power curve is performed to assess the further approach in this sensitivity analysis. Then, the sensitivity of the wind farm performance to a change in rotor diameter of the same turbine is investigated.

### 6.1.1. Down-scaling the IEA Wind Turbine

Altering the rotor diameter of the IEA Wind turbine (RD = 190.8 m) results in changes in both the power curve and thrust coefficient curve which are input to WindPRO. The power curve of the turbine with a smaller rotor diameter is derived from the IEA Wind turbine using the power density. The IEA Wind turbine will be referred to as IEA Base and the turbine with decreased rotor diameter is referred to as IEA Small. The power density and rotor diameter of the IEA Base and IEA Small turbines are presented in Table 6.1.

Table 6.1: Rotor diameter and nominal power density of reference IEA base (190.8 m) and IEA small (178.3 m) turbine.

| | Rotor Diameter [m] | Nominal Power Density [$W/m^2$] |
|---|---|---|
| **IEA Base** | 190.8 | 349.8 |
| **IEA Small** | 178.3 | 400.5 |

The ratio of power density multiplied with the IEA Wind turbine power curve results in an estimate of the power curve for the IEA Small turbine as shown in Figure 6.1 [1]. Above the rated wind speed of the IEA Small turbine, the IEA Small turbine power curve is set identical to the power curve of the IEA Base turbine.

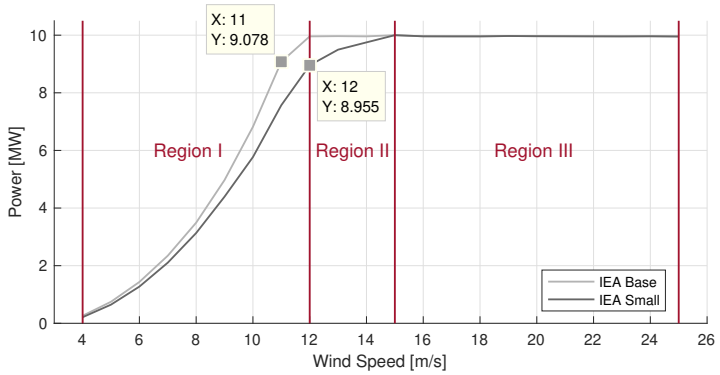


Figure 6.1: Power curve for IEA Base and IEA Small turbine of 190.8 m and 178.3 m rotor diameter. The control regions are identified in red.

First, the control regions are identified. Control region II is assumed to start where the cubic relation between the power and wind speed ends. The control regions for the IEA Small turbine can then be defined as indicated in Figure 6.1. The objective in control region II is to maintain the rotational speed while varying the generator torque. The maximum tip speed of the rotor is thus reached at the beginning of this control region. The two turbines have the same maximum tip speed of 90 m/s. This means that the rotational speed of the IEA Small turbine is approximately 7 % higher than that of the IEA Base turbine. It is assumed that both turbines have the same tip-speed-ratio (Equation 6.1.

$$\lambda = \frac{\omega_r R}{V_2} \tag{6.1}$$

To obtain the same tip-speed ratio, the ratio between the rotor radius and velocity at the start of control region II for both turbines needs to be approximately the same. The ratio of the IEA Base turbine is found to be approximately 0.128 and the ratio of the IEA Small turbine is 0.124. The power curve is therefore deemed suitable for use in this sensitivity analysis based on this analysis. The thrust coefficient is very turbine specific. The potential to model a turbine thrust coefficient was investigated with the help of ir. A. Walvis [2]. It was decided to use the thrust coefficient used in the 10 MW DTU reference wind turbine with a rotor diameter of 178.3 m [93].

### 6.1.2. Sensitivity: Energy Yield

The same procedure as described in section 3.2 is implemented to calculate the annual energy production for the wind farm with the IEA Small turbines. The same layout as the base regular and irregular wind farms is used, and only the WTG type is changed in WindPRO. The results obtained from this simulation are presented in Table 6.2. The results of the initial simulation with the IEA Base turbines are also presented in this table for reference.

[1] In this chapter the reference case is always visualised in light-grey and the changed case is presented in dark-grey.
[2] Wind Specialist at Ventolines BV.

Table 6.2: WindPRO PARK results for the wind farm IEA base (with 190.8 m turbines) and IEA small (with 178.3 m turbines). The annual energy production of the irregular wind farm is compared to the regular wind farm, which is presented in the right-most column.

| | **AEP [GWh/y]** | | **Wake Loss [%]** | | **Difference** |
|---|---|---|---|---|---|
| | Regular | Irregular | Regular | Irregular | |
| **IEA Base** | 3138.7 | 3159.5 | 8.2 | 7.5 | 0.66% |
| **IEA Small** | 2888.3 | 2906.4 | 8.5 | 7.9 | 0.63% |

It can be observed that independent of the rotor diameter, the irregular wind farm layout performs better than the regular wind farm layout.

The wind farm with the IEA Base turbine shows a higher yield which can be explained with the Weibull distribution and power curve. A relatively large difference in power output for high probability wind speeds is observed for the IEA Base turbine which results in a higher power output than for the IEA Small turbine. The increase in AEP of the irregular wind farm relative to the regular wind farm is found to be 0.66% and 0.63% for wind farm with the IEA Base turbines and IEA Small turbines respectively.

The wake losses also influence the annual energy production. The N.O. Jensen wake model is used in the PARK calculations. The thrust coefficient is an inherent part of this wake loss model, for the IEA Small turbine the thrust coefficient is higher for the high probability wind speeds, resulting in higher wake losses which decrease the power output. Although a smaller rotor diameter means the wake volume becomes smaller, the strength of the wake increases with thrust coefficient resulting in an overall negative effect of a decreased rotor diameter with increased thrust coefficient.

Computing the difference in relative performance for the irregular wind farm to the regular wind farm results in an increase of 0.66 % and 0.63 %, which leads to a percentage point change of 0.03 %. The effect of a smaller rotor diameter on the AEP of the wind farm is thus considered marginal.

### 6.1.3. Sensitivity: Persistence to Wind Direction

The persistence to wind direction sensitivity to a change in rotor diameter is analysed. Subjecting the wind farm to a mean wind speed of 9.5 m/s from each wind direction with the IEA Base turbine results in Figure 6.2. The power output in MW is presented as a function of wind direction.

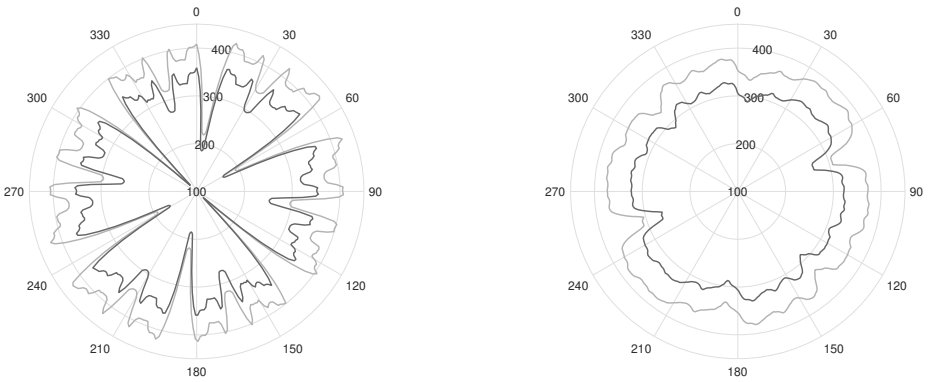


(a) Regular (b) Irregular

Figure 6.2: Power output in MW as a function of wind direction for the (a) Regular and (b) Irregular wind farm layout with the IEA Base (light-grey) and IEA Small (dark-grey) turbines, with a mean wind speed of 9.5 m/s.

A negative offset of the IEA Small wind farm compared to the original IEA Base wind farm is observed in both the regular and irregular layout power output plots. This can be explained looking at Figure 6.1. At the wind speed of 9.5 m/s, the power curve of the IEA Base turbine has a value of 5.89 MW, and the IEA Small turbine has a value of 5.08 MW. The wind farm consisting of the IEA Base turbines is thus expected to generate less power at the same wind speed.

Assessing the difference in maximum power deficit and the standard deviation of the power as a function of wind direction results in Table 6.3.

Table 6.3: Maximum power decrease per wind direction bin of 33° for the IEA base and IEA small wind farms subjected to 9.5 m/s mean wind speed.

| | **Max. Δ Power [MW]** | | **Difference** | **$\sigma_P$ [MW]** | | **Difference** |
|---|---|---|---|---|---|---|
| | Regular | Irregular | | Regular | Irregular | |
| **IEA Base** | 70.6 | 269.5 | - 73.8 % | 67.6 | 16.6 | - 75.5 % |
| **IEA Small** | 60.3 | 232.9 | - 74.1 % | 59.8 | 14.5 | - 75.8 % |

Again, both irregular wind farms perform better than the regular wind farms, independent of the rotor diameter. The maximum power output change and the standard deviation of power as a function of wind direction decrease significantly for the irregular wind farms. For the IEA Small turbine irregular layout the decrease in maximum power drop is 74.1 % compared to the IEA Small turbine regular layout, and the standard deviation decreases with 75.8 %. Compared to the same analysis performed for the IEA Base turbine wind farm, this is an increase of 0.3 % and 0.4 % for the for the maximum power drop and standard deviation respectively.

This analysis indicates that the maximum power drop and standard deviation as a function of wind direction have a low sensitivity to changes in rotor diameter. It also indicates that the positive effect of choosing the irregular wind farm for persistence to wind direction might increase even further with altering rotor diameter.

### 6.1.4. Sensitivity: Wake Induced Tower Fatigue

The wake induced tower fatigue is governed by the wake added turbulence described by Frandsen [66] as presented in subsection 4.3.1. The Frandsen model includes turbines in a rotor diameter distance of 10 RD. Decreasing the rotor diameter is thus expected to exclude turbines at the edge. The decreased rotor diameter is therefore expected to have a decreased effective turbulence. The difference in effective turbulence intensity for both turbine wind farm layouts is calculated and presented in Figure 6.3.

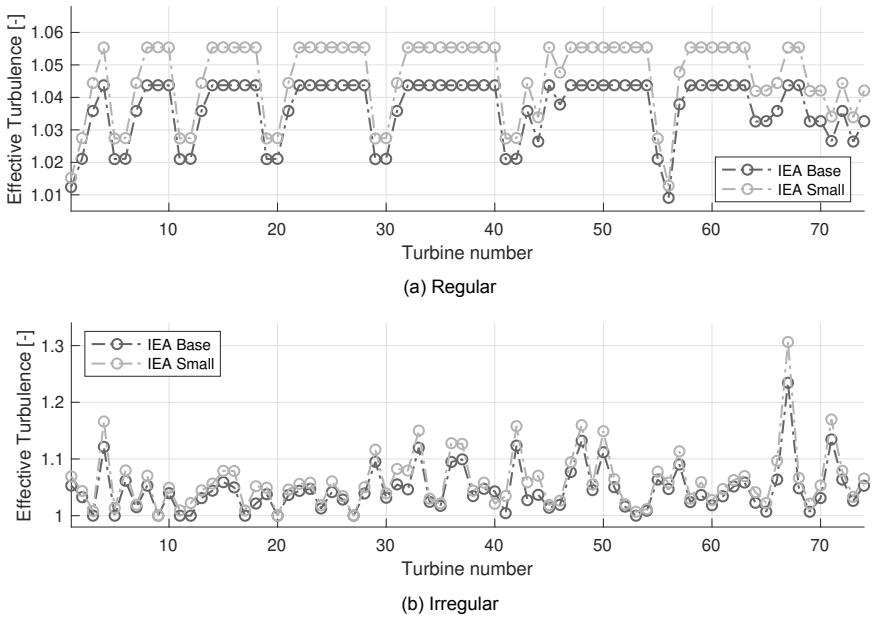


Figure 6.3: Effective turbulence intensity for the wind farm with IEA Small and IEA Base turbines at Borssele wind farm site.

A negative offset for the effective turbulence intensity of the regular wind farm per turbine is observed. For the irregular wind farm, this offset differs per turbine. The possible driving factors for this are discussed below for the regular and irregular wind farm respectively.

First, the distance between the turbines is constant for the regular wind farm. When the rotor diameter is decreased, the distance to the same turbine normalised by rotor diameter is higher. Therefore, the weight of the turbines is lower for the wind farm with the IEA Small turbines, resulting in a lower effective turbulence. It was expected that some turbines would fall outside the 10 RD radius used in the

Frandsen model for the turbines in the regular wind farm due to the decreased rotor diameter. However, investigating the number of surrounding turbines in both regular wind farms with IEA Base and IEA Small turbines, results in exactly the same number of turbines in each 10 RD circle. The difference in effective turbulence intensity is thus only caused by the larger normalised distance to the surrounding turbines. Second, the thrust coefficient (in the denominator of Equation 4.5) for the IEA Small wind turbine is higher for high probability wind speeds. This means that a positive effect on the effective turbulence intensity can be expected (decreasing $I_{eff}$).

For the irregular wind farms, a different behaviour is observed than for the regular wind farm when decreasing the rotor diameter of the turbines. This is caused by two factors. First, the same effect of the increased normalised distance to surrounding turbines as for the regular wind farm is observed. Second, the expectation of exclusion of turbines based on the 10 RD radius used in the Frandsen model holds for the irregular wind farm. Looking more closely at Figure 6.7b, turbine 40 in the irregular wind farm shows a higher effective turbulence for the IEA Small wind farm than for the IEA Base wind farm. For visualisation the 10 RD radius for both rotor diameters is presented for turbine 40 in Figure 6.4 below.

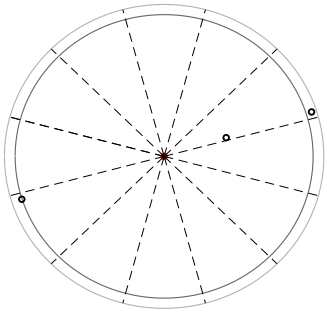

Figure 6.4: Frandsen 10 RD radius visualisation for turbine 40 of the irregular wind farm with RD = 178.3 m (dark-grey, inner circle) and RD - 190.8 m (light-grey, outer circle).

It can be observed that for the decreased rotor diameter, the two outer surrounding turbines fall outside the Frandsen investigation [3]. For 28 turbines this exclusion of turbines is observed, with the highest number of turbines excluded found to be two.

To quantify the difference in performance, the maximum and standard deviation of the effective turbulence intensity and number of turbines with the highest effective turbulence intensity are presented in Table 6.4.

Table 6.4: Maximum and standard deviation of the effective turbulence intensity and number of turbines with the highest effective turbulence intensity for a rotor diameter of 178.3 m (IEA Small) and 190.8 m (IEA Base).

| | **Max. $\mathbf{I_{eff}}$ [-]** | | **Difference** | **$\sigma$ $\mathbf{I_{eff}}$ [-]** | | **Difference** | **$\mathbf{N_{turb}}$ [-]** | |
|---|---|---|---|---|---|---|---|---|
| | Regular | Irregular | | Regular | Irregular | | Regular | Irregular |
| **IEA Base** | 1.0554 | 1.3063 | + 23.8 % | 0.0119 | 0.0508 | + 325.4 % | 42 | 1 |
| **IEA Small** | 1.0437 | 1.2343 | + 18.3 % | 0.0096 | 0.0407 | + 321.9 % | 42 | 1 |

The effective turbulence intensity for both irregular wind farms increases significantly, with 23.8% and 18.3% for the wind farm with IEA Base and IEA Small turbines respectively. This confirms that also for a change in rotor diameter, the irregular layouts perform worse on effective turbulence intensity. The percentage change between the two maximum effective turbulence changes obtained is 5.5 %. The standard deviation as a function of wind direction also shows similar behaviour comparing the irregular and regular wind farm layouts with the IEA Base and IEA Small turbines. The percentage change between the relative performance of the irregular and regular wind farm for this sub-performance indicator is approximately 3.5 %. Furthermore, the number of turbines which experience the highest effective turbulence intensity is equal for both wind farms with the IEA Base and IEA Small turbines.

[3]The turbine in wind direction sector 9 has the highest probability and mean wind speed and is thus expected to add significant effective turbulence.

The high potential to decrease the worst-case effective turbulence intensity for the irregular wind farm thus remains the same.

Overall, the sensitivity of the results obtained for the persistence to wind direction is no longer marginal. The percentage points change of 5.5 % and 3.5 % show that the results are certainly influenced by a change in rotor diameter. Still, the better performance of the regular wind farms compared to the irregular wind farms remains.

### 6.1.5. Rotor Diameter Sensitivity Conclusion

The sensitivity of the performance indicator results is assessed for a change in rotor diameter from 190.8 m (IEA Base turbine) to 178.3 m (IEA Small turbine). The results of the irregular wind farm compared to the regular wind farm are calculated in absolute percentages as presented in this sensitivity analysis (Figure 6.5a). Going one step further, the percentage points change of these obtained percentages are computed comparing the IEA Base wind farm and IEA Small wind farm (Figure 6.5b).

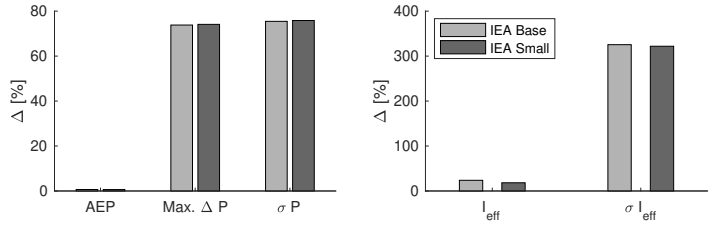


(a) Percentage change comparing the performance of the irregular wind farm to the regular wind farm.

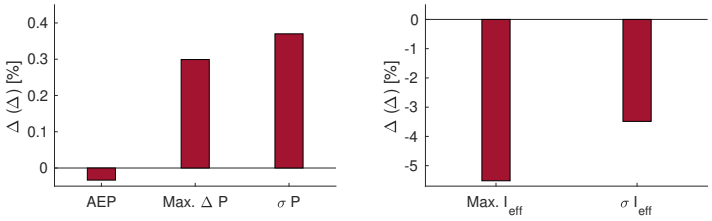


(b) Percentage points change obtained computing the difference in Figure 6.5a compared to the wind farm with IEA Base turbines.

Figure 6.5: Sub-performance indicator results for the power performance and wake induced tower fatigue performance indicator groups for a change in rotor diameter.

Figure 6.5a visualises the relative performance of the irregular wind farm compared to the regular wind farm for the wind farms consisting of IEA Base and IEA Small turbines. For clarification, the difference between the dark-grey (new) and light-grey (base) bars from Figure 6.5a is computed, and presented in percentage point changes as the red bars in Figure 6.5b.

The values on the x-axis can strictly speaking not be compared. The aim of the visualisation of the percentage points in Figure 6.5b is to obtain a feeling of which results vary more with changes of rotor diameter.

Assessing Figure 6.5a, it can be observed that the difference in performance of the wind farms with irregular layout compared to the wind farms with regular layout is very similar regardless of the turbine rotor diameter selected. Looking closer at the percentage points difference presented in Figure 6.5b, the largest percentage point change is observed for the effective turbulence intensity of approximately 5.5%. From this analysis, it can be concluded that a change in rotor diameter for the same rated power will not have a large effect on the results obtained in this research. However, although not changing the overall conclusion regarding irregular vs. regular layouts, turbulence intensity is found to be impacted more significantly by the rotor size than the power performance results.

## 6.2. Wind Climate Sensitivity

In this section the sensitivity of the performance results to a change in wind climate is analysed. The wind climate varies per wind farm site. Both the annual energy production and effective turbulence intensity

results are analysed for altering wind roses. For the analysis of the persistence to wind direction, the mean wind speed is altered. The wind roses for the three cases used in this analysis are:

- **Borssele**, the wind rose from Wind and Zone [48] is used as measured at the Borssele wind farm location.
- **Uniform**, a uniform wind rose is developed with uniform wind speed and probability from each wind direction bin. The wind speed is chosen as the mean wind speed obtained from the Borssele wind farm site.
- **Unidirectional**, the prevailing wind direction bin is set as the only occurring wind direction for the wind farm. The mean wind speed from Borssele is again chosen to limit the additional variations.

The wind rose Weibull parameters, probability, and mean wind speed distributions are presented in Appendix C.

### 6.2.1. Sensitivity: Energy Yield

The production of a wind farm changes with distribution of wind speed and direction. First, the different wind speeds cause a difference in power per turbine and the wake loss effect. Second, the wind direction influences the direction of the wake, influencing the wake losses. To analyse the influence of altering wind climates, the base regular and irregular wind farm layout are subjected to the three wind rose cases in WindPRO using the standard PARK with MEASURE model.

Table 6.5: Annual Energy Production for three wind rose cases: Borssele, Uniform, and Unidirectional.

| | **AEP [GWh/y]** | | **Wake Loss [%]** | | **Difference** |
|---|---|---|---|---|---|
| | Regular | Irregular | Regular | Irregular | |
| **Borssele** | 3138.7 | 3159.5 | 8.1 | 7.5 | + 0.66 % |
| **Uniform** | 3154.0 | 3182.2 | 8.1 | 7.3 | + 0.90 % |
| **Unidirectional** | 3097.7 | 3148.8 | 9.8 | 8.3 | + 1.65 % |

The annual energy production is driven by two factors: the mean wind speed and the wake losses which vary with per selected wind rose. The results show that the irregular wind farms perform better for all three cases, corresponding to lower wake losses. The percentage difference between the AEP of the wind farm with irregular layout compared to the AEP of the wind farm with regular layout 0.66%, 0.90% and 1.65% for the three respective cases. The latter higher result can be addressed to the layout of the regular wind farm, the turbine rows are almost aligned with the unidirectional wind bin to which it is subjected.

The same wake loss percentage is observed for the regular Borssele and uniform distribution, but the AEP is higher for the uniform distribution. This can be explained looking at the capacity factors which are 48.4% and 48.6% for the Borssele and Uniform wind direction distributions.

The percentage point change computed from the last column of Table 6.5 results in -0.23 % and -0.99 %. The sensitivity of the AEP to a change in wind climate is considered low. Noteworthy is the relation to profit, the AEP is the driving factor for the revenue of a wind farm which means the impact on the profit is certainly significant.

### 6.2.2. Sensitivity: Persistence to Wind Direction

The persistence to wind direction is simulated at the mean wind speed at Borssele of 9.5 m/s for the base case. In this analysis, the wind farm is subjected to two different wind speeds to assess their effect on the obtained results. The wind speeds selected are 8 m/s and 12 m/s respectively, and presented in Figure 6.6. These wind speeds are selected to have one wind speed below rated and one wind speed above rated.

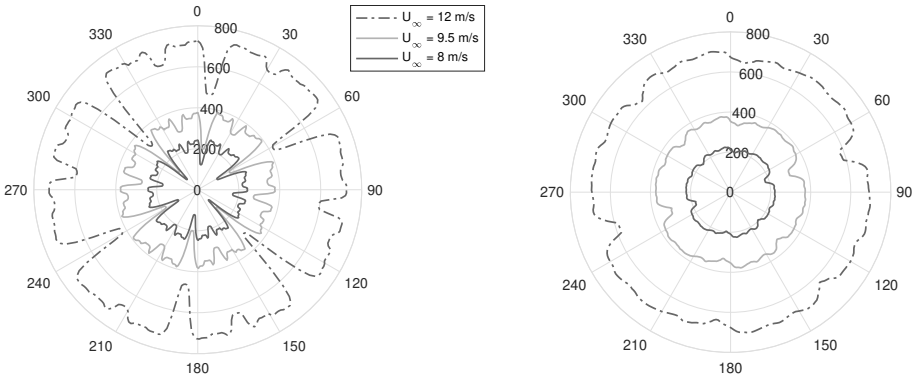


(a) Regular (b) Irregular

Figure 6.6: Power output as a function of wind direction in MW, subjected to mean wind speed of 8.0 m/s, 9.5 m/s and 12.0 m/s for 10 minutes from each direction.

The irregular wind farm layout shows less variation in power output over the wind directions compared to the regular wind farm layout independent of the mean wind speed chosen. To quantify the difference, the maximum power drop and standard deviation as a function of wind direction for each case is computed as shown in Table 6.6.

Table 6.6: Persistence to wind direction results for Low (8.0 m/s), Base (9.5 m/s) and High (12.0 m/s) mean wind speed.

| | **Max. Δ Power [MW]** | | **Difference** | **$\sigma_P$ [MW]** | | **Difference** |
|---|---|---|---|---|---|---|
| | Regular | Irregular | | Regular | Irregular | |
| **Low** | 170.0 | 42.3 | - 75.1 % | 43.1 | 10.3 | - 76.1 % |
| **Base** | 251.7 | 70.6 | - 73.8 % | 63.2 | 16.6 | - 75.5 % |
| **High** | 415.6 | 114.2 | - 72.5 % | 99.5 | 25.6 | - 74.3 % |

Again, the irregular wind farm layouts perform better regardless of the subjected mean wind speed for both maximum power drop and standard deviation as a function of wind direction. The maximum power drop for the irregular wind farms compared to the regular wind farms decrease with 75.1 %, 73.8 %, and 72.5 % for the mean wind speeds of 8.0, 9.5 and 12.0 m/s respectively. This results in a percentage point change of -1.28 % and -2.57 % compared to the Base mean wind speed case. The difference in standard deviation shows the similar behaviour as the maximum power drop. The percentage points change for the standard deviation are -0.68 % and -1.85 % compared to the base mean wind speed case.

The sensitivity of the results in the persistence to wind direction analysis to changes in wind climate is higher than the sensitivity to changes in rotor diameter. For higher wind speeds this change is expected to become even more significant as the wake losses decreases or disappear at high wind speeds (+ 15 m/s).

### 6.2.3. Sensitivity: Wake Induced Tower Fatigue

The Frandsen model is implemented to assess the effective turbulence for altering wind roses. The result of the effective turbulence intensity for the Borssele wind direction distribution and uniform wind direction distribution is presented in Figure 6.7. The standard value used for the probability of wake condition from a certain turbine is based on the assumption that each wind direction occurs with an equal probability, and a deterministic assessment of the wake geometry. Combining these aspects results in the value of 0.06 used in the Frandsen model.

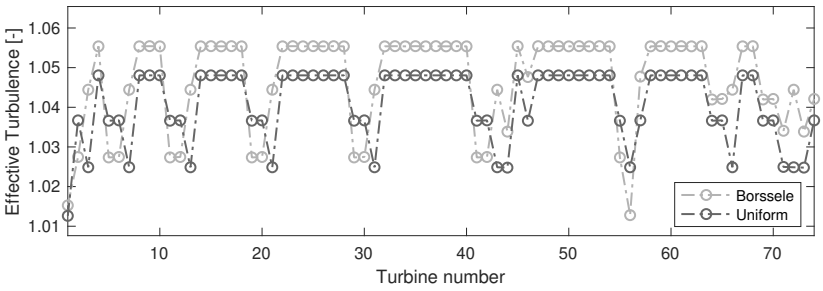


(a) Regular

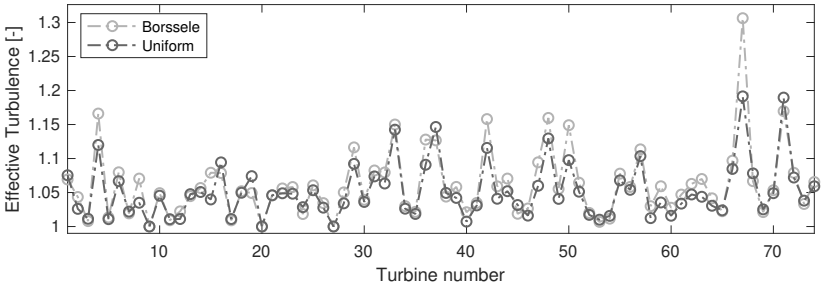


(b) Irregular

Figure 6.7: Effective Turbulence Intensity for Borssele and Uniform wind rose.

The maximum effective turbulence is driving for the tower design of the wind turbines, these maxima for the regular and irregular wind farm for both wind roses are presented in Table 6.7.

Table 6.7: Maximum effective turbulence results for two wind roses: Actual wind direction distribution at Borssele and Uniform distribution.

| | **Max. $I_{eff}$ [-]** | | **Difference** | **$\sigma$ $I_{eff}$ [-]** | | **Difference** | **$N_{turb}$ [-]** | |
|---|---|---|---|---|---|---|---|---|
| | Regular | Irregular | | Regular | Irregular | | Regular | Irregular |
| **Borssele** | 1.0554 | 1.3063 | + 23.8 % | 0.0119 | 0.0508 | + 325.4 % | 42 | 1 |
| **Uniform** | 1.0481 | 1.1914 | + 13.7 % | 0.0093 | 0.0407 | + 335.3 % | 42 | 1 |

For both cases, the irregular wind farm layout performs worse compared to the regular wind farm layout. A decrease of 23.8 % and 13.7 % is observed for the Borssele and Uniform wind direction distribution respectively. This corresponds to percentage point changes of + 10.1 % and + 9.9 % for the maximum effective turbulence and standard deviation. The wake turbulence is normalised with the ambient turbulence which decreases for increasing wind speeds. The actual wind direction distribution contains higher wind speeds than the annual average mean wind speed with corresponding lower ambient turbulence levels, resulting in higher effective turbulence levels. Furthermore, the thrust coefficient is in the denominator of the wake turbulence equation (Equation 4.4), meaning a smaller thrust coefficient (at higher wind speeds) will result in a higher effective turbulence.

The sensitivity of the maximum effective turbulence and standard deviation of the effective turbulence are both found to be relatively high compared to the other previous sensitivity studies. With a percentage point change of 10.1 % and 9.9 %, the wind climate distribution is found to significantly change the effective turbulence results.

### 6.2.4. Windrose Climate Sensitivity Conclusion

The sensitivity of the sub-performance indicator results to a change in wind climate is quantified by simulating the power performance and effective turbulence results using additional wind direction distributions. Three distribution are selected: Borssele, Uniform with mean wind speed from Borssele, and Unidirectional with mean wind speed from the prevailing wind direction at Borssele. For the persistence to wind direction, two additional mean wind speeds are subjected to the wind farm: 8.0, 9.5, and 12.0 m/s. The absolute percentage difference found in this analysis are combined in Figure 6.8a. From this the

percentage point change between the different cases is computed and presented in Figure 6.8b.

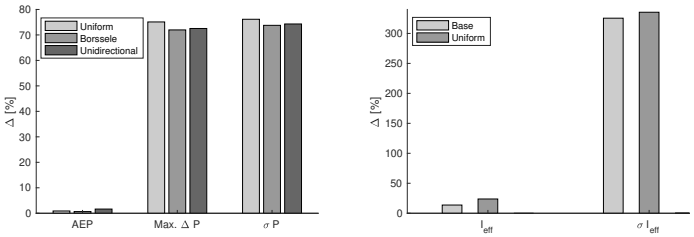


(a) Percentage change of irregular wind farm compared to regular wind farm.

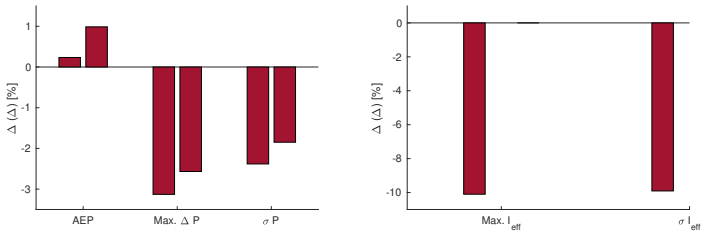


(b) Percentage points change obtained computing the difference in Figure 6.8a compared to the base case.

Figure 6.8: Sub-performance indicator results for the power performance and wake induced tower fatigue performance indicator groups for a change in wind climate.

The relative change in performance of the irregular wind farm layout compared to the regular wind farm layout is presented in Figure 6.8a. It should be noted that the persistence to wind direction changes is computed with mean wind speeds of 8, 9.5, and 12 m/s instead of the wind rose cases described earlier. The percentage points change are shown in Figure 6.8b. This shows a significant change in all performance indicators except the AEP. Noteworthy is that the relatively small change in percentage points of the AEP are expected to have a larger effect on the profit. So, for the performance of the wind farm overall this change is significant. For this sensitivity study based only on the parameters which are considered a driving factor for the profit it is considered to have a low sensitivity to a change in wind climate.

Overall, the sensitivity of the performance indicator group results to changes in wind climate is higher than to changes in rotor diameter. Especially the results regarding the effective turbulence change significantly between the uniform and Borssele wind rose. It should be noted that the wind rose cases chosen for this sensitivity analysis are extremes. Actual wind roses are expected to range between the extreme cases used.

## 6.3. Re-optimisation of Wind Farm Layouts

The preceding results in the sensitivity analysis are obtained by changing the input parameters for the optimised wind farm layout developed by Sanchez Perez Moreno [45], without re-optimising this wind farm layout. A change in rotor diameter or wind climate is expected to affect the positioning of turbines in the optimised wind farm layout. In this section, a re-optimisation of the WindPRO optimised layout is done to assess the change in turbine positioning. The aim of this section is not to understand the turbine placement by the algorithm, but to investigate the change in layout as a result of changing input parameters.

The WindPRO irregular optimisation is run for the changes in input parameters. The optimisation is performed in WindPRO with the base case input parameters described in section 2.3. Elaboration on the optimisation procedure can be found in Appendix B. First, the rotor diameter is changed as input to the optimisation tool, second the wind climate is changed. The analysis is only performed for the irregular optimisation. The regular optimisation procedure is described in subsection B.2.1. The irregular optimisation tool searches for the best position of a turbine where the regular optimisation tool has a regular pre-defined grid. To assess the change in layout for a change in input, the irregular optimisation is deemed a better fit for the analysis.

### 6.3.1. Rotor Diameter Optimisation

The rotor diameter change described in subsection 6.1.1 is implemented in the WindPRO optimisation tool. The rotor diameter of the IEA Base turbine is down-scaled from 190.8 m to 178.3 m, the new turbine is referred to as IEA Small turbine. The result of the optimisation with the IEA Base and IEA Small turbines is presented in Figure 6.9b.

The performance curves of this IEA Small turbine are altered with the scaling method described in subsection 6.1.1. Although an initial verification showed that the scaled curves are fit to use for the sensitivity analysis, an additional check is done. An exiting wind turbine from industry is implemented to assess the impact of using a different WTG type. For this, the *'V164 8 MW of MVOW (MHI Vestas Offshore Wind) with a rotor diameter of 164 m'* is used as input for the optimisation (from now on this will be referred to as Vestas). This layout with this turbine will from now on be referred to as Vestas layout. The results of both optimisations are presented in Figure 6.9c.

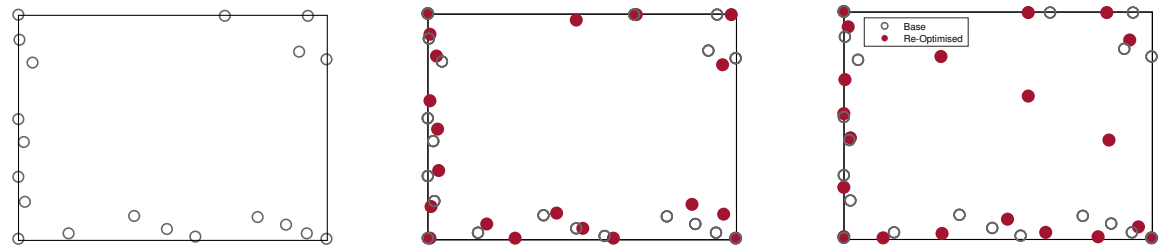


(a) IEA Base turbine with RD = 190.8 m (b) IEA Small turbine with RD = 178.3 m (c) Vestas turbine with RD = 164.0 m

Figure 6.9: WindPRO optimisation results for (a) IEA Base turbine with 190.8 m rotor diameter, (b) IEA Small turbine with 178.3 m rotor diameter, and (c) Vestas turbine with 164.0 m rotor diameter. The red filled dots represent the new positions, and the grey empty circles depict the starting positions of the wind turbines.

It can be observed that most turbines in Figure 6.9a are placed near the south and west border of the WTG area. With the prevailing wind direction coming from the south-west-west sector, this places these turbines in a free-stream wind speed. At the north-east corner, another set of turbines is placed. Moving diagonally from the south-west corner to the north-east corner, the wake has a distance of approximately 5 km to recover.

The optimised layout with the IEA Small turbines to a large extent shows the same positioning of the turbines in the WTG area (Figure 6.9b). Qualitatively analysing the positioning, it can be said that the turbine positions only vary slightly between the optimised wind farm layout with the IEA Base and IEA Small turbines.

The optimised wind farm with the Vestas turbine shows more difference compared to the optimised wind farm with the IEA Base turbines. The IEA Base turbine rotor diameter is decreased with approximately 7 % for the IEA Small turbine, and 16 % for the Vestas turbine. The difference in turbine positioning due to the altering rotor diameter is therefore also expected to be higher for the latter comparison.

Overall, the wind farm layout is concluded not to change significantly for changes in rotor diameter up to at least 7 %. The change in turbine positioning for larger changes is expected to be influenced more but not drastically. The basis of placing turbines at the WTG area edges which face the prevailing wind direction of the wind farm is still observed independent of rotor diameter size.

### 6.3.2. Wind Climate Optimisation

The WindPRO optimisation is also performed for altering wind rose cases. The same wind rose cases selected for the sensitivity study in section 6.2 are used. Those are the Borssele, Uniform, and Unidirectional wind roses. The Borssele wind rose is the base case, with which the other wind farm optimised layouts are qualitatively compared. The resulting optimised wind farm layouts are presented in Figure 6.10.

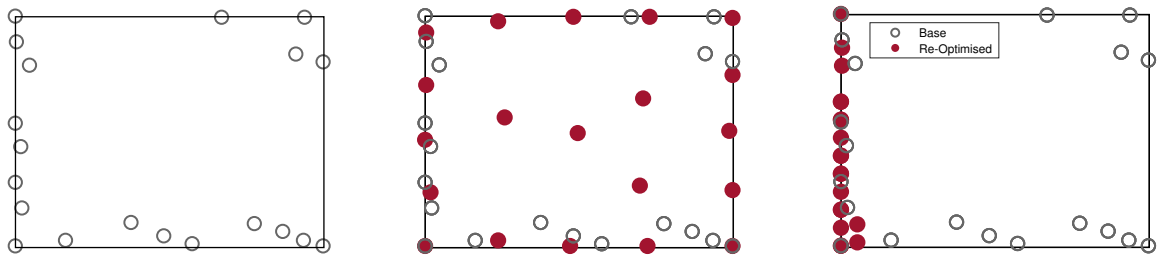


(a) Borssele (b) Uniform (c) Unidirectional

Figure 6.10: WindPRO optimisation results for (a) Borssele wind rose, (b) Uniform wind rose, and (c) Unidirectional wind rose. The red filled dots represent the new positions, and the grey empty circles depict the starting positions of the wind turbines.

The turbines in Figure 6.10b are spaced approximately equal in all directions in the WTG optimisation area. The regularity of this wind farm layout is higher than that of the wind farm layout optimised for the Borssele wind rose. This suggests that for more uniform wind direction and wind speed distributions regular wind farm layouts with a higher degree of regularity would yield a higher annual energy production than wind farm layouts with a lower degree of regularity.

In Figure 6.10c it appears as if only 14 turbines are positioned in the WTG optimisation area. Investigating this further shows that some turbines pairs have an exceptionally close inter-turbine spacing. The WindPRO optimisation has an input option for the minimum spacing of turbines. The option has two possible results: omit the turbines with smaller inter-turbine spacing, or keep the turbines with smaller inter-turbine spacing.

Overall, the WindPRO optimised wind farm layouts are concluded to change significantly for the uniform and unidirectional wind rose. Therefore, the sensitivity analysis performed in section 6.2 does not provide a fair representation of the wind farm layouts. This sensitivity can thus only be used to assess what happens to the wind farm performance indicator group results if the wind rose for the base case alters from the Borssele wind rose it is designed for.

## 6.4. Additional Optimised Layout Cases

In this section, the global effect of the wind farm layout on the performance indicator groups is analysed. This is done through means of additional optimised regular and irregular wind farm layout pairs. First, the optimised layout pairs are presented and briefly elaborated upon. Then, the sub-performance indicator results are computed for each wind farm layout.

### 6.4.1. Optimised Layouts Selection

The first optimised wind farm layout pair is developed by Sanchez Perez Moreno [45]. This layout has the same origin as the base layouts (with sequential design approach), but an alternative optimisation procedure (MDAO design approach). The optimisation approach for the MDAO couples different components and disciplines represented by computational tools in a workflow to simulate the entire system. Additional information on the MDAO workflow can be found in Appendix B. The MDAO regular and irregular wind farm layout are presented in Figure 6.11.

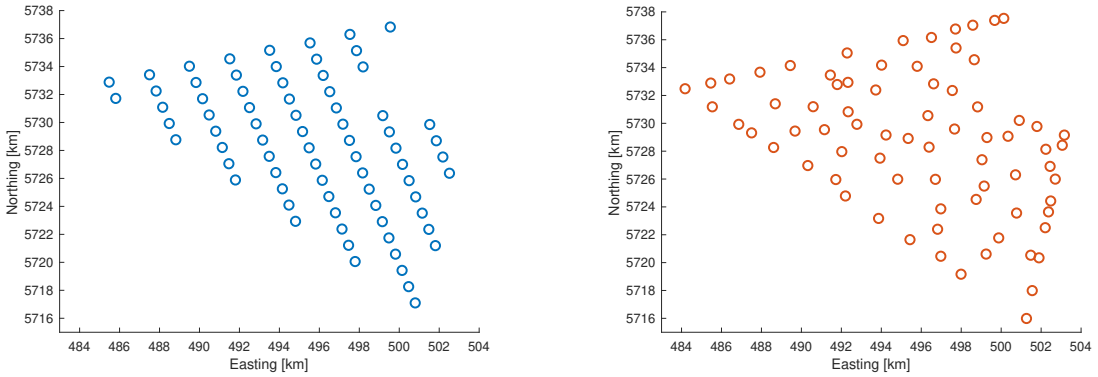


(a) Regular (b) Irregular

Figure 6.11: Regular and irregular MDAO layout from Sanchez Perez Moreno [45] consisting of 74 turbines with a rated power of 10 MW at Borssele.

The same wind farm area of Borssele III and IV is used as can be seen in Figure 6.11. Again, it can be observed that the optimisation algorithm for the irregular wind farm pushes the turbines to the boundaries.

The irregular wind farm developed in section 6.3 is used for the second wind farm layout pair. A regular wind farm layout is developed using the optimisation tool in WindPRO, for which the procedure is explained in Appendix B. The resulting regular and irregular wind farm layout is presented in Figure 6.12.

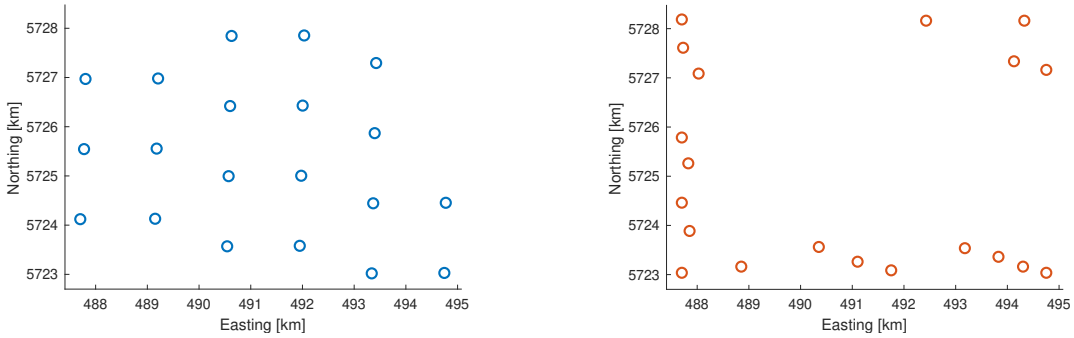


(a) Regular (b) Irregular

Figure 6.12: Optimised regular and irregular wind farm layout using WindPRO with Borssele wind climate data.

Similar to the base layout presented in section 2.3, some initial observations are quantified. First, the sum of the distances to surrounding turbines in a 10 RD radius is computed for each turbine in the respective wind farms. Second, the minimum spacing between two turbines is computed normalised with rotor diameter. Both are presented in Table 6.8.

Table 6.8: Number of turbines with the same sum of distances to surrounding turbines with a tolerance of 0.001 RD ($N_{turb}$), and the minimum distance between two turbines ($x_{min}$). For the regular and irregular wind farm layouts of both the MDAO and WindPRO optimisation.

| | | $\mathbf{N_{turb}}$ $(\sum \mathbf{d_i})$ [-] | $\mathbf{x_{min}}$ [RD] |
|---|---|---|---|
| **MDAO** | Regular | 3 | 6.33 |
| | Irregular | 58 | 2.38 |
| **WindPRO** | Regular | 8 | 7.36 |
| | Irregular | 18 | 2.45 |

The number of unique values for the sum of distances to surrounding turbines in the 10 RD radius for the

regular wind farm is 3. This indicates a high degree of regularity. This value for the irregular wind farm is found to be 58. The minimum spacing between two turbines in the wind farm is again significantly smaller for the irregular wind farm. This is in line with the findings from the base layout, where the density of the turbines around the edge of the wind farm was also higher causing a decrease in inter-turbine spacing.

### 6.4.2. Annual Energy Production

The annual energy production, wake losses, and capacity factors of the additional MDAO and optimised layouts are computed in WindPRO. The results, together with the base results, are presented in Table 6.9. The layouts will from now on be referred to as Base, MDAO, and WindPRO layout.

Table 6.9: Calculated annual energy for Base, MDAO, and WindPRO optimised regular and irregular layouts.

| | | AEP [GWh/y] | Wake Loss [%] | Difference | Capacity Factor [%] | Difference |
|---|---|---|---|---|---|---|
| Base | **Regular** | 3138.7 | 8.1 | + 0.66 % | 48.4 | + 0.62 % |
| | **Irregular** | 3159.5 | 7.5 | | 48.7 | |
| MDAO | **Regular** | 3133.96 | 8.2 | + 1.04 % | 48.3 | + 1.04 % |
| | **Irregular** | 3166.4 | 7.3 | | 48.8 | |
| WindPRO | **Regular** | 866.4 | 6.1 | + 0.67 % | 49.4 | + 0.61 % |
| | **Irregular** | 872.2 | 5.5 | | 49.7 | |

For all wind farm layout pairs, the AEP of the wind farms with the irregular layout is higher, corresponding to the lower found wake losses. The capacity factor indicates the ratio of the amount of energy generated and the maximum amount of energy that can be produced in the same amount of time [94]. This capacity factor is higher for the irregular wind farm layout. Comparing the regular and irregular wind farm AEP performance then results in an increase of 0.66, 1.04 and 0.67% between the Base, MDAO, and WindPRO layout pairs respectively.

### 6.4.3. Persistence to Wind Direction

The persistence to wind direction is also assessed for the three optimised layouts. The WindPRO optimised wind farm consists of 20 turbines, so the power output is lower, as can be observed in Figure 6.13. The maximum power drop for the MDAO regular layout is expected to occur at an angle between 150 and 180°, as this wind direction is in alignment with the wind turbine rows. The prevailing wind direction is from the south-west-west (sector 9) which means that a power drop at this angle occurs less. The power drop of the irregular Base layout occurring around 240° lays in the prevailing wind direction sector. Although the peak is less than that of the irregular MDAO layout, the effect on the predictability and hence value on the e-market might be higher. The power output of all layouts for a mean uniform wind speed of 9.5 m/s is presented in Figure 6.13 below.

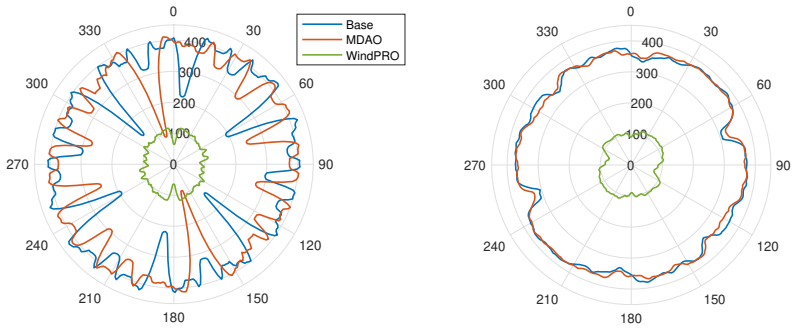


(a) Regular (b) Irregular

Figure 6.13: The multi-directional power curve for mean wind speed of 9.5 m/s for the Base, MDAO, and WindPRO optimised regular and irregular wind farm in megawatt as a function of wind direction.

First, it can be observed that the irregular wind farm power output shows a less severe power drop as a function of wind direction. Furthermore, the same preferred overall behaviour characterises all three irregular layouts. The MDAO layout seems to show a lower frequency of large power drops than the Base layout. Quantifying the maximum power drop and standard deviation as a function of wind direction results in Table 6.10.

Table 6.10: Persistence to wind direction results for additional optimised layouts for a mean wind speed at Borssele of 9.5 m/s.

| | **Max. Δ Power [MW]** | | **Difference** | **$\sigma_P$ [MW]** | | **Difference** |
|---|---|---|---|---|---|---|
| | Regular | Irregular | | Regular | Irregular | |
| **Base** | 269.5 | 70.6 | - 73.8 % | 67.6 | 16.6 | - 75.5 % |
| **MDAO** | 324.2 | 44.7 | - 86.2 % | 69.5 | 12.9 | - 81.4 % |
| **WindPRO** | 53.3 | 36.2 | - 32.2 % | 11.3 | 10.5 | - 7.4 % |

The irregular wind farm layouts indeed have better performance for both the maximum power drop and standard deviation of the power output as a function of wind direction. As the WindPRO optimised layout consists of less turbines, the percentages increase in performance are assessed to compare the layouts. The maximum power drop decreases with 73.8, 86.2, and 32.2% for the Base, MDAO, and WindPRO optimised layouts, respectively. This corresponds to a percentage change of -12.4 % and +41.6 %. This could indicate that the positive effect of the irregular wind farm increases with the number of turbines in the wind farm. This is in line with the previous observation of increased magnitude of the power drop for a larger number of turbines aligned in a row.

Overall, the sensitivity of the results is significant for the WindPRO optimisation layout compared to the Base and MDAO layouts. However, the same trend of better performance is observed for all irregular wind farms compared to their regular counterpart.

### 6.4.4. Wake Induced Tower Fatigue

The effective turbulence intensity is determined for the MDAO and WindPRO optimised wind farm layouts. The visualisation of these turbulence levels are presented in Figure 6.14a and Figure 6.14b.

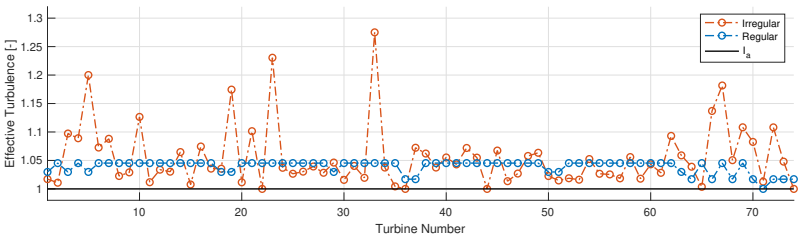


(a) MDAO

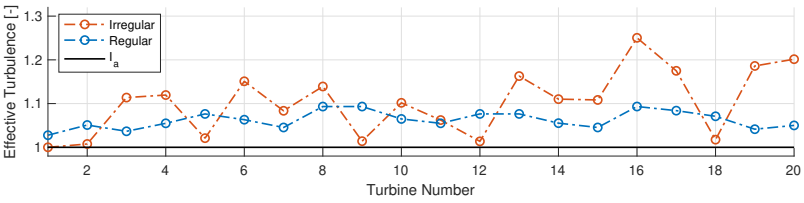


(b) WindPRO

Figure 6.14: Effective turbulence intensity normalised with ambient turbulence for the MDAO and WindPRO optimised wind farm layouts.

The irregular wind farm layouts show significantly higher effective turbulence intensity levels, as was also found for the Base wind farm layout. Again, the regular effective turbulence intensity shows more consistent behaviour among the turbines. Quantifying the maximum effective turbulence levels for each wind farm layout results in Table 6.11.

Table 6.11: Maximum effective turbulence results for two wind roses; Actual wind direction distribution at Borssele and Uniform distribution.

| | **Max. $I_{eff}$ [-]** | | **Difference** | **$\sigma$ $I_{eff}$ [-]** | | **Difference** | **$N_{turb}$ [-]** | |
|---|---|---|---|---|---|---|---|---|
| | Regular | Irregular | | Regular | Irregular | | Regular | Irregular |
| **Base** | 1.055 | 1.306 | + 23.8 % | 0.0119 | 0.0508 | + 325.4 % | 42 | 1 |
| **MDAO** | 1.045 | 1.275 | + 22.0 % | 0.0110 | 0.0537 | +388.5 % | 55 | 1 |
| **WindPRO** | 1.093 | 1.250 | + 14.4 % | 0.0196 | 0.0740 | + 274.9 % | 4 | 1 |

The maximum effective turbulence for each irregular wind farm in the regular and irregular layout pairs, performs significantly worse. The maximum effective turbulence increases with 23.8 %, 22.0 %, 14.4 % for the Base, MDAO, and WindPRO wind farm layouts. This results in a percentage point change of + 5.9 % and - 1.7%. As observed in the case selection, this is likely caused by the tendency of optimisation algorithms to place turbines at the edge of the wind farm area section 2.3. This leads to lower (average) spacing. The standard deviation of the effective turbulence over the turbines in the wind farm also shows similar behaviour between the irregular and regular wind farm layouts.

Overall, the effective turbulence intensity results for the additional wind farm layouts indicate that the results found in chapter 4 are generally applicable for irregular wind farm layouts. The degree to which this negative performance of the irregular wind farm is observed depends on the layout case.

### 6.4.5. Additional Layout Conclusion

The effect of different optimised wind farm layouts on the performance indicator group results is assessed by implementing the already developed MDAO wind farm layout, and developing a new optimised layout in WindPRO.

First, the irregular wind farm layout sub-performance indicator results are compared to the regular wind farm layout results. The absolute percentage change of the irregular wind farm relative to the regular wind farm is presented in Figure 6.15a. This results in three percentages for the three different wind farm layout optimisation strategies. To analyse the effect on the results of using different wind farm layout optimisation strategies, the percentage points change are computed as the difference between the MDAO and WindPRO wind farm layout results obtained in Figure 6.15a. These percentage points change are visualised in Figure 6.15b.

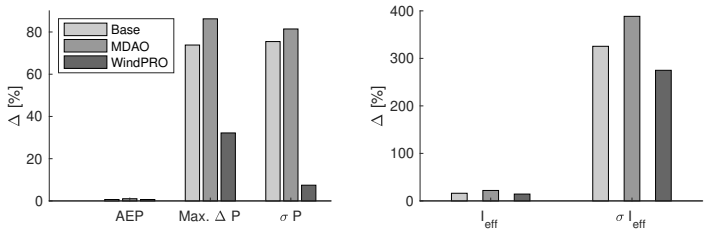


(a) Percentage change of irregular wind farm compared to regular wind farm.

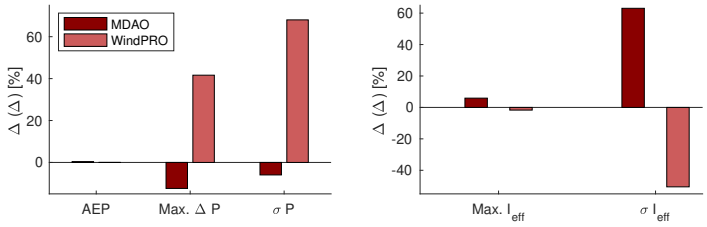


(b) Percentage points change obtained computing the difference in Figure 6.15a compared to the base case.

Figure 6.15: Sub-performance indicator results for the power performance and wake induced tower fatigue performance indicator groups for different optimised wind farm layouts.

Again, it is important to note that this section does not serve as a sensitivity study. It serves as a means to assess whether the conclusions formulated based on the performance indicator group results of the Base wind farm layout are also valid when using other optimised wind farm layout pairs.

The percentage points change between the Base and MDAO layout are lower in magnitude than the percentage points change between the Base and WindPRO optimised layout. An explanation for this can be that the design objectives and approach differ more between the Base and WindPRO layout optimisation. The MDAO optimisation is developed in the same study taking into account the same input parameters [45]. The WindPRO optimisation tools objective is to maximise the annual energy production of the layout, not to minimise the LCOE.

Furthermore, it can be observed that the percentage points change in maximum power drop is significantly smaller for the WindPRO optimised wind farm layout. This can be explained comparing the arrangement of turbines in Figure 6.12a and Figure 6.11a. The maximum number of turbines aligned in the MDAO regular wind farm layout is 17, where that in the WindPRO regular wind farm layout is 4. With larger regular wind farms, the losses for wind direction in alignment with the wind turbine rows increase with the number of turbines in the row.

The percentage points difference in effective turbulence shows less change between the wind farm optimisation layouts. The difference between the minimum spacing in the regular and irregular wind farm is of similar magnitude for the MDAO and WindPRO optimisation approach as shown in Table 6.8. Comparing the results in Figure 6.15a for the Base and MDAO wind farm layout indicates two things regarding the effective turbulence intensity. First, the maximum turbulence intensity percentage points difference between the regular and irregular layout decreases. This means the tower wall thickness in the MDAO layout will not increase as much as the Base tower. Second, looking at the standard deviation, the percentage points change between the MDAO and Base wind farm layout show a positive magnitude. The percentage points change between the WindPRO and Base optimised wind farm layouts show a negative magnitude. Both magnitudes are significant which means that the standard deviation of the effective turbulence is highly dependent on the wind farm layout.

Overall, the behaviour of the irregular wind farms compared to their regular counterpart is similar to a large extent. The largest difference is observed in the persistence to wind direction results for the standard deviation as a function of wind direction. This sub-performance indicator result is concluded to be to a large degree dependent on the size of the regular wind farm. The results obtained in this research regarding the relative performance of irregular wind farms compared to regular wind farms is thus found generally applicable based on these additional case studies. To further substantiate this claim it is recommended to perform the analysis with numerous additional wind farm layout pairs. Due to the time constraints of this thesis it is not feasible to perform these additional studies in this research.

## 6.5. Conclusion

The performance indicator (PI) group analyses in the first phase of this research are performed using only the specific Borssele case study. Through means of sensitivity studies and additional layout cases, the global effect of the wind farm layout on these PI group results is analysed. The sensitivity analysis serves as a method to predict the outcome of the PI group results of the Borssele case for a change in rotor diameter size or wind climate. While this may not inform global effects of different layouts, it provides a first step towards evaluating the general trends of their effects. To assess this global effect of different layouts, the effect of other optimised wind farm layouts on the PI group results is quantified. The results of the sensitivity studies are shown on the left-hand side of the red dashed line in Figure 6.16, and the additional layout case studies are shown on the right of this line.

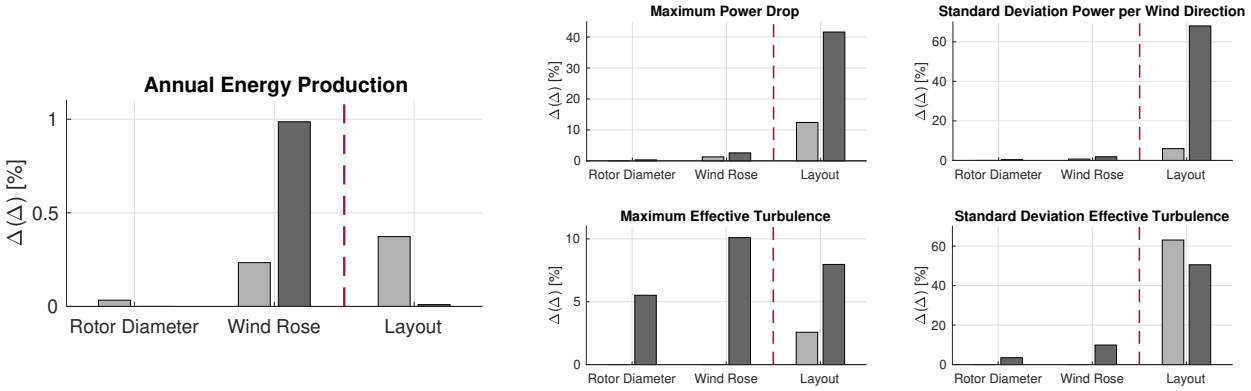


Figure 6.16: Absolute percentage points change obtained from the sensitivity (left of the red dashed line) and additional case studies (right of the dashed red line). The absolute percentage points change are computed based on the layout pair relative performance compared to the base layout pair performance.

For the sensitivity studies, first the IEA Wind turbine rotor diameter is down-scaled from 190.8 m to 178.3 m. The turbines in the Borssele case are replaced with these down-scaled turbines. Comparing the two layouts then shows that the relative sub-performance indicator results between the irregular and regular layouts are only marginally affected by this change in rotor diameter size. The same analysis is performed for a change in wind rose. The results are re-determined for a uniform and unidirectional wind rose. The sensitivity of the PI group results to a change in wind rose is no longer negligible. Especially the results obtained for the sub-performance indicator 'effective turbulence' change significantly between the Borssele and Uniform wind rose.

It is recognised that the wind farm layout is not optimised for the changes in input parameter, which creates an unrealistic situation. WindPRO is utilised to develop an additional wind farm layout for the Borssele case study. Two additional optimisations for a change in rotor diameter show that the wind farm layout does not change significantly as a function of this input change. The uniform and unidirectional wind rose alter the optimised wind farm layout significantly.

Finally, the MDAO and WindPRO optimised wind farm layout pairs are compared. The aim of performing these additional case studies is to assess the global effect of these wind farm layouts on the PI group results. From this analysis it is found that the relative behaviour of the layout pairs (Base, MDAO, and WindPRO) show very similar results. The largest difference is observed in the persistence to wind direction results for the standard deviation as a function of wind direction. This sub-performance indicator result is very dependent on the size of the regular wind farm.

Different analysis methods are implemented to assess the global effect of the wind farm layout on the PI group results. It is found that regardless of the changes in layout cases, wind rose or rotor radius, the absolute inter-pair results are identical as to which layout outperforms the other. For example, in the base case, the irregular wind farm is found to perform worse on the maximum effective turbulence. The same negative behaviour is found with respect to the regular wind farm layout for a change in rotor diameter, wind climate, and also for alternative wind farm layouts.

# 7

# Mitigation of Effective Turbulence for Irregular Wind Farms

## 7.1. Introduction

In this chapter, two models are implemented to develop a recommendation for minimum spacing when optimising irregular wind farms for their power output. In general, from the research performed in the previous chapters, the irregular wind farm layout performs better than the regular wind farm layout. However, the maximum effective turbulence intensity is found to increase in the order of 20%. This significant increase is caused by a limited number of turbines with minimum distance. The maximum effective turbulence in the wind farm is driving for the tower wall thickness and thus cost. The potential to alleviate this downside of the irregular wind farm is investigated by implementing a minimum spacing limit.

Initially, the N.O. Jensen [95] and Frandsen [66] models are analysed in more depth to quantify the relation between turbine spacing, energy loss, and effective turbulence intensity for two turbines. Vermeer et al. [96] observed in large field experiments that the turbulence intensity behind a wind turbine is more persistent than the velocity deficit. This means the velocity deficit will decay more rapidly than the turbulence intensity. In Figure 7.1 the setup for the analysis is presented with the spacing defined as the distance between two turbines, normalised by rotor diameter.

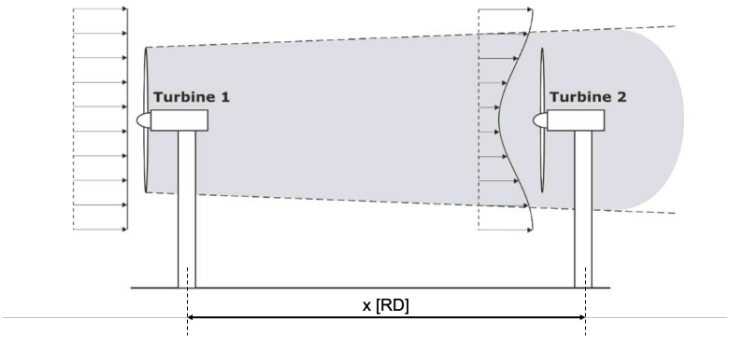


Figure 7.1: Wind turbine wake visualisation, spacing between the turbines is indicated with distance normalised by rotor diameter [97].

The minimum spacing limit found with this in-depth analysis is then implemented to the base irregular wind farm. The PARK and effective turbulence calculations are then performed and compared to the base layout to assess the effect of this attempt to mitigate the effective turbulence of the irregular wind farm.

## 7.2. Minimum Spacing Limit

In the design phase of the wind farm, the turbulence intensity needs to be predicted for each individual turbine in the wind farm. This gives an indication whether the wind turbine layout is suitable for the site conditions. In this research, an estimate of a recommended turbine spacing to mitigate the tower fatigue damage is the objective. Therefore, the effective turbulence intensity for a range of turbine spacing is computed. Using the Frandsen model, the effective turbulence is computed for varying hub-height wind speed and turbine spacing.

The wind-speed-dependent results from the Frandsen model are compared with the respective design curves of the IEC 64100-1 for the wind turbine design class. Between the hub-height wind speeds ranging from $0.6U_{rated}$ and $U_{cut-out}$, the Frandsen results must not exceed by these design curves. The representative value of the turbulence standard deviation is determined using Equation 7.1, as per IEC 64100-1 standards for the normal turbulence model. This representative value for the standard deviation is given by the 90% quantile of the turbine free-stream hub-height mean wind speed.

$$\sigma_1 = I_{ref}(0.75U_{hub} + 5.6) \tag{7.1}$$

Dividing this representative value for the turbulence standard deviation with the mean wind speed at hub-height then results in the turbulence intensity. The representative effective turbulence intensity a function of hub-height mean wind speed is plotted for different spacing in Figure 7.2.

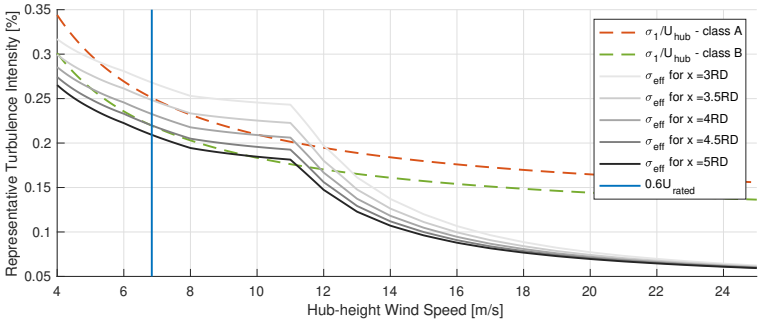


Figure 7.2: Graphical depiction of effective turbulence intensity as a function of hub-height mean wind speed for turbine spacing of 3 to 5 rotor diameter distance. The representative turbulence intensity limit of the IEC 61400-1 is added for wind turbine class A and B.

The IEA Wind turbine is a class A turbine, therefore the red dotted line in Figure 7.2 is relevant for this limiting turbine spacing. Assessing the curves ranging from a turbine spacing of 3 RD to 5 RD with steps of 0.5 RD, the limiting minimum spacing to adhere to the IEC 64100-1 requirements can be established. The curve showing a turbine spacing of 4 RD only exceeds the representative turbulence intensity at a wind speed ranging between approximately 10.1 m/s and 11.2 m/s. Sector-wise curtailment can be implemented when a certain combination of wind speed and direction cause the effective turbulence level to exceed the IEC 64100-1 limit [74]. Therefore, this turbine spacing is selected as the minimum turbine spacing limit to mitigate the tower fatigue damage turbulence in the wind farm.

## 7.3. Wake Energy Loss

To assess the effect of this turbine spacing on the energy production of the turbines, the N.O. Jensen wake model is implemented to assess the energy loss in the wake. To assess the potential energy a turbine can generate at varying distance from the first turbine, the power is computed at the reduced wind speed in the wake, to obtain the reduced power as a function of spacing between turbine 1 and 2. The total energy loss over all operational wind speeds is determined using Equation 7.2.

$$E_w(U_w) = \int_{U_{cut_{in}}}^{U_{cut_{out}}} P(U_w) \cdot W(U_{hub}, A, k) dU$$
$$\Delta E = E_{free}(U_{hub}) - E_w(U_w) \tag{7.2}$$

In which E is the annual energy, P is power curve of the IEA Wind turbine, and W is the Weibull distribution function of the Borssele wind climate. The difference between the free-stream operating turbine and the turbine located in the wake is then compared to assess the annual energy loss. The percentage of the free-stream potential energy of the wake energy is presented in Figure 7.3.

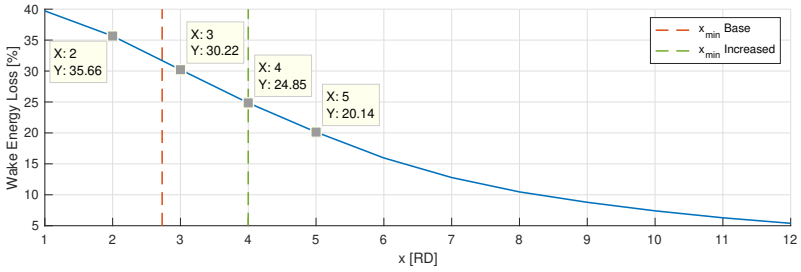


Figure 7.3: Wake energy loss as a function of turbine spacing.

It can be observed that at one rotor diameter spacing the wake energy loss is approximately 40%. With increased spacing the velocity deficit decreases and hence the energy loss decreases. The smallest spacing between two turbines found in the base wind farm layout is 2.73 RD. The reduced energy in the wake, percentage energy loss, and change in wake energy from the 2.73 RD spacing of the base layout compared to the increased spacing of 4 RD is presented in Table 7.1.

Table 7.1: Energy wake loss with respect to distance, the no-loss energy is 6689 kWh.

| | x [RD] | $E_w$ [kWh] | Loss $E_w$ [%] | $\Delta E_w$ [kWh] |
|---|---|---|---|---|
| **Base** | 2.73 | 4565 | 31.8 | + 462 |
| **4RD** | 4.0 | 5027 | 24.9 | |

The base spacing of 2.73 RD corresponds to a wake energy loss of approximately 31.8%, and a spacing of 4 RD corresponds to 24.9%. On a yearly basis, this means that the downstream turbine will generate 503 kWh more when it is positioned at a distance of 4 RD downstream of the turbine compared to 2.73 RD. It should be noted that this analysis is performed for a setup of two turbines. In a wind farm, when increasing the spacing from one turbine, the spacing to another turbine inherently decreases. Depending on the density of the wind farm this increased spacing is possible without decreasing the spacing to another turbine significantly. The effect on the whole complete wind farm therefore needs to be assessed to ensure the overall energy production indeed increases.

## 7.4. Implementation of the Minimum Spacing Limit

To assess the effect on the energy production and effective turbulence, the limiting spacing of 4 RD is applied to the base irregular wind farm. The irregular base wind farm contains three pairs of turbines with a distance smaller than the recommended 4 RD from the effective turbulence intensity analysis. One turbine from each of the three turbine pairs is manually moved to a distance of 4 RD from the other turbine. This manual displacement of individual turbines is performed in WindPRO. The turbines which are moved are indicated with the filled blue circles in Figure 7.4.

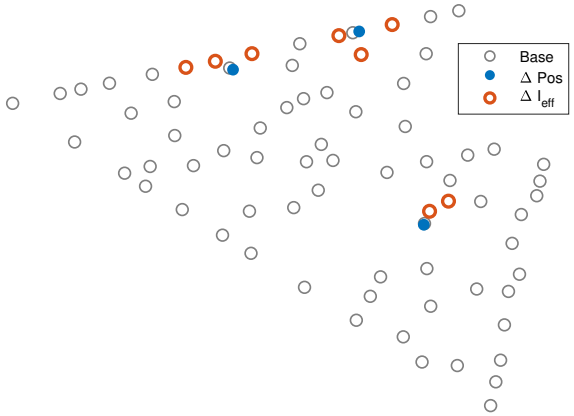


Figure 7.4: Turbines which are moved to adhere to the recommended 4 RD limiting spacing (Δ Pos). The turbines in bold red are the turbines which are not displaced, but do experience a change in effective turbulence intensity (Δ $I_{eff}$).

### 7.4.1. Annual Energy Yield

The energy yield of the wind farm is assessed for the new design with minimum inter-turbine spacing of 4 RD. This is done using the same method as described in section 3.2. The results are presented in Table 7.2 below.

Table 7.2: Energy yield and effective turbulence intensity levels for revised irregular layout with 4 RD as minimum turbine spacing.

| | AEP [GWh/y] | Wake Loss [%] | Difference |
|---|---|---|---|
| **Base** | 3159.5 | 7.49 | + 0.043 % |
| **4 RD** | 3160.8 | 7.45 | |

Increasing the inter-turbine spacing results in reduced wake losses as the wake has more distance to recover between the turbines. The annual energy production increases with 1369 MWh per year, corresponding to an increase of 0.043 % compared to the base layout.

### 7.4.2. Effective Turbulence

To assess the change in effective turbulence the same method described in section 4.3 is implemented for the revised wind farm with 4 RD minimum spacing. The effective turbulence of all the turbines is computed and the result is presented in Figure 7.5.

First, the light-grey lines represent the base irregular wind farm described in . Second, the revised layout where a minimum inter-turbine spacing of 4 RD is implemented, is presented with the dark-grey lines. The re-positioned turbines (from base to 4 RD layout) are depicted with filled black dots. Naturally, these displaced turbines experience a change in effective turbulence intensity. From Figure 7.5, it can also be observed that the turbines surrounding the re-positioned turbines experience a change in effective turbulence. The change in effective turbulence is not directly visible from Figure 7.5 so these turbines are highlighted with red. To link the positions of these turbines, they are also presented with bold red (empty) circles in Figure 7.4. Finally, the maximum effective turbulence for the base and 4 RD layouts are presented with the continuous and dashed red horizontal lines.

Previously it was discussed that the energy production of the turbines surrounding the re-positioned turbine will also be affected. This is also the case for the effective turbulence. Looking at the effective turbulence levels of the two respective layouts (Figure 7.5), it should be noted that by reducing the effective turbulence of one turbine, the effective turbulence of another turbine may increase. In this case example, the effective turbulence of the surrounding turbines does not increase drastically, but with a higher density wind farm this side-effect should be taken into consideration for the implementation of this limiting inter-turbine spacing.

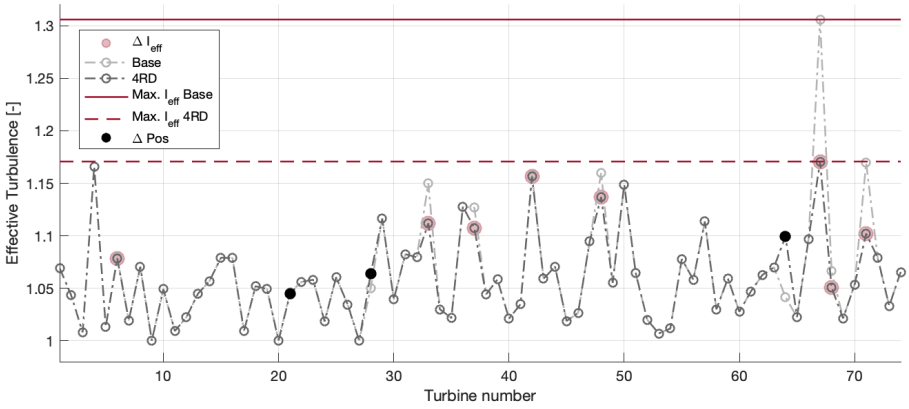


Figure 7.5: Effective turbulence intensity of the Base and 4 RD wind farm layout. The re-positioned turbines are indicated with a filled black dot. The turbines which are not re-positioned, but do experience a change in effective turbulence, are highlighted. The maximum effective turbulence value is indicated with the horizontal red lines for the respective layouts.

The maximum and standard deviation of the effective turbulence are presented in Table 7.3.

Table 7.3: Maximum and standard deviation of the effective turbulence for the base and 4 RD wind farm irregular layouts.

| | **Max. $I_{eff}$** | **Difference** | **$\sigma$ $I_{eff}$ [-]** | **Difference** |
|---|---|---|---|---|
| **Base** | 1.306 | - 10.4 % | 0.05 | - 20.5 % |
| **4 RD** | 1.171 | | 0.04 | |

A significant improvement of the effective turbulence performance is observed for the 4 RD irregular wind farm. The maximum effective turbulence is decreased with 10.4% and the standard deviation is decreased with 20.5%. The standard deviation change is higher as some additional peaks in Figure 7.5 are also mitigated as a result of mitigating the maximum effective turbulence. To give a rough estimation of the tower steel material cost this would save, the same procedure as presented in subsection 4.4.2. The resulting reduction in tower steel material cost is then found to be almost 1 million euros.

## 7.5. Conclusion

The minimum spacing to adhere to the IEC 64100-1 design curves is computed with the Frandsen model, resulting in a minimum inter-turbine spacing of 4 RD. The base irregular layout has three turbine pairs which have a smaller inter-turbine spacing than this limit. Three turbines (one of each turbine pair) is re-positioned to an inter-turbine distance of 4 RD. The annual energy production of the resulting wind farm is found to be 0.043%. For a wind farm consisting of 74 turbines, this result is positive but not significant. Computing the effective turbulence intensity of the 4 RD wind farm results in noteworthy improvements both for the maximum effective turbulence and standard deviation of the effective turbulence. The maximum effective turbulence decreases with approximately 10.4%, which corresponds to (roughly estimated) almost 1 million euros in total tower wall steel cost. It is thus possible to mitigate the maximum effective turbulence intensity for the base irregular layout. Important to note is that when re-positioning one turbine, the effective turbulence for a neighboring turbine might increase. Especially for high density wind farms, the potential to mitigate the maximum effective turbulence might not be as high as for this base layout.

# 8

# Conclusion and Recommendation

The main conclusions that can be drawn from the analyses throughout this research are presented in this chapter. section 8.1 presents the conclusions that can be drawn within the framework of this thesis, whereas section 8.2 discusses the limitations of this framework and makes recommendations for future research.

## 8.1. Conclusions

Improving the performance of wind farms lays the foundation for the wind farm layout optimisation problem. Irregular wind turbine patterns are inherent to the use of optimisation algorithms. To verify whether such wind farm layouts perform better than a regular layouts, the following research question is formulated:

*'To what extent does a regular or irregular geometrical pattern of wind turbines affect the performance of an offshore wind farm?'*

In this research, three performance indicators are identified and investigated to quantify an answer to the above question by means of a comparative case study. These selected indicator groups are (1) power performance; (2) wake-induced tower fatigue; and (3) inter-array cabling system. The performance indicators in this group are affected by the wind farm layout, feasible, site independent, and technical as identified by a multi-criteria decision analysis. Each performance indicator is assessed for three regular and irregular wind farm layout pairs.

In line with expectations, the irregular wind farm performs better in energy production by reducing overall wake losses. It has an increase in annual energy production ranging from 0.66 % in the case study to 1.04 % in the MDAO layout pair. A notable finding is that the irregular layouts also increase the persistence to wind direction, which means that the power output is less sensitive to fluctuations in wind direction. In the case study the regular wind farm shows a power drop up to 66.6% for a limited change in wind direction, whilst the irregular layout shows a power drop of 18.8% under the same conditions. This characteristic improves the predictability of the power output and increases the value of power on the electricity market. In an electricity market dominated by renewable energy, this predictability is even more valuable as the energy price will fluctuate more based on supply and demand.

The regular layout is preferred for tower steel weight. Based on the Frandsen model, the irregular wind farm layout generates significantly higher worst-case wake-induced turbulence levels that result in higher fatigue loads. For fatigue-driven tower design this leads to an increase in wall thickness and therefore material consumption. The increase in maximum effective turbulence for the irregular wind farm compared to the regular wind farm ranges between 14.4 % and 23.8 %. Based on current industry practises, the tower is designed based on the worst case turbulence conditions within a wind farm. The analysis shows that wake-induced turbulence is mostly driven by the smallest inter-turbine spacing in the wind farm. This is demonstrated by implementation of the minimum spacing from the IEC 61400-1, which reduces the worst case turbulence intensity by 20% (as compared to the case study). Nevertheless, few turbines positioned with limited spacing is inherent to the irregular layouts, therefore this conclusion is valid for all wind farm layout pairs.

It was found that the irregular layout results in inter-array cabling costs that are 1.15% higher than that of the regular wind farm layout, due to less efficient routing. The inter-array cabling system is much dependent on site-specific factors such as soil conditions, cable type, and sub-station position. Based on this marginal difference and the high site-dependency, this performance indicator is excluded from further conclusions.

Based on the selected three performance indicators, the performance of the irregular wind farm layouts is higher than that of the regular wind farm layouts. It shows higher energy yield and higher persistence to wind direction. A drawback of irregular wind farm layouts is the increase of wake induced tower fatigue. For comparative purposes an attempt was made to quantify these positive and negative effects for this case study. The net present value of the increase in AEP results to 10 million Euros, whereas the cost for additional tower steel is 3.9 million Euros. The increase of energy production at the cost of tower material consumption leads to an increase in net present value of approximately 6 million Euros.

For future wind farm development, the use of irregular wind farm patterns is expected to increase the performance of the wind farm as a whole. Caution is required with respect to the minimum inter-turbine spacing to limit the negative effect of increased fatigue-loads.

## 8.2. Recommendations

Due to the time constraints of this research and the complexity of the topic, developing an optimisation tool to solve the wind farm layout problem was not feasible. Therefore, as a starting point a pre-defined regular and irregular wind farm layout pair is selected. The exact trade-off between the disciplines and components, and design space are not taken into consideration. To remove this uncertainty, the underlying optimisation algorithm should be analysed with respect to the performance indicator results.

The persistence to wind direction is analysed assuming that the entire wind farm sees the change in wind direction at one instance. In reality it takes minutes or hours before all wind turbines experience a shift in wind conditions. The power drop or wake losses presented in this research are based on a static calculation and do not take into account this dynamic character of inflow conditions. To remove this simplification error, a time-dependent calculation should be performed. Furthermore, only hourly wind data is available for this wind farm site, which means that the variation in wind direction within the hour is unknown.

For the analysis of the wake induced tower fatigue it is assumed that the tower design is driven by fatigue limit states. In reality, the tower design might be driven by ultimate limit states. This doesn't change the results regarding the effective turbulence, but does influence the increase in the tower material consumption. Furthermore, it is assumed that the tower is designed based on the worst-fatigue position in the wind farm. In the future a solution may be found using multiple tower designs in one wind farm. This introduces numerous practical complications which is why this is currently not yet implemented. Finally, the wake added fatigue damage is calculated using a low fidelity model to generate an initial estimation of the added fatigue rather than developing a detailed fatigue analysis. Suggestions for higher fidelity models to accurately quantify the fatigue loads are HAWC2, FAST, or PHATAS.

Regular wind farms are often characterised by straight rows of wind turbines. The negative effect around this characteristic can be reduced when rows are (slightly) bent, by application of yaw misalignment, or other forms of turbine control. Further research is necessary to understand the complex relation between the predictability of a wind farm and the value of its power on the energy market. Factors such as strategic bidding and prediction tools are not considered in this research, but are expected to influence the value on the energy market.

The cost-benefit analysis between regular and irregular wind farm layouts is very complicated, making this comparison a great challenge for further investigation. Analysis of additional performance indicators identified in this research would lead to a more complete review. Especially performance indicators which concern dependency on site-specific input could alter the conclusion that irregular wind farms have better overall performance.

# A

# Multi-Criteria Decision Analysis

## A.1. Performance Indicator Inventory & Rating

| PI | SPI | Layout specific (2) | Technical (0.5) | Feasible (2) | Site independent (1) | Relevance Master (0.5) | Score |
|---|---|---|---|---|---|---|---|
| **Annual Energy Production** | Raw/stand-alone yield | 1 | 3 | 3 | 3 | 3 | 7.8 |
| | Wake losses | 3 | 3 | 3 | 3 | 3 | 10 |
| | Electrical losses | 2 | 3 | 3 | 3 | 2 | 8.6 |
| | Availability | 2 | 2 | 2 | 3 | 3 | 7.5 |
| **Electricity Price** | Predictability | 3 | 3 | 3 | 3 | 3 | 10 |
| | Value on e-market | 3 | 3 | 2 | 2 | 3 | 8.3 |
| **Predevelopment & Consenting** | Project management | 1 | 2 | 2 | 3 | 2 | 6.1 |
| | Legal authorization | 1 | 1 | 2 | 1 | 1 | 4.4 |
| | Surveys | 1 | 1 | 3 | 2 | 1 | 6.1 |
| | Engineering | 2 | 2 | 2 | 3 | 1 | 6.9 |
| | Contingencies | 1 | 2 | 1 | 3 | 2 | 5.0 |
| **Production & Acquisition** | Wind turbines | 2 | 3 | 2 | 3 | 3 | 8.9 |
| | Foundation | 3 | 2 | 1 | 1 | 2 | 6.1 |
| | Power transmission system | 3 | 3 | 3 | 3 | 2 | 9.7 |
| | Monitoring system | 2 | 2 | 2 | 3 | 1 | 6.9 |
| **Installation & Commissioning** | Port | 1 | 1 | 3 | 1 | 2 | 5.8 |
| | Installation of components | 2 | 2 | 2 | 2 | 2 | 6.7 |
| | Commissioning | 2 | 1 | 2 | 2 | 1 | 6.1 |
| | Insurance | 1 | 1 | 3 | 2 | 1 | 6.1 |
| **Operation & Maintenance** | Rental | 1 | 2 | 3 | 2 | 1 | 6.4 |
| | Insurance | 1 | 1 | 3 | 2 | 1 | 6.1 |
| | Transmission charges | 1 | 2 | 3 | 1 | 1 | 5.8 |
| | Maintenance hours | 2 | 3 | 2 | 3 | 3 | 7.8 |
| | Component replacement | 3 | 3 | 2 | 3 | 3 | 8.9 |
| **Decommissioning & Disposal** | Decommissioning | 2 | 1 | 2 | 2 | 1 | 6.1 |
| | Waste management | 1 | 1 | 3 | 3 | 1 | 6.6 |
| | Site clearance | 2 | 1 | 2 | 2 | 1 | 6.1 |
| | Post monitoring | 1 | 1 | 3 | 2 | 1 | 6.1 |

## A.2. Selected Performance Indicator Groups

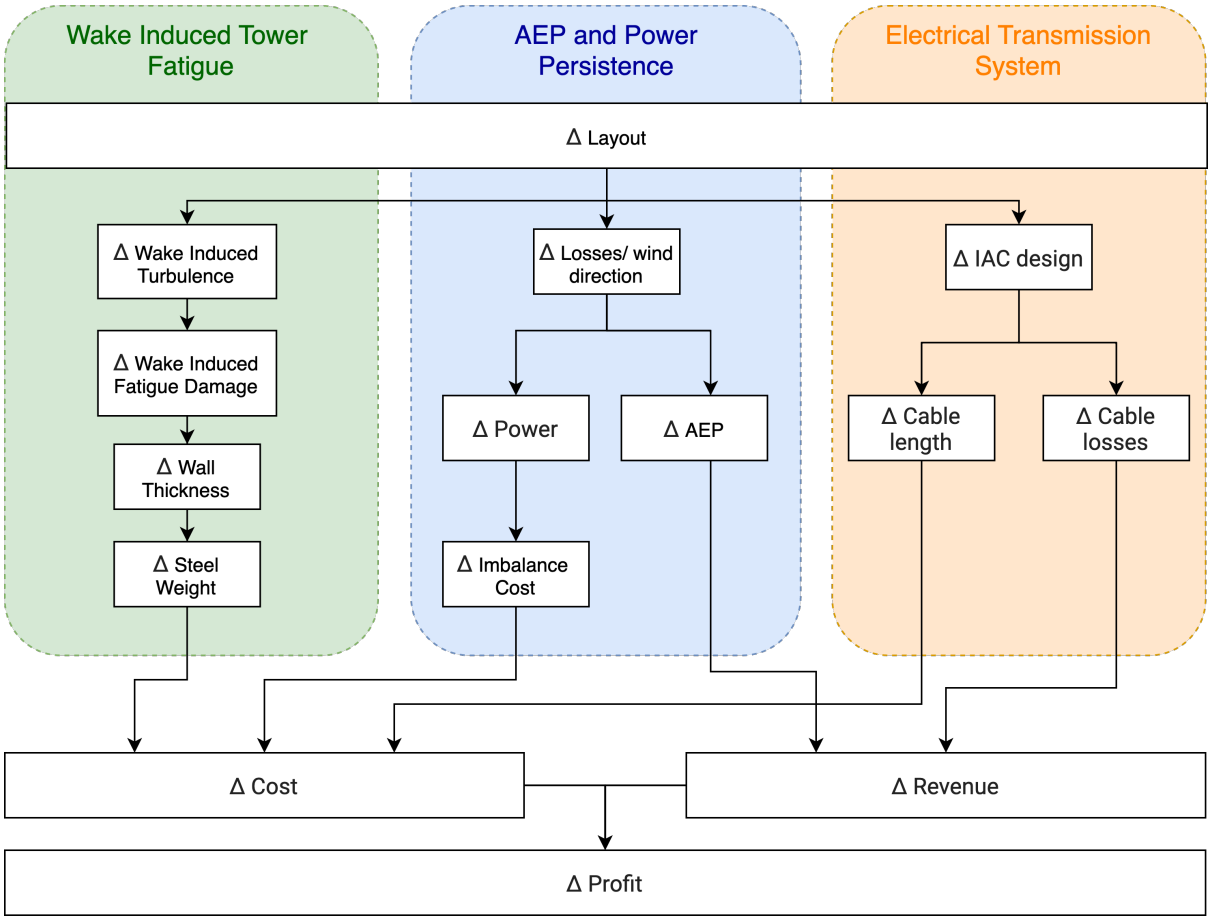


Figure A.1: Schematic overview performance indicator groups

# B

# Optimised Layouts

## B.1. MDAO Design Approach

The 'Multidisciplinary Design Analysis and Optimisation' (MDAO) approach couples different components and disciplines represented by computational tools in a workflow to simulate the entire system. The MDAO workflow is visualised by Sanchez Perez Moreno [45] in Figure B.1.

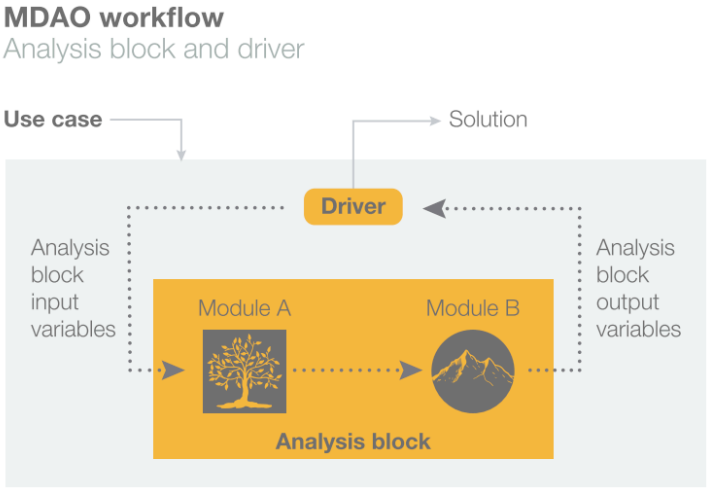


Figure B.1: MDAO workflow diagram consisting of analysis block, drivers, and use case [45].

The workflow has three important aspects that need to be discussed in further detail to understand the MDAO procedure. The flow diagram starts with the **use case** which indicates in what scenario the workflow diagram can be implemented. An **analysis block** is defined consisting of multiple coupled computational tools. The **drivers** then determine which computational tools are implemented and when to obtain a certain desired output such as minimum LCOE in this case. The final proposed layout of the MDAO approach takes into consideration the layout, electrical infrastructure, and foundations.

## B.2. WindPRO Optimisation Module

WindPRO recognises the site-specific constraints and drivers for wind farm layout and therefore allows for a high degree of interactivity between the program and user [30]. WindPRO's optimisation algorithms cover four situations: regular pattern, random pattern, and noise optimization. Noise is not considered in this project, so the latter optimisation algorithm is not discussed. Both optimisation algorithms use a simplified version of the N.O. Jensen model to decrease computational time.

### B.2.1. Regular Optimisation

In the regular optimisation algorithm, as the name already indicates, there are strict geometrical requirements. A choice can be made between the following regular pattern layouts: parallel rows, arcs with same radius, arcs with some origin, and parallel rows in radials. The optimisation of the regular pattern layout is

simply a comparison between all possible regular layouts with the chosen constraints and requirements. The variables that can be altered are the following:

- Starting point X and Y of the fixed WTG
- Number of rows and turbines in each row
- Row and in-row distance
- Base and side angle
- Row off set

A minimum required efficiency can be set to decrease the computational time, excluding layouts with lower efficiency from the analysis. To further decrease the computational time, the input parameters are first varied with large step-size. Then, a refined step size is implemented once the region for the optimised input parameter is known.
The sequence in which the optimisation is performed is as follows:

1. Define a WTG are with a maximum number of turbines allowed in the area, with a resolution of 25m and elevation of 119 m (hub-height) above ground level
2. Define the origin of the regular grid projected onto the WTG area
3. Run optimisation with large step-size for variable input parameters
4. Run optimisation with refined step-size for variable input parameters
5. Compare efficiency and yield of all optimisation results and select best performing layout

The regular layout is largely defined by the input parameters of the user. Therefore, the process of optimisation is both time consuming and prone to sub-optimal solutions caused by user-input constraints. The highest accuracy possible in WindPRO is used for each input parameter to obtain the highest possible yield.

### B.2.2. Irregular Layout Optimisation WindPRO

The number of turbines in the random pattern optimisation algorithm can either be set from the start or included in to optimisation process. Three options are available for the optimisation:

- Auto-fill, this approach will aim to place a maximum number of turbines within a set space, taking into account the minimum spacing. The power output of this layout will be high, but the efficiency will be relatively low due to high power losses.
- Fast Energy Layout, generates a first indication of the optimised layout which allows for alteration of the input parameters. This will not result in an optimised layout but does give an estimate of what this optimised layout will look like.
- Full Energy Optimisation, can be performed where the array losses are continuously calculated, increasing the computational time significantly. First, a wind turbine is placed on the best node point after which a second is added taking into consideration the park efficiency. The position of the first turbine is changed to allow for the best result from both turbines. This continues until all turbines are placed inside the confined space.

The irregular pattern optimisation include interactivity with the user and is an iterative process. Changing the input parameters or manually changing turbine locations can be made to improve the efficiency.

## B.3. WindPRO Optimised Layout Results

WindPRO's optimisation tool is implemented to generate a regular and irregular wind farm layout. This is done to investigate the general applicability of the results found for the performance indicator groups. Following the procedure described in subsection B.2.1, the regular wind farm optimisation with the regular patterns is found as presented in Table B.1.

Table B.1: Table with Input regular optimisation module WindPRO for 20 turbines and Borssele wind climate.

| Input Regular Optimisation | Value |
|---|---|
| X (Easting [km]) | 487.7 |
| Y (Northing [km]) | 5721.3 |
| Row count | 12 |
| WTGs per row | 12 |
| Row distance [m] | 1425 |
| In-row distance [m] | 1425 |
| Base angle [deg] | 349 |
| Side angle [deg] | 100 |
| Row offset | 0.2 |

# C

# Wind Direction Distribution

The sensitivity of the results for different wind roses determines the applicability of the research to generic wind turbine layout cases. Three wind rose distributions are developed to assess this effect. For this, one realistic and two extreme wind roses are selected.

Table C.1: **Borssele** wind direction distribution at hub-height (119 m) [48]. P = probability of the wind direction occurring, A and k are the scale and shape parameters of the Weibull distribution respectively, and $U_{mean}$ = mean wind speed.

| Sector | Direction [°] | A [m/s] | k [-] | P [%] | $\mathbf{U_{mean}}$ [m/s] |
|---|---|---|---|---|---|
| 1 | 345 - 15 | 9.57 | 2.20 | 6.76 | 8.48 |
| 2 | 15 - 45 | 9.49 | 2.26 | 8.07 | 8.41 |
| 3 | 45 - 75 | 9.12 | 2.26 | 7.83 | 8.08 |
| 4 | 75 - 105 | 8.75 | 2.14 | 6.68 | 7.75 |
| 5 | 105 - 135 | 7.89 | 2.07 | 4.81 | 6.99 |
| 6 | 135 - 165 | 8.65 | 2.01 | 4.87 | 7.67 |
| 7 | 165 - 195 | 11.22 | 2.04 | 7.72 | 9.94 |
| 8 | 195 - 225 | 12.39 | 2.12 | 1.23 | 10.97 |
| 9 | 225 - 255 | 12.89 | 2.43 | 1.83 | 11.43 |
| 10 | 255 - 285 | 11.30 | 2.14 | 9.54 | 10.01 |
| 11 | 285 - 315 | 10.55 | 2.08 | 6.88 | 9.34 |
| 12 | 315 - 345 | 10.52 | 2.10 | 6.34 | 9.32 |
| OD | - | 10.72 | 2.08 | 100 | 9.5 |

Table C.2: **Uniform** wind speed distribution derived from Borssele wind climate data [48], at hub-height (119 m). P = probability of the wind direction occurring, A and k are the scale and shape parameters of the Weibull distribution respectively, and $U_{mean}$ = mean wind speed.

| Sector | Direction [°] | A [m/s] | k [-] | P [%] | $\mathbf{U_{mean}}$ [m/s] |
|---|---|---|---|---|---|
| 1 | 345 - 15 | 10.72 | 2.08 | 8.33 | 9.5 |
| 2 | 15 - 45 | 10.72 | 2.08 | 8.33 | 9.5 |
| 3 | 45 - 75 | 10.72 | 2.08 | 8.33 | 9.5 |
| 4 | 75 - 105 | 10.72 | 2.08 | 8.33 | 9.5 |
| 5 | 105 - 135 | 10.72 | 2.08 | 8.33 | 9.5 |
| 6 | 135 - 165 | 10.72 | 2.08 | 8.33 | 9.5 |
| 7 | 165 - 195 | 10.72 | 2.08 | 8.33 | 9.5 |
| 8 | 195 - 225 | 10.72 | 2.08 | 8.33 | 9.5 |
| 9 | 225 - 255 | 10.72 | 2.08 | 8.33 | 9.5 |
| 10 | 255 - 285 | 10.72 | 2.08 | 8.33 | 9.5 |
| 11 | 285 - 315 | 10.72 | 2.08 | 8.33 | 9.5 |
| 12 | 315 - 345 | 10.72 | 2.08 | 8.33 | 9.5 |
| OD | - | 10.72 | 2.08 | 100 | 9.5 |

Table C.3: **Unidirectional** wind speed distribution derived from Borssele wind climate data [48], at hub-height (119 m). P = probability of the wind direction occurring, A and k are the scale and shape parameters of the Weibull distribution respectively, and $U_{mean}$ = mean wind speed.

| Sector | Direction [°] | A [m/s] | k [-] | P [%] | $\mathbf{U_{mean}}$ [m/s] |
|---|---|---|---|---|---|
| 1 | 345 - 15 | 0 | - | 0 | 9.5 |
| 2 | 15 - 45 | 0 | - | 0 | 9.5 |
| 3 | 45 - 75 | 0 | - | 0 | 9.5 |
| 4 | 75 - 105 | 0 | - | 0 | 9.5 |
| 5 | 105 - 135 | 0 | - | 0 | 9.5 |
| 6 | 135 - 165 | 0 | - | 0 | 9.5 |
| 7 | 165 - 195 | 0 | - | 0 | 9.5 |
| 8 | 195 - 225 | 0 | - | 0 | 9.5 |
| 9 | 225 - 255 | 10.72 | 2.08 | 100 | 9.5 |
| 10 | 255 - 285 | 0 | - | 0 | 9.5 |
| 11 | 285 - 315 | 0 | - | 0 | 9.5 |
| 12 | 315 - 345 | 0 | - | 0 | 9.5 |
| OD | - | 10.72 | 2.08 | 100 | 9.5 |

# D

# Sensitivity Overview

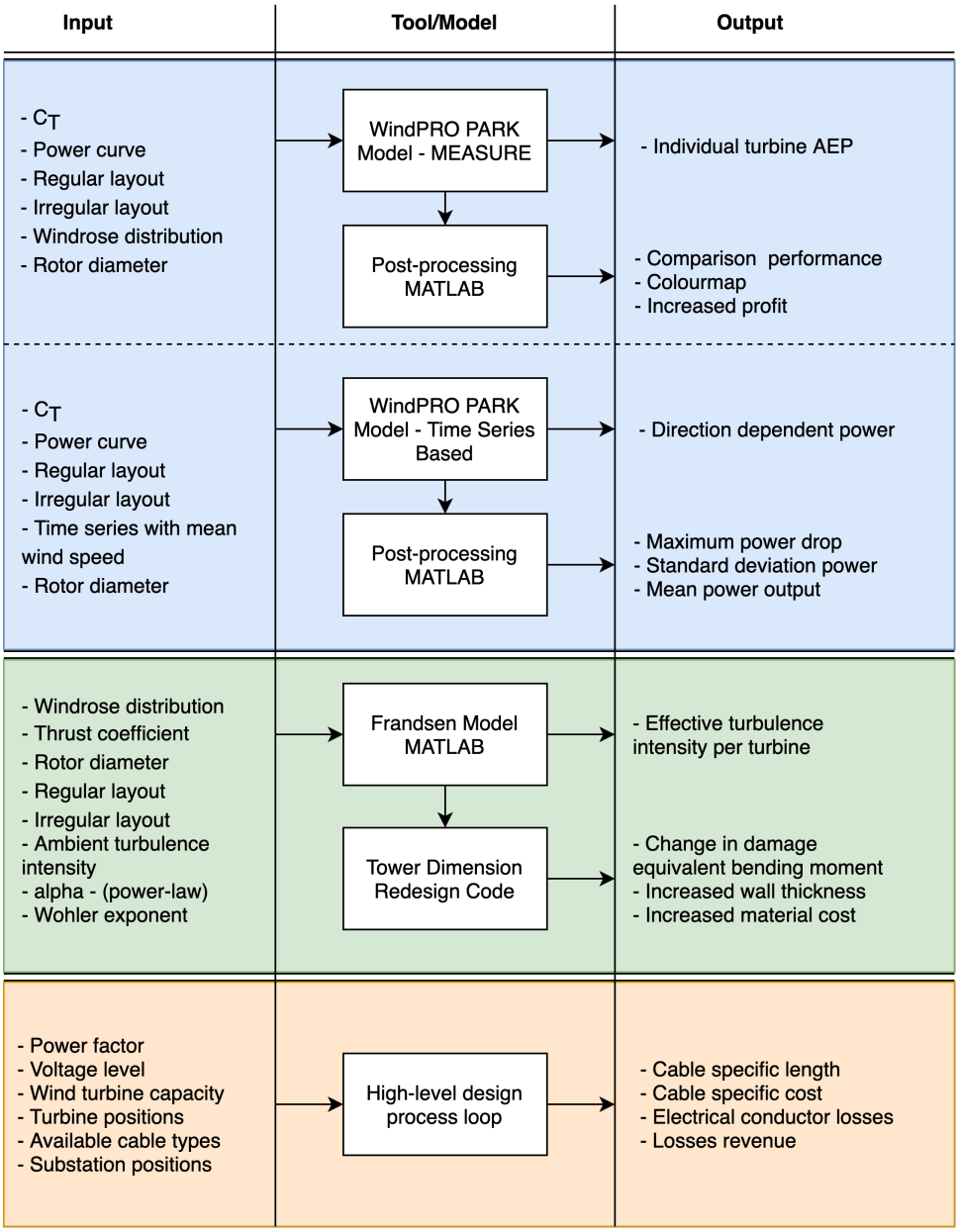


Figure D.1: Input parameters, models/tools, and output per respective performance indicator analysis.

# Sensitivity Study Inter-Array Cable Layout

In this appendix an explanation of the detailed design loop, and sensitivity study of the inter-array cable (IAC) design to both the cable type and substation position is analysed.

## E.1. Detailed Design Loop

The second design loop consist of a detailed design, and verification of the first design loop. As site-dependent variables are required for this design loop this design phase is not performed for the preliminary analysis of the comparison in IAC performance, some of the main aspects that need to be considered are discussed below.

- The selected cable cross-section from the first design loop needs to be verified for both the thermal limit and power losses. In the initial design loop the cable selection is performed based on only the current carrying capacity. Verification that the short circuit power and thermal limits are not exceeded in the cables needs to be performed in the second loop. The soil type and burying depth of the cable are of high importance for the current carrying capacity of the cables. This in turn determines how many turbines can be connected to one string which means an iteration with design loop one is necessary.
- The permissible threshold for temperature within all sub-components needs to be confirmed. Hotspot locations originate when the thermal resistivity of the surrounding (soil) is greater than the one used for the entire wind farm. This needs to be done for at least the following potential hotspot carrying sub-components as identified by dr. ir. Bart Ummels:
  - Inside WTG foundation/monopile, above hang-off, in air, single-core
  - Inside monopile, below hang-off, in air, three-core
  - Inside monopile, in water (possibly: in J-tube)
  - Outside monopile, in water, inside cable protection system (CPS) or J-tube
  - In seabed, in CPS
  - In seabed
  - In seabed, in CPS towards offshore substation
  - In J-tube, each turbine is connected to the cable trench in the seabed with a J-shaped plastic tube [98].
  - Inside substation, below hang-off, in air, three-core
  - Inside substation, above hang-off, in air, single-core

  This is visually presented in Figure E.1.

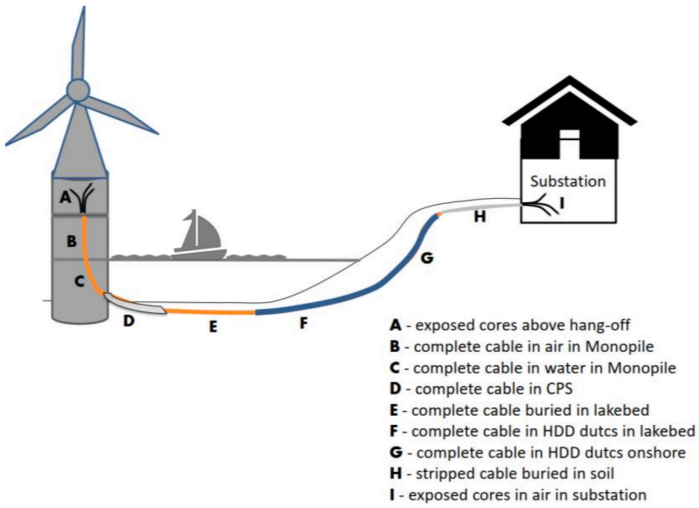


Figure E.1: Visualisation of potential hotspot locations in the offshore electrical inter-array cable system [99].

Both the current dependent losses and voltage dependent losses need to be assessed [100]. The thermal limit is set to 90°C according to IEC 60287 [101]. When the thermal limit is exceeded, a larger cross-sectional cable has to be selected.

- The number and positioning of the substation(s) can vary per location depending on the export cable location often determined by the electricity company maintaining the onshore grid connection according to dr. ir. Bart Ummels, including multiple substations in the second design loop results in a lower cross-section for the cables as less turbines are connected, this will require iteration with the initial design loop.
- The assessment should involve the installation cost which are highly dependent on the site-specific situation. For laying and burying a generic cost value can be assigned per meter, which should include downtime and the chosen risk (P50 or P90), this means the installation cost can differ largely between projects according to ir. Daniël Vree [1]. A cost indication lays between 100-150€, for a large and complex offshore wind farm as Borssele 150€ is deemed a suitable choice, which is not a representative figure but merely serves as an indicative figure to quantify the difference between the regular and irregular wind farm layout.
- Aspects such as obstacles, fishing zones, protected animal species and many more form considerable constraints for the design of an offshore wind farm. These are likely to change the 'ideal' cable design developed in the initial design phase described in Figure 5.2.

Due to both the complexity and the need to use site-specific input parameters from the wind farm, the second design loop is not implemented in this preliminary estimation of the IAC performance.

## E.2. Cable Selection

From the analysis of the design process it became apparent that the cable selection can vary within the same IAC design. In the base calculations the cables selected are 400, 630, 800 $mm^2$ (Case 1). However, the sensitivity of the results to this input parameter need to be investigated to assess the influence of this choice on the results. Therefore, as a sensitivity study the cable ratings are down-scaled to 240, 400, and 630 $mm^2$ (Case 2). The cable specifications for this additional smaller cable are presented together with the cable specifications of the previously used cables in Table E.1.

[1] Electrical power systems consultant at Energy Solutions B.V. with extensive experience regarding offshore electrical power systems.

Table E.1: Selected cable types with their corresponding specifications for two cable type selections. Base design consists of cable 1, 2, and 3. Reduced diameter design consists of cable 2, 3, and 4.

| | Type [$mm^2$] | Ampacity [A] | Conductor resistance [Ω/km] | Phase operating voltage [kV] | Number of turbines [-] | Cost [€/m] |
|---|---|---|---|---|---|---|
| **Cable 1** | 240 | 267 | 0.161 | 66 | 2 | 105 - 121 |
| **Cable 2** | 400 | 424 | 0.101 | 66 | 4 | 145 - 160 |
| **Cable 3** | 630 | 584 | 0.063 | 66 | 6 | 165 - 180 |
| **Cable 4** | 800 | 750 | 0.037 | 66 | 7 | 240 - 255 |

Due to the lower current carrying capacity of the 240 $mm^2$ cable, only two turbines can be connected. Therefore, the minimum number of strings found in the design process described in Figure 5.2, is found to be 13 instead of 11. The IAC design process is implemented for the new cable selection, which results in Figure E.2.

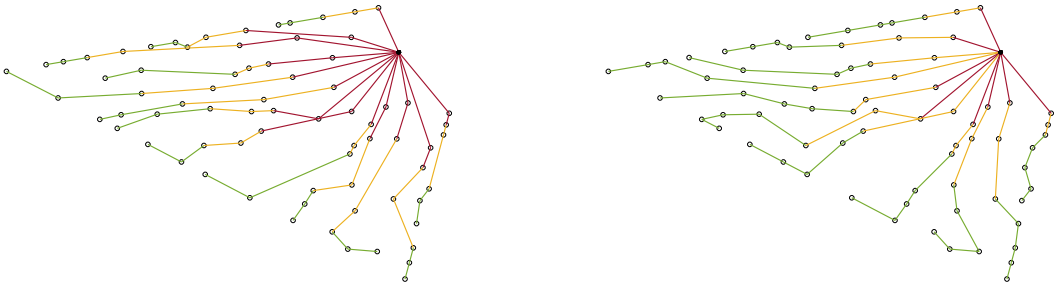

(a) Base Design

(b) Reduced Diameter Design

Figure E.2: Initial Cable Layout for Regular Sequential base design and reduced diameter cable selection. Base design = 400, 630, 800 $mm^2$. Reduced Diameter = 240, 400, 630 $mm^2$.

It should be noted that an attempt was made to keep the arrangement of the strings of both cases largely similar, however, due to the varying number of turbines that can be connected this is not entirely possible. Therefore, there is an uncertainty in the results regarding the level of optimization of the string arrangement. The difference in length, losses, and initial investment cost is calculated for both cases which is presented in Table E.2

Table E.2: Sensitivity study results for the base design and reduced diameter design, for the irregular sequential layout of Borssele. Length, approximate full load losses and initial investment cost. Base: cable1 = 240 $mm^2$, cable 2 = 400 $mm^2$, cable 3 = 630 $mm^2$. Reduced: cable1 = 400 $mm^2$, cable 2 = 630 $mm^2$, cable 3 = 800 $mm^2$.

| | Length [km] | | Full load loss [MW] | | Cost [$10^6$€] | |
|---|---|---|---|---|---|---|
| | Base | Reduced | Base | Reduced | Base | Reduced |
| **Cable 1** | 78.26 | 51.51 | 6.01 | 2.67 | 11.89 | 5.78 |
| **Cable 2** | 54.17 | 56.51 | 4.97 | 4.34 | 8.88 | 8.59 |
| **Cable 3** | 18.98 | 64.66 | 1.90 | 5.92 | 4.75 | 10.6 |
| **Total** | **151.4** | **172.68** | **12.87** | **12.94** | **25.53** | **24.96** |
| **Difference** | + 14.0 % | | + 0.5 % | | - 2.2 % | |

The total length of reduced diameter design is higher than the base case. This is due to the increase in number of strings used in the reduced diameter design versus the base case, using 13 strings instead of 11 strings will increase the total length of cable needed to reach the turbines further away from the offshore substation. With an increase of 14.0% due to the increased number of strings, both the loss and the cost are expected to increase for the irregular wind farm. The same procedure is performed

for the regular grid, which results in an increase of approximately 13.2% However, this is not directly proportional due to the difference in conductor resistance and cost per unit length for the cable types. Case 1 uses higher rated cables than base case, which have higher losses corresponding to higher cable ratings. However, the increase in cable length of the base case is such that the benefit of having lower cable losses in the reduced diameter case does not result in lower power losses. The difference in total loss between both cases is 0.50% which is deemed negligible due to the uncertainty of the calculations. Following, again, the same procedure for the regular grid a similar percentage of 0.52% is found. The difference in cable losses is thus very small for both the regular and irregular grid using different cable types.

The price per unit length also increases with cable rating, here the difference in price is such that the longer distance of the base case does not lead to a higher cost, and in fact results in a lower total initial investment cost of the cables. From Table E.1 it can be seen that the highest rated cable has a significant increase in cost, which is only used in the reduced diameter case. Looking at the total initial investment cost, a decrease of 2.21% is observed which equals to half a million euros. The same procedure was executed for the regular layout which results in an increase of 0.05%. The difference between the regular and irregular grid for the cost is significant and can be explained with the difference in total length, this has most effect on the total initial investment cost. It should also be noted that for the base case, the amount of 'zig-zag' in the cable is increased which will likely result in higher installation cost according to ir. Ana-Maria Ringlever-Dospinescu, due to the increased complexity of the installation procedures.

Looking at the three result categories obtained in this sensitivity study, it can be observed that the cable type used in the wind farm has most effect on the total length of the IAC used. However, the effect on both the losses and cost are relatively small compared with the effect of the length. The regular grid is less sensitive to changes in the cable type used than the irregular grid.

## E.3. Substation Location

As presented in the design process visualised in Figure 5.2, the location of the sub-station can vary as a design choice in the first design loop. The sensitivity of the length, losses and initial investment cost to the location of the substation is investigated in this section. For this sensitivity study, the base design with base case (400, 630, 800 $mm^2$) is used. The substation of the 11-string irregular layout is changed from $5.01 \cdot 10^5$ m nourthing and $5.735 \cdot 10^6$ m Southing to $4.965 \cdot 10^5$ m Northing and $5.725 \cdot 10^6$ m Southing. The visualization of the cable design for both cases is presented in Figure E.3 below.

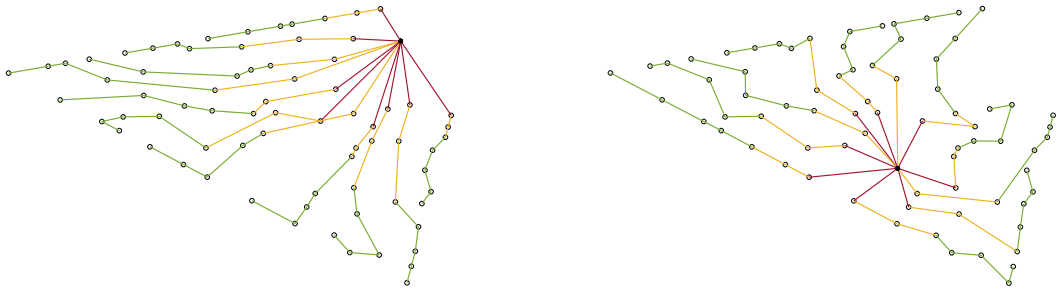

(a) Base position

(b) Alternative position

Figure E.3: Initial Cable Layout for Regular Sequential string design, red = cable 3, orange = cable 2, green = cable 1.

The resulting length, approximate full load losses, and initial investment cost of each cable type are presented in Table E.3 below.

Table E.3: Sensitivity study results for base substation position and the alternative substation position, for the irregular sequential layout of Borssele. Length, approximate full load losses and initial investment cost. Base position = $5.01 \cdot 10^5$ m northing and $5.735 \cdot 10^6$ m Southing. Alternative position = $4.955 \cdot 10^5$ m northing and $5.725 \cdot 10^6$ m Southing.

| | **Length [km]** | | **Full load loss [MW]** | | **Cost [$10^6$ €]** | |
|---|---|---|---|---|---|---|
| | Base | Alternative | Base | Alternative | Base | Alternative |
| **Cable 1** | 40.86 | 30.06 | 3.14 | 2.31 | 6.21 | 4.57 |
| **Cable 2** | 37.40 | 25.56 | 3.43 | 2.34 | 6.13 | 4.19 |
| **Cable 3** | 73.16 | 63.32 | 7.30 | 7.30 | 18.29 | 15.83 |
| **Total** | **151.42** | **118.95** | **13.87** | **10.98** | **30.63** | **24.59** |
| **Difference** | - 22.2 % | | - 21.4 % | | - 20.8 % | |

Assessing the results in Table E.3, the total length of the cables used for the design with alternative substation position is found to decrease with 21% compared to the base substation position. The largest difference is found in cable length 2 which is decreased with approximately 32%, followed by cable 1 with 26% and cable 3 with 13%. This result is in line with the expectations as the same number of strings is used, but now the distance between the offshore substation and turbines on the edge of the wind farm is decreased significantly. For the regular design a similar result is found, with a reduction of 15%, during the clustering of the strings of the regular design it was found that there are limited possibilities for the regular IAC layout.

Looking at the total losses of both base case and alternative case, a decrease of 21% is observed, equal to approximately 2.9 MW. For the regular wind farm this is a reduction of 15% equal to approximately 2.1 MW. Using the same cables and thus having a constant loss per unit length will result in a direct proportionality between the length and losses. Comparing these losses with the nominal electrical power output of the wind farm only results in 0.4%.

For the initial investment cost of the semi-dry cables, a decrease in cost for the irregular wind farm is observed of approximately 21%, and 17% for the regular wind farm. The smaller difference between the regular and irregular layout can be attributed to the smaller difference in length used of cable 3 which has the highest impact on the cable cost.

Overall, the IAC performance with respect to the length, losses, and cost is better for the irregular layout than the regular layout with different substation positions. However, for the regular layout the same substation position would be considerably harder to install as the export cable transmitting the electrical power from the wind farm to the grid becomes challenging. Irregular turbine placement shows more possibilities for the positioning of substation(s), which allows for a significant decrease of both the initial cost of the cables as well as the electrical power losses.

# Bibliography


[1] Peter Musgrove. *Wind Power*. Number 9780521762380 in Cambridge Books. Cambridge University Press, Enero 2009. URL https://ideas.repec.org/b/cup/cbooks/9780521762380.html.

[2] M. Z. Jacobson. Review of solutions to global warming, air pollution and energy security. *Geochimica Et Cosmochimica Acta*, 73(13):A581–A581, 2009. ISSN 0016-7037. URL <GotoISI>://WOS:000267229901394.

[3] S. Keivanpour, A. Ramudhin, and D. A. Kadi. The sustainable worldwide offshore wind energy potential: A systematic review. *Journal of Renewable and Sustainable Energy*, 9(6):18, 2017. ISSN 1941-7012. doi: 10.1063/1.5009948. URL <GotoISI>://WOS:000416106300020.

[4] Jacqueline Yujia Tao and Anton Finenko. Moving beyond LCOE: impact of various financing methods on PV profitability for SIDS. *Energy Policy*, 98:749–758, 2016. ISSN 03014215. doi: 10.1016/j.enpol.2016.03.021.

[5] Wenwen Li, Ender Özcan, and Robert John. Multi-objective evolutionary algorithms and hyper-heuristics for wind farm layout optimisation. *Renewable Energy*, 105:473–482, 2017. ISSN 18790682. doi: 10.1016/j.renene.2016.12.022.

[6] S Tegen, M Hand, B Maples, E Lantz, P Schwabe, and A Smith. 2010 Cost of Wind Energy. *Contract*, 303(March):275–3000, 2012.

[7] Ørsted. Key question about green power, 2020. URL https://orsted.com/en/About-us/whitepapers/taking-action/Key-questions-about-green-power.

[8] F. González-Longatt, P. P. Wall, and V. Terzija. Wake effect in wind farm performance: Steady-state and dynamic behavior. *Renewable Energy*, 39(1):329–338, 2012. ISSN 09601481. doi: 10.1016/j.renene.2011.08.053. URL http://dx.doi.org/10.1016/j.renene.2011.08.053.

[9] Eftun Yilmaz. Benchmarking of Optimization Modules for Two Wind Farm Design Software Tools. pages 1–117, 2012. URL file:///C:/Users/AlexaderPrada/Desktop/Articulosderevistascientificas/FULLTEXT01.pdf.

[10] R. J. Barthelmie, K. Hansen, S. T. Frandsen, O. Rathmann, J. G. Schepers, W. Schlez, J. Phillips, K. Rados, A. Zervos, E. S. Politis, and P. K. Chaviaropoulos. Modelling and measuring flow and wind turbine wakes in large wind farms offshore. *Wind Energy*, 12(5):431–444, 2009. ISSN 1095-4244. doi: 10.1002/we.348. URL https://doi.org/10.1002/we.348.

[11] S. Markarian, F. Fazelpour, and E. Markarian. Optimization of wind farm layout considering wake effect and multiple parameters. *Environmental Progress & Sustainable Energy*, 38 (5):16, 2019. ISSN 1944-7442. doi: 10.1002/ep.13193. URL <GotoISI>://WOS:000486024400055https://aiche.onlinelibrary.wiley.com/doi/full/10.1002/ep.13193.

[12] Regular | definition of regular by oxford dictionary on lexico.com also meaning of regular, jul 2020. URL https://www.lexico.com/definition/regular.

[13] Irregular | definition of irregular by oxford dictionary on lexico.com also meaning of irregular, jul 2020. URL https://www.lexico.com/definition/irregular.

[14] B. Akay, D. Ragni, C. S. Ferreira, and G J W Van Bussel. Investigation of the root flow in a Horizontal Axis. *Wind Energy*, (July 2015):1–20, 2013. doi: 10.1002/we.

[15] Andrew P.J. Stanley and Andrew Ning. Coupled wind turbine design and layout optimization with nonhomogeneous wind turbines. *Wind Energy Science*, 4(1):99–114, 2019. ISSN 23667451. doi: 10.5194/wes-4-99-2019.

[16] Wiesław Ostachowicz, Malcolm McGugan, Jens Uwe Schröder-Hinrichs, and Marcin Luczak. MARE-WINT: New materials and reliability in offshore wind turbine technology. *MARE-WINT: New Materials and Reliability in Offshore Wind Turbine Technology*, pages 1–432, 2016. doi: 10.1007/978-3-319-39095-6.

[17] Nicolai Gayle Nygaard. Wakes in very large wind farms and the effect of neighbouring wind farms. *Journal of Physics: Conference Series*, 524(1), 2014. ISSN 17426596. doi: 10.1088/1742-6596/524/1/012162.

[18] Naima Charhouni, Mohammed Sallaou, and Khalifa Mansouri. Realistic wind farm design layout optimization with different wind turbines types. *International Journal of Energy and Environmental Engineering*, 10(3):307–318, 2019. ISSN 22516832. doi: 10.1007/s40095-019-0303-2. URL https://doi.org/10.1007/s40095-019-0303-2.

[19] Yassine Karouani and Ziyati Elhoussaine. *Toward an intelligent traffic management based on big data for smart city*, volume 37. 2018. ISBN 9783319744995. doi: 10.1007/978-3-319-74500-8_47.

[20] Thomas Corke. Triton Knoll offshore wind farm. *Wind Energy Design*, 44(January):183–194, 2018. doi: 10.1201/b22301-8.

[21] CMS. Cms expert guide to offshore wind in northern europe - offshore wind in the netherlands | regulatory framework for offshore wind, 2019. URL https://cms.law/en/INT/Expert-Guides/CMS-Expert-Guide-to-Offshore-Wind-in-Northern-Europe/Netherlands.

[22] S. Sanchez Perez-Moreno, K. Dykes, K. O. Merz, and M. B. Zaaijer. Multidisciplinary design analysis and optimisation of a reference offshore wind plant. *Journal of Physics: Conference Series*, 1037:042004, 2018. ISSN 1742-6588 1742-6596. doi: 10.1088/1742-6596/1037/4/042004. URL http://dx.doi.org/10.1088/1742-6596/1037/4/042004.

[23] Ying Chen, Hua Li, Bang He, Pengcheng Wang, and Kai Jin. Multi-objective genetic algorithm based innovative wind farm layout optimization method. *Energy Conversion and Management*, 105:1318–1327, 2015. ISSN 0196-8904. doi: https://doi.org/10.1016/j.enconman.2015.09.011. URL http://www.sciencedirect.com/science/article/pii/S0196890415008468.

[24] Naima Charhouni, Mohammed Sallaou, and Khalifa Mansouri. Realistic wind farm design layout optimization with different wind turbines types. *International Journal of Energy and Environmental Engineering*, 10(3):307–318, 2019. ISSN 2251-6832. doi: 10.1007/s40095-019-0303-2. URL https://doi.org/10.1007/s40095-019-0303-2.

[25] S. A. Grady, M. Y. Hussaini, and M. M. Abdullah. Placement of wind turbines using genetic algorithms. *Renewable Energy*, 30(2):259–270, 2005. ISSN 0960-1481. doi: https://doi.org/10.1016/j.renene.2004.05.007. URL http://www.sciencedirect.com/science/article/pii/S0960148104001867.

[26] Grigorios Marmidis, Stavros Lazarou, and Eleftheria Pyrgioti. Optimal placement of wind turbines in a wind park using monte carlo simulation. *Renewable Energy*, 33:1455–1460, 2008. doi: 10.1016/j.renene.2007.09.004.

[27] Bryony DuPont, Jonathan Cagan, and Patrick Moriarty. *Optimization of Wind Farm Layout and Wind Turbine Geometry Using a Multi-Level Extended Pattern Search Algorithm That Accounts for Variation in Wind Shear Profile Shape*, volume 3. 2012. doi: 10.1115/DETC2012-70290.

[28] Rabia Shakoor, Mohammad Yusri Hassan, Abdur Raheem, and Nadia Rasheed. Wind farm layout optimization using area dimensions and definite point selection techniques. *Renewable Energy*, 88:154–163, 2016. ISSN 0960-1481. doi: https://doi.org/10.1016/j.renene.2015.11.021. URL http://www.sciencedirect.com/science/article/pii/S0960148115304390.

[29] Henrik Mattsson. Evaluation of the Software Program WindFarm and Comparisons with Measured Data from Alsvik. 2000.

[30] EMD International A/S. WindPRO user manual. page 193, 2019.

[31] SETIS - TPWind. Key Performance Indicators for the European Wind Industrial Initiative. page 9, 2011.

[32] Ulrich Nissen and Nathanael Harfst. Shortcomings of the traditional "levelized cost of energy" [LCOE] for the determination of grid parity. *Energy*, 171:1009–1016, 2019. ISSN 03605442. doi: 10.1016/j.energy.2019.01.093. URL https://doi.org/10.1016/j.energy.2019.01.093.

[33] Giuseppe Bertalero, Pagamento Addebito, C C Bancario, and Comunicazioni A L Cliente. Co Co Co. (xxxx):1–2, 2013.

[34] Katherine Dykes, Paul Veers, Eric Lantz, Hannele Holttinen, Ola Carlson, Aidan Tuohy, A. M. Sempreviva, A. Clifton, J. S. Rodrigo, Derek Berry, Daniel Laird, Scott Carron, Patrick Moriarty, M. Marquis, C. Meneveau, J. Peinke, J. Paquette, Nick Johnson, L. Pao, Paul Fleming, C. Bottasso, V. Lehtomaki, Amy Robertson, M. Muskulus, Latha Sethuraman, Owen Roberts, and Jason Fields. Results of IEA Wind TCP Workshop on a Grand Vision iea wind. (April), 2019.

[35] DS Remer and AP Nieto. A compendium and comparison of 25 project evaluation techniques. Part 1: net present value and rate of return methods. *International Journal of Production Economics*, 42:101–129, 1995. URL http://www.sciencedirect.com/science/article/pii/0925527395001050.

[36] Elena Gonzalez, Emmanouil M. Nanos, Helene Seyr, Laura Valldecabres, Nurseda Y. Yürüşen, Ursula Smolka, Michael Muskulus, and Julio J. Melero. Key Performance Indicators for Wind Farm Operation and Maintenance. *Energy Procedia*, 137:559–570, 2017. ISSN 18766102. doi: 10.1016/j.egypro.2017.10.385.

[37] Mahmood Shafiee, Feargal Brennan, and Inés Armada Espinosa. A parametric whole life cost model for offshore wind farms. *International Journal of Life Cycle Assessment*, 21(7):961–975, 2016. ISSN 16147502. doi: 10.1007/s11367-016-1075-z. URL http://dx.doi.org/10.1007/s11367-016-1075-z.

[38] María Isabel Blanco. The economics of wind energy. *Renewable and Sustainable Energy Reviews*, 13(6-7):1372–1382, 2009. ISSN 13640321. doi: 10.1016/j.rser.2008.09.004.

[39] IEC. International standard IEC 61400-1, Wind turbines Part 1: Design requirements. *International standard*, 2005, 2005. URL www.iec.ch.

[40] Junying Chang, Bart C. Ummels, Wilfried G.J.H.M. van Sark, Huub P.G.M. den Rooijen, and Wil L. Kling. Economic evaluation of offshore wind power in the liberalized Dutch power market. *Wind Energy*, 12(5):507–523, 2009. ISSN 10954244. doi: 10.1002/we.334.

[41] F. Miceli. Offshore wind turbines foundation types, dec 2012. URL http://www.windfarmbop.com/offshore-wind-turbines-foundation-types/.

[42] S. D. Pohekar and M. Ramachandran. Application of multi-criteria decision making to sustainable energy planning - A review. *Renewable and Sustainable Energy Reviews*, 8(4):365–381, 2004. ISSN 13640321. doi: 10.1016/j.rser.2003.12.007.

[43] Poul Sørensen, Nicolaus Antonio Cutululis, Antonio Vigueras-Rodríguez, Leo E. Jensen, Jesper Hjerrild, Martin Heyman Donovan, and Henrik Madsen. Power fluctuations from large wind farms. *IEEE Transactions on Power Systems*, 22(3):958–965, 2007. ISSN 08858950. doi: 10.1109/TPWRS.2007.901615.

[44] M. A. Mikitarenko and A. V. Perelmuter. Safe fatigue life of steel towers under the action of wind vibrations. *Journal of Wind Engineering and Industrial Aerodynamics*, 74-76:1091–1100, 1998. ISSN 01676105. doi: 10.1016/S0167-6105(98)00100-7.

[45] Sebastian DOI Sanchez Perez Moreno. *A GUIDELINE FOR SELECTING MDAO WORKFLOWS WITH AN APPLICATION IN OFFSHORE WIND ENERGY*. PhD thesis, 2019. URL https://doi.org/10.4233/uuid:ea1b4101-0e55-4abe-9539-ae5d81cf9f65.

[46] SINTEF Energy Research. Total Control: Advanced integrated supervisory and wind turbine control for optimal operation of large Wind Power Plants - Reference Wind Power Plant. (727680): 1–15, 2018.

[47] David Guirguis, David A. Romero, and Cristina H. Amon. Toward efficient optimization of wind farm layouts: Utilizing exact gradient information. *Applied Energy*, 179:110–123, 2016. ISSN 03062619. doi: 10.1016/j.apenergy.2016.06.101. URL http://dx.doi.org/10.1016/j.apenergy.2016.06.101.

[48] Borssele Wind and Farm Zone. Site Studies Wind Farm Zone Borssele. Technical report, 2015. URL https://english.rvo.nl/sites/default/files/2015/02/SiteStudiesWindFarmZoneBorssele{_}MorphodynamicsofBorsseleWindFarmZone.pdf.

[49] Pietro Bortolotti, Helena Canet Tarrés, Katherine Dykes, Karl Merz, Latha Sethuraman, David Verelst, and Frederik Zahle. Systems Engineering in Wind Energy - WP2.1 Reference Wind Turbines. *IEA Wind TCP Task 37*, (May), 2019. URL https://www.osti.gov/biblio/1529216-iea-wind-tcp-task-systems-engineering-wind-energy-wp2\-reference-wind-turbines.

[50] Peter Yun Zhang. Topics in Wind Farm Layout Optimization: Analytical Wake Models, Noise Propagation, and Energy Production. 2013.

[51] Souma Chowdhury, Jie Zhang, Achille Messac, and Luciano Castillo. Unrestricted wind farm layout optimization (uwflo): Investigating key factors influencing the maximum power generation. *Renewable Energy*, 38:16–30, 2011. doi: 10.1016/j.renene.2011.06.033.

[52] Anshul Mittal and Lafayette Taylor. *Optimization of Large Wind Farms Using a Genetic Algorithm*, volume 7. 2012. doi: 10.1115/IMECE2012-87816.

[53] Jim Y. J. Kuo, David A. Romero, J. Christopher Beck, and Cristina H. Amon. Wind farm layout optimization on complex terrains – integrating a cfd wake model with mixed-integer programming. *Applied Energy*, 178:404–414, 2016. ISSN 0306-2619. doi: https://doi.org/10.1016/j.apenergy.2016.06.085. URL http://www.sciencedirect.com/science/article/pii/S0306261916308595.

[54] Stephan Meier and Philip C. Kjr. Benchmark of annual energy production for different wind farm topologies. *PESC Record - IEEE Annual Power Electronics Specialists Conference*, 2005: 2073–2080, 2005. ISSN 02759306. doi: 10.1109/PESC.2005.1581918.

[55] Shafiul Murshed Maruf. WIND RESOURCE ASSESSMENT AND SITE SUITABILITY Dissertation in partial fulfillment of the requirements for the degree of WIND RESOURCE ASSESSMENT AND SITE SUITABILITY. page 69, 2015. URL http://www.diva-portal.org/smash/get/diva2:824303/ATTACHMENT01.pdf.

[56] Zhenzhou Shao, Ying Wu, Li Li, Shuang Han, and Yongqian Liu. Multiple wind turbine wakes modeling considering the faster wake recovery in overlapped wakes. *Energies*, 12(4), 2019. ISSN 19961073. doi: 10.3390/en12040680.

[57] Nicholas Jenkins, A Burton, D Sharpe, and E Bossanyi. *Wind Energy Handbook*. John Wiley & Sons Ltd, United Kingdom, 2001. ISBN 0-4714-8997-2.

[58] R. J. Barthelmie, S. T. Frandsen, M. N. Nielsen, S. C. Pryor, P. E. Rethore, and H. E. Jørgensen. Modelling and measurements of power losses and turbulence intensity in wind turbine wakes at middelgrunden offshore wind farm. *Wind Energy*, 10(6):517–528, 2007. ISSN 10954244. doi: 10.1002/we.238.

[59] Fernando Porté-Agel, Yu Ting Wu, and Chang Hung Chen. A numerical study of the effects ofwind direction on turbine wakes and power losses in a largewind farm. *Energies*, 6(10):5297–5313, 2013. ISSN 19961073. doi: 10.3390/en6105297.

[60] Hannele Holttinen. Handling of wind power forecast errors in the Nordic power market. *2006 9th International Conference on Probabilistic Methods Applied to Power Systems, PMAPS*, 2006. doi: 10.1109/PMAPS.2006.360288.

[61] C. Obersteiner, T. Siewierski, and A. N. Andersen. Drivers of imbalance cost of wind power: A comparative analysis. *2010 7th International Conference on the European Energy Market, EEM 2010*, pages 1–9, 2010. doi: 10.1109/EEM.2010.5558699.

[62] M. Y. Othman, B. Yatim, K. Sopian, Bakar, and M. N. A. Improving Air-Cooled Condenser Performance in Combined Cycle Power Plants Improving Air-Cooled Condenser Performance in Combined. *Journal of Energy Engineering*, December(December):121–126, 2006. doi: 10.1061/(ASCE)0733-9402(2006)132.

[63] Ju Feng and Wen Zhong Shen. Wind farm power production in the changing wind: Robustness quantification and layout optimization. *Energy Conversion and Management*, 148:905–914, 2017. ISSN 0196-8904. doi: https://doi.org/10.1016/j.enconman.2017.06.005. URL http://www.sciencedirect.com/science/article/pii/S0196890417305484.

[64] Kenneth Thomsen and Poul Sørensen. Fatigue loads for wind turbines operating in wakes. *Journal of Wind Engineering and Industrial Aerodynamics*, 80(1-2):121–136, 1999. ISSN 01676105. doi: 10.1016/S0167-6105(98)00194-9.

[65] Victor Igwemezie, Ali Mehmanparast, and Athanasios Kolios. Current trend in offshore wind energy sector and material requirements for fatigue resistance improvement in large wind turbine support structures – A review. *Renewable and Sustainable Energy Reviews*, 101(October 2018): 181–196, 2019. ISSN 18790690. doi: 10.1016/j.rser.2018.11.002. URL https://doi.org/10.1016/j.rser.2018.11.002.

[66] Sten Tronaes Frandsen. *Turbulence and turbulence- generated structural loading in wind turbine clusters*, volume 1188. 2007. ISBN 8755034586. doi: Riso-R-1188.

[67] Peter Frohboese and Christian Schmuck. Thrust coefficients used for estimation of wake effects for fatigue load calculation. *European Wind Energy Conference and Exhibition 2010, EWEC 2010*, 5:3434–3444, 2010.

[68] Tim Cooper and Burton Street. *Product Lifetimes And The Environment conference proceedings*. 2015. ISBN 9780957600997.

[69] Katherine Dykes, Rick Damiani, Owen Roberts, and Eric Lantz. Analysis of ideal towers for tall wind applications. *Wind Energy Symposium, 2018*, (210029), 2018. doi: 10.2514/6.2018-0999.

[70] J. Angelina and M. Andrew. Imperfection analysis and optimized design of tapered spirally-welded wind turbine towers. *Structural Stability Research Council Annual Stability Conference 2014, SSRC 2014*, (May 2015):607–616, 2014.

[71] C. Amzallag, J. P. Gerey, J. L. Robert, and J. Bahuaud. Standardization of the rainflow counting method for fatigue analysis. *International Journal of Fatigue*, 16(4):287–293, 1994. ISSN 01421123. doi: 10.1016/0142-1123(94)90343-3.

[72] Anders Ahlstr. Aeroelastic Simulation of by. *Technology*, (April), 2005.

[73] Carlo Tibaldi Leonardo Bergami David Verelst Georg Pirrung Riccardo Riva Morten Hartvig Hansen, Lars Christian Henriksen. *HAWCStab2: User Manual*. Department of Wind Energy, October 2018.

[74] Morten Nielsen, Hans E. Jørgensen, and Sten T. Frandsen. Wind and wake models for IEC 61400-1 site assessment. *European Wind Energy Conference and Exhibition 2009, EWEC 2009*, 6:3765–3770, 2009.

[75] Mesfin Belayneh Ageze, Yefa Hu, and Huachun Wu. Wind Turbine Aeroelastic Modeling: Basics and Cutting Edge Trends. *International Journal of Aerospace Engineering*, 2017, 2017. ISSN 16875974. doi: 10.1155/2017/5263897.

[76] Martin Shan. Load Reducing Control for Wind Turbines: Load Estimation and Higher Level Controller Tuning based on Disturbance Spectra and Linear Models. 2017. URL https://kobra.bibliothek.uni-kassel.de/bitstream/urn:nbn:de:hebis:34-2017050852519/3/DissertationMartinShan.pdf.

[77] Erik Asp Hansen. Site Studies Wind Farm Zone Borssele. page 127, 2015. URL https://english.rvo.nl/sites/default/files/2015/02/SiteStudiesWindFarmZoneBorssele{_}MorphodynamicsofBorsseleWindFarmZone.pdf.

[78] Paul S. Veers. *Fatigue loading of wind turbines*. Woodhead Publishing Limited, 2010. ISBN 9781845695804. doi: 10.1533/9780857090638.1.130. URL http://dx.doi.org/10.1533/9780857090638.1.130.

[79] Victor Igwemezie, Ali Mehmanparast, and Athanasios Kolios. Materials selection for XL wind turbine support structures: A corrosion-fatigue perspective. *Marine Structures*, 61(May 2018): 381–397, 2018. ISSN 09518339. doi: 10.1016/j.marstruc.2018.06.008. URL https://doi.org/10.1016/j.marstruc.2018.06.008.

[80] David Milborrow. Global costs analysis – the year offshore wind costs fell, jan 2016. URL https://www.windpowermonthly.com/article/1380738/global-costs-analysis-year-offshore-wind-costs-fell.

[81] Peter Argyle, Simon Watson, Christiane Montavon, Ian Jones, and Megan Smith. Modelling turbulence intensity within a large offshore wind farm. *Wind Energy*, 21(12):1329–1343, 2018. ISSN 10991824. doi: 10.1002/we.2257.

[82] Juan Andres Perez-Rua and Nicolaos A. Cutululis. Electrical Cable Optimization in Offshore Wind Farms - A Review. *IEEE Access*, 7:85796–85811, 2019. ISSN 21693536. doi: 10.1109/ACCESS.2019.2925873.

[83] Xiaojing Sun, Diangui Huang, and Guoqing Wu. The current state of offshore wind energy technology development. *Energy*, 41(1):298–312, 2012. ISSN 03605442. doi: 10.1016/j.energy.2012.02.054. URL http://dx.doi.org/10.1016/j.energy.2012.02.054.

[84] P. Gardner, L. M. Craig, and G.J. Smith. Electrical Systems for Offshore Wind Farms. *Switch Onto Wind Power 20th (BWEA)*, pages 309–317, 1998. ISSN 2193-1801. doi: 10.1186/2193-1801-3-418.

[85] Javier Serrano González, Manuel Burgos Payán, Jesús Manuel Riquelme Santos, and Francisco González-Longatt. A review and recent developments in the optimal wind-turbine micro-siting problem. *Renewable and Sustainable Energy Reviews*, 30:133–144, 2014. ISSN 13640321. doi: 10.1016/j.rser.2013.09.027. URL http://dx.doi.org/10.1016/j.rser.2013.09.027.

[86] A. Endegnanew, H. Svedsen, R. Torres-Olguin, and L. Faiella. Design procedure for in array electric design. *EERA DTOC report*, 2013. URL http://www.eera-dtoc.eu/wp-content/uploads/files/D2.2-Design-procedure-for-inter-array-electric-design.pdf.

[87] Martina Fischetti and David Pisinger. Optimizing wind farm cable routing considering power losses. *European Journal of Operational Research*, 270(3):917–930, 2018. ISSN 03772217. doi: 10.1016/j.ejor.2017.07.061. URL https://doi.org/10.1016/j.ejor.2017.07.061.

[88] Bengt Franken. Reliability study. analysis of electrical systems within offshore wind parks, Nov 2007.

[89] Anna Ferguson, Phil De Villiers, Brendan Fitzgerald, and Jan Matthiesen. Benefits in moving the inter-array voltage from 33 kV to 66 kV AC for large offshore wind farms. *European Wind Energy Conference and Exhibition 2012, EWEC 2012*, 2(1):902–909, 2012.

[90] Ernst Camm and Charles Edwards. Reactive Compensation Systems for Large Wind Farms. *IEEE*, pages 1–5, 2008. URL https://ieeexplore.ieee.org/stamp/stamp.jsp?arnumber=4517085.

[91] Laura Castro-Santos and Vicente Diaz-Casas. Sensitivity analysis of floating offshore wind farms. *Energy Conversion and Management*, 101:271–277, 2015. ISSN 01968904. doi: 10.1016/j.enconman.2015.05.032. URL http://dx.doi.org/10.1016/j.enconman.2015.05.032.

[92] Jérme Morio. Global and local sensitivity analysis methods for a physical system. *European Journal of Physics*, 32(6):1577–1583, 2011. ISSN 01430807. doi: 10.1088/0143-0807/32/6/011.

[93] Zahle R. Bitsche T.Kim A. Yde L.C. Henriksen P.B. Andersen A. Natarajan M.H. Hansen C. Bak, F. Design and performance of a 10 mw wind turbine. *J. Wind Energy*, 138, jul 2013.

[94] NRC: Glossary. Capacity factor (net), may 2020. URL https://www.nrc.gov/reading-rm/basic-ref/glossary/capacity-factor-net.html.

[95] N.O. Jensen and Forskningscenter Risø. *A Note on Wind Generator Interaction*. Risø National Laboratory, 1983. ISBN 9788755009714. URL https://books.google.nl/books?id=5w3tvgEACAAJ.

[96] L. J. Vermeer, J. N. Sørensen, and A. Crespo. Wind turbine wake aerodynamics. *Progress in Aerospace Sciences*, 39(6-7):467–510, 2003. ISSN 03760421. doi: 10.1016/S0376-0421(03)00078-2.

[97] Ali C. Kheirabadi and Ryozo Nagamune. A quantitative review of wind farm control with the objective of wind farm power maximization. *Journal of Wind Engineering and Industrial Aerodynamics*, 192(June):45–73, 2019. ISSN 01676105. doi: 10.1016/j.jweia.2019.06.015. URL https://doi.org/10.1016/j.jweia.2019.06.015.

[98] Sanjeev Malhotra. Selection, Design and Construction of Offshore Wind Turbine Foundations. *Wind Turbines*, 2011. doi: 10.5772/15461.

[99] TKF Connectivity Solutions. Ampacity Calculation for all Hotspots - 630mm2 Cable Ampacity Calculation for all Hotspots -. 2019.

[100] J. Pilgrim, S. Catmull, R. Chippendale, R. Tyreman, and P. Lewin. Offshore Wind Farm Export Cable Current Rating Optimisation. *EWEA Offshore Wind*, (November), 2013.

[101] IEC 61851. International Standard International Standard. *61010-1 © Iec:2001*, 2006:13, 2006.